ВЕСТНИК ТУРИНСКОГО ПОЛИТЕХНИЧЕСКОГО УНИВЕРСИТЕТА В ГОРОДЕ ТАШКЕНТЕ

ACTA OF TURIN POLYTECHNIC UNIVERSITY IN TASHKENT

ВЫПУСК
EDITION 1/2022

TOSHKENT SHAHRIDAGI TURIN POLITEXNIKA UNIVERSITETI
AXBOROTNOMASI
1/2022 SONI

ВЕСТНИК
ТУРИНСКОГО ПОЛИТЕХНИЧЕСКОГО УНИВЕРСИТЕТА В ГОРОДЕ ТАШКЕНТЕ
ВЫПУСК 1/2022

ACTA
OF TURIN POLYTECHNIC UNIVERSITY IN TASHKENT
EDITION 1/2022

TASHKENT – 2022

Журнал Ўзбекистон Ахборот ва оммавий коммуникациялар агентлиги томонидан 0890-сонли гувоҳнома билан рўйҳатга олинган.
ISSN 2181-8886
E-ISSN 2181-1512

№ 3/2021

Тошкент шаҳридаги Турин политехника университети 100095, Тошкент ш., Кичик Халқа Йўли 17 уй.

Тел.: (+99871) 246-70-82
E-mail: actattpu@polito.uz
www.actattpu.polito.uz

Журнал зарегистрирован в Узбекском Агентстве информации и массовых коммуникаций. Свидетельство о регистрации № 0890.
ISSN 2181-8886
E-ISSN 2181-1512

№ 3/2021

Туринский Политехнический Университет в городе Ташкенте 100095, г. Ташкент, ул. Кичик Халка Йули 17.

Тел.: (+99871) 246-70-82
E-mail: actattpu@polito.uz
www.actattpu.polito.uz

The journal was registered at the Agency of Information and Mass Communications of Uzbekistan. Certificate of Registration № 0890.
ISSN 2181-8886
E-ISSN 2181-1512

№ 3/2021

Turin Polytechnic University in Tashkent 100095, Tashkent city, Kichik Halqa Yo’li str. 17.

Tel.: (+99871) 246-70-82
E-mail: actattpu@polito.uz
www.actattpu.polito.uz

CONTENTS

ACTA TTPU

Preface

Dear readers! I am pleased to announce a new edition of the journal of the Turin Polytechnic University ACTA TTPU. It is an № 1 issue to be published in 2022 year which includes selected articles submitted to the Editors. We observed an increase of the number of submissions to our journal during a year and I believe that the growth of the popularity of the journal is due to excellent work of the Editorial Board as well. We will continue our efforts in increasing the quality, as well as requirements for the submissions and simplification of the selection procedures bringing the quality to higher standarts.

I appreciate very much our Editorial board for their contribution to improving the quality of our journal and all authors for presented papers. We are always open to any criticism and suggestions to improve the readability and content of the submitted papers published in our journal.

Editor in-chief
DSc. J.Sh.Inoyatkhodjaev

Acta of Turin Polytechnic University in Tashkent, 2022, 31, 7-13
Published Online March 2022 in Acta TTPU (http://www.acta.polito.uz/)

MODELLING OF ENERGY CONSUMPTION OF THE BATTERY ELECTRIC VEHICLE

Jamshid Mavlonov[1] *, **Sanjarbek Ruzimov**[2] **and Akmal Mukhitdinov**[3]
Turin Polytechnic University in Tashkent, Kichik khalka yuli 17, Tashkent, Uzbekistan[1 2]
Tashkent state transport university, Adilkhodjaev street 1, Tashkent, Uzbekistan[3]
*Corresponding author email: j.mavlonov@polito.uz

Abstract– Battery electric vehicles (BEVs) are gaining large market share. Accurate computation of the BEV's energy consumption is important to avoid running out of energy while driving. Therefore, it is important to develop a model which estimates the energy consumption of the BEV. This article describes a model that evaluates a BEV's energy consumption. The aim of this paper is modeling of BEV using MATLAB/Simulink software based on a real BMW i3 BEV 2014 data. The model consists of vehicle dynamics, single-speed transmission gearbox, electric machines and battery blocks. The detailed analysis on each block is performed and the governing equations for each block is derived taking into account both traction and regeneration modes. Moreover, constraints in terms of limitation in power for each block is considered. Finally, the results of the model are compared with the experimental data which obtained from Argonne national laboratory database in EPA Urban Dynamometer Driving Schedule (EPA UDDS) driving cycle.

Key words– BEV, EM, MATLAB, simulation, electric battery, UDDS

I INTRODUCTION

One of the main cause of environmental degradation around the world is global warming. CO2 and other gases exhausted by systems are main causes of global warming [1]. Therefore, the main goal of car manufactures all over the world is to develop zero-emission vehicles. On the other hand, measures are being taken to regulate the usage of natural resources. In this context, electrified vehicles are seen as the suitable solution [2]. One of the main advantage of BEV is the regenerative braking feature. However, still the market share of BEVs is not very fast. The main reasons for that are some limitations on charging stations, batteries cost and their life. The assessment of BEV's energy consumption has become an important task. The literature devoted to estimation of energy consumption of the electrified vehicle. Miri et al. used the MATLAB / Simulink based simulation modeling and estimation a BEV. The BEV energy consumption was modeled using longitudinal dynamics [2]. Synák et al. has used a dynamometric stand to determine the energy consumption of the BEV, experimentally. Dynamometer generates the mechanical energy transmitted through the car wheels to the traction motor and records the results using sensors connected to different parts [3]. Experimenting using this stand will also incur additional costs. The same dynamometric roller has also used in the work done by Konzept at al. The purpose of their work was to predict energy consumption of BEV in different driving cycles. In the end, the results were compared with a real driving speed profile and energy consumption recorded by an onboard computer of the vehicle [4]. The article does not take into account the influence of weather conditions and battery degradation. Thus, it can be concluded that vehicle modeling is the highest priority in the analysis of energy consumption. In an article presented by Suvak and Ersan, BEV was simulated in the MATLAB/Simulink program. Their article provided an analysis of the EM torque and power changes during the driving cycle. In addition, the power and torques generated by the wheels during the movement of the car was analyzed [5]. Simple yet efficient model for estimation of energy consumption of the BEV is missing. This article focuses on the analysis of energy consumption of the BEVs. The work describes a backward model to estimate energy consumption of BEV on different driving cycles. The model is validated using publicly available data from ANL [6].

II VEHICLE MODELLING

In this section, full model of the BEV has been described. This analysis performed in the MATLAB / Simulink software and EPA UDDS drive cycle selected as the cycle of action which has shown in Figure 3. Simulated results are also compared with the experimental results in the section of RESULT. A detailed description of the measurement process has also given. In addition, the formulas used to calculate the vehicle's electric motor and battery parameters are given. The full model of the BEV has shown in Figure 1. This model allows to determine the state of charge (SOC) of the battery and energy consumption of BEV.

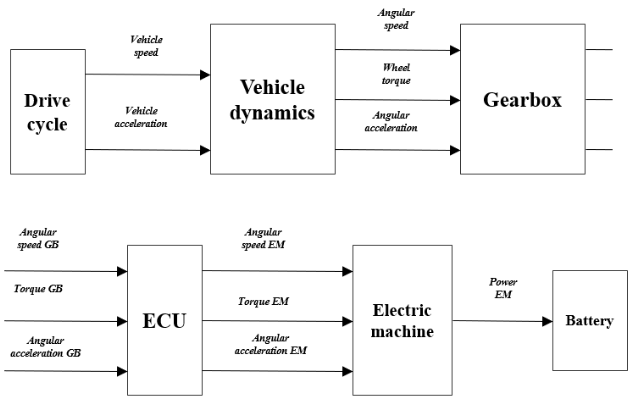

Fig. 1: Data flow for Backward model of BEV [7,8]

1 *VEHICLE SPECIFICATION*

BMW i3 BEV 2014 was selected for further analysis as the main technical specifications of the vehicle is publicly available and the most complete. The technical specifications of a vehicle are given in Table 1.

2 *VEHICLE MODEL*

Since this article focuses on evaluating the energy consumption of BEV, the following power analyzes are important for the implementation of this model:

- Analysis of the power from the battery to the wheels for the moving the vehicle
- Analysis of the power as a result of the regenerative braking of the vehicle
- Auxiliary power required to turn the additional equipment in the vehicle (air conditioning, etc.) and its analysis.

The data flow along each block is depicted in the Figure 1 are described sequentially.

3 *DRIVE CYCLE*

Drive cycle - is a time history of the vehicle speed. The drive cycle is used for vehicle testing and simulation as a standard form. Specifically, it is used to predict the performance of a vehicle's dynamics, emissions and comfort.

VEHICLE BODY	
Curb weight, (kg)	1443.3
Aerodynamic drag coefficient	0.3
Frontal area, (m^2)	2.38
POWERTRAIN	
Motor operating range, (rpm)	0-11 400
Maximum power kW / @ rpm	125 / @ 4777
Maximum torque Nm / @ rpm	250 / @ 0-4475
TRANSMISSION	
Type	Single-speed automatic transmission
Final gear ratio	8.2:1
Front/rear tyres radius, (m)	0.3290 (175/70 R19)
BATTERY	
Chemistry	Lithium-ion
Battery configuration	8 Modules (96 Cells Connected in Series)
Nominal cell voltage, (V)	3.7
Nominal cell capacity, (Ah)	60
Nominal battery pack voltage, (V)	355.2
Nominal battery pack capacity, (Ah)	60
Nominal battery pack energy, (kWh)	22

TABLE 1: BMW I3 BEV 2014 SPECIFICATIONS [2,6,9]

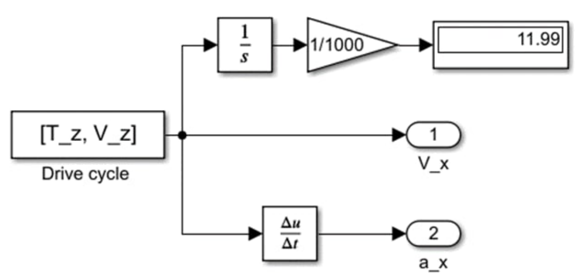

Fig. 2: Driving cycle model

The plot of the change in speed shown in Figure 3 and these values loaded into the block diagram in Figure 2. This block can also be used to represent the time dependence of a vehicle's acceleration (Eq.1.). Both experimental and theoretical data can be loaded into the driving cycle.

$$a_x = \frac{dV}{dt} \tag{1}$$

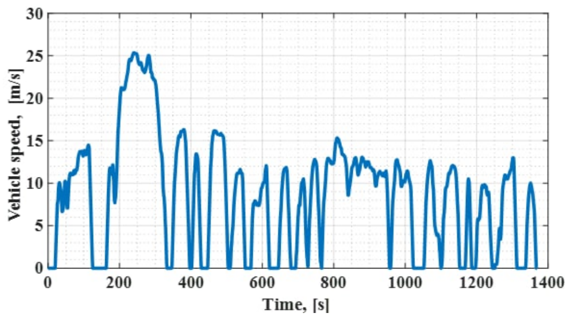

Fig. 3: Vehicle speed on EPA UDDS driving cycle

4 VEHICLE DYNAMICS

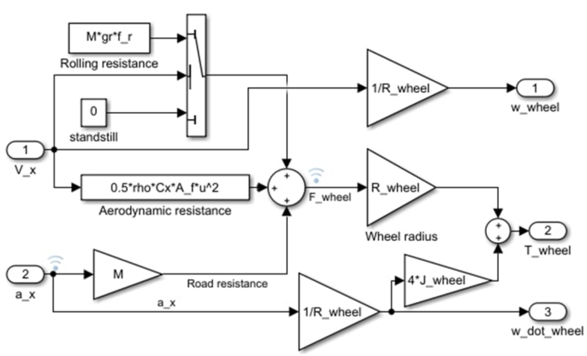

Fig. 4: Vehicle dynamics block

Vehicle dynamics - block studies the factors (angular velocity, forces, torque, etc.) that affect the movement of the vehicle and it is made up of forces that resist movement. Vehicle dynamics block is shown in Figure 4. The forces play a key role for driving the vehicle. This means that while the forces help the vehicle to move, they also resist the movement. These forces are transmitted from the electric motor to the wheels by means of a propulsion device to move the vehicle. The motion of a vehicle consists of the following forces that affect it: rolling resistance, aerodynamic drag force and the force generated by linear acceleration. The vehicle has to overcome resistance forces to move. Total force (F_t) determined by sum of the rolling resistance force (F_r), aerodynamic resistance force (F_a) and linear acceleration resistance force (F_m).

$$F_t = F_r + F_a + F_m \tag{2}$$

$$F_r = f_r \cdot M \cdot g \tag{3}$$

$$F_a = \frac{1}{2} \cdot \rho \cdot C_x \cdot A_f \cdot V^2 \tag{4}$$

$$F_m = M \cdot a_x \tag{5}$$

The output results from this block are shown in figure 4. They are angular speed (ω_w), angular acceleration ($\dot{\omega}_w$) and torque (T_w) in the wheels. Delivered power (P_w) to the wheel can determined by using Eq.9.

$$\omega_w = \frac{V_x}{R} \tag{6}$$

$$\dot{\omega}_w = \frac{a_x}{R} \tag{7}$$

$$T_w = F_t \cdot R + \dot{\omega}_w \cdot 4 \cdot J_w \tag{8}$$

$$P_w = F_t \cdot V_x \tag{9}$$

The output from this block to the GEARBOX block are the wheel torque Knowing (T_w) which depends also moment of inertia of the wheel (J_w) (Eq.8), wheel angular speed (ω_w) and acceleration ($\dot{\omega}_w$)

5 GEARBOX

In the Gearbox the angular speed and the torque generated from the vehicle's engine/motor are increased or decreased by a certain amount equal to transmission ratio (Fig.5.). In previous section, it was mentioned that the considered vehicle has a single – speed transmission. Hence, the value of the angular speed and the angular acceleration are changed while passing through the gearbox. These parameters are multiplied by the final gear ratio (U_f). U_f and efficiency of a gearbox (η_w) do not change due to the reason of single – speed transmission is used. One of the main functions of the transmission system is increasing of the torque between the electric motor and the wheel. The efficiency of the gearbox in the traction and braking mode can be inverted. For finding the torque and the efficiency of the gearbox, in the traction and braking modes approach proposed in [7] have been used.

The resulting equations are input parameters for the electric motor. It is necessary to determine the direction of power flow and this block is divided into two sub-blocks which are traction and braking modes. Depending on the movement of the vehicle, traction or braking mode is activated. The determined parameters are realized by the following equations 10 and 11.

$$\omega_{em} = \omega_w \cdot U_f \tag{10}$$

$$\dot{\omega}_{em} = \dot{\omega}_w \cdot U_f \tag{11}$$

Power mode block contains of following structure [7]:

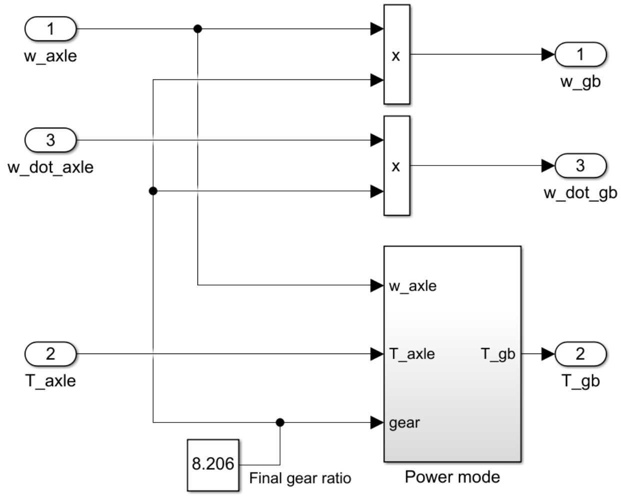

Fig. 5: GEARBOX block

$$T_{em} = \begin{cases} \frac{T_w}{\eta_{gb} \cdot U_f} & \text{– Traction mode} \\ \frac{\eta_{gb} \cdot T_w}{U_f} & \text{– Braking mode} \end{cases} \tag{12}$$

Where,

ω_{em} - angular velocity of electric machine [rad/s]

$\dot{\omega}_{em}$- angular acceleration of electric machine [rad/s^2]

η_{gb} - efficiency of a gearbox [-]

The transmission model is determined based on the following equation:

$$T_{em} = F_{tr} \cdot R \cdot U_f \cdot \eta_{gb} \tag{13}$$

Where,

F_{tr} – Traction force [N]

6 ELECTRIC MACHINE

Electric machine – is a machine which can convert electrical energy to mechanical energy when it works as a motor. In electric machine block, electric power can be determined from the electric motor torque and angular speed. The electric machine acts as a generator during the regenerative braking mode.

In backward model, Electric machine block demands an electric power from the battery packs. In general, the electric power from the battery is delivered to the electric motor. The movement of a vehicle is ensured as a result of the transmission through the gearbox to the wheels. The angular velocity and the torque can determine by using the Eq.10 and Eq.12. By using these parameters the electrical power (P_{em}) is determined. The auxiliary power (P_{aux}) is used by auxiliary components (air conditioner and etc.) of the BEV. It should be noted that the value of P_{aux} varies depending on the climate.

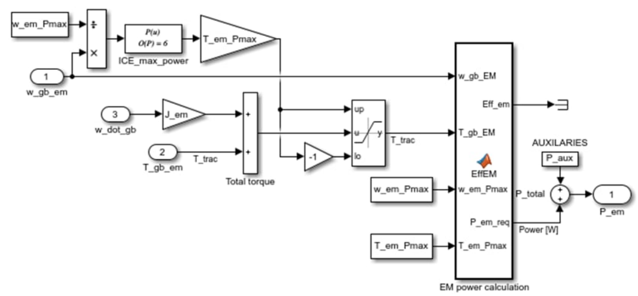

Fig. 6: Electric Machine block

For example, on a hot ambient temperature, more power is required as a result of using the air conditioner. So, the total electric power is determined by using the Eq.14. Model of the electric machine aims in calculating power demand from battery pack for given mechanical power, i.e., torque and speed of the electric machine at its output shaft. Scheme of this block is shown in Figure 6.

$$P_{em} = \omega_{em} \cdot T_{em} + P_{aux} \tag{14}$$

In this case, the maximum characteristic of the operation of electric machine is used in determining the minimum and maximum torque [8].The limits of T_{em} are following:

$$T_{max_{em}} < T_{em} < T_{min_{em}} \tag{15}$$

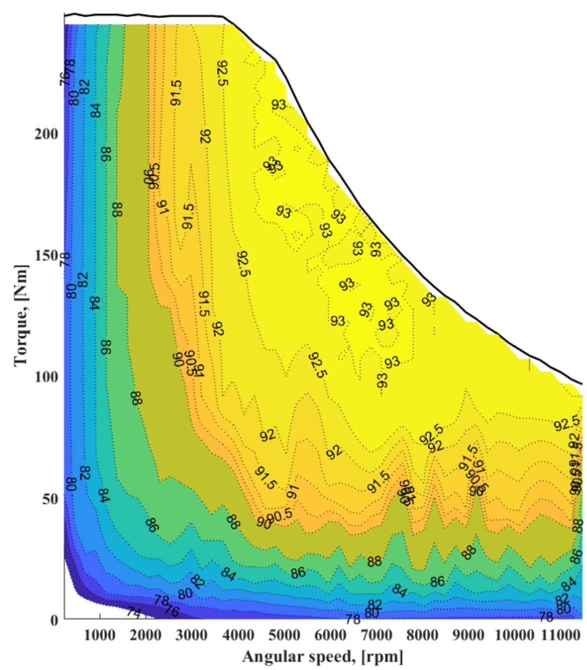

Fig. 7: BEV motor efficiency [2]

The efficiency of the electric motor (η_{em}) is formed as a function of the angular velocity (ω_{em}) and torque ($T_{tot_{em}}$) defines as follows:

$$\eta_{em} = f(\omega_{em}, T_{em}) \tag{16}$$

$$T_{tot_{em}} = T_{em} + J_{em} \cdot \dot{\omega}_{em} \tag{17}$$

where,
J_{em} - moment of inertia of electric machine [$kg \cdot m^2$]

7 BATTERY

Battery – is the main source of the vehicle to power the electric motor. Battery block analyses the required electric current and voltage during the driving cycle. In addition, it can study variation of state of charge (SOC).

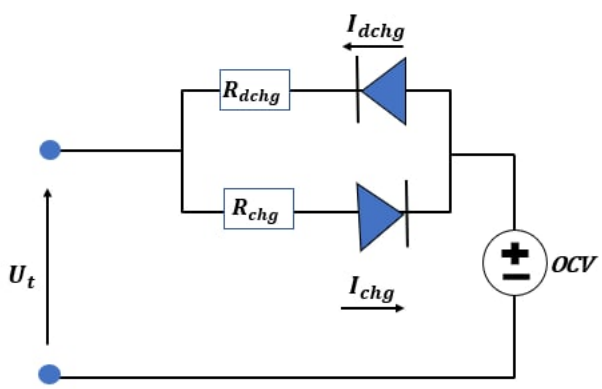

Fig. 8: Battery electrical circuit model (Thevenin model)

Thevenin model it can be used to model Open circuit voltage (OCV), charging (R_{chg}) and discharging (R_{dchg}) resistance as functions of SOC:

$$OCV = f(SOC), \;\; R_{chg} = f(SOC), \;\; and \;\; R_{dchg} = f(SOC) \tag{18}$$

The SOC of the battery is if charge and discharge modes are calculated in the following equation:

$$SOC = \begin{cases} SOC_i - \frac{\int_o^t I_{dchg} dt}{Q_{nom}} & - \quad \text{Traction mode} \\ SOC_i + \frac{\int_o^t I_{chg} dt}{Q_{nom}} & - \quad \text{Braking mode} \end{cases} \tag{19}$$

Where,
SOC_i – initial value of state of charge [-]
Q_{nom} – nominal value of the battery capacity [Ah]
I_{dchg} – value of discharge current [A]
I_{chg} – value of charge current [A]

By knowing the value of charging (R_{chg}) and discharging (R_{dchg}) resistances and OCV it should be evaluated the I_{dchg} and I_{chg} by solving the following quadratic equations:

$$I_{dchg} = SOC_i - \frac{OCV - \sqrt{OCV^2 - 4 \cdot R_{dchg} \cdot P_{bat}}}{2R_{dchg}} \tag{20}$$

$$I_{chg} = SOC_i - \frac{-OCV + \sqrt{OCV^2 - 4 \cdot R_{chg} \cdot P_{bat}}}{2R_{chg}} \tag{21}$$

There are restrictions on the battery performance in terms of maximum charging and discharging currents values. It is therefore important to ensure that the current discharged from the batteries does not overcome the limiting conditions.

$$I_{chg} < I_{chg_{max}} \;\; and \;\; I_{dchg} < I_{dchg_{max}} \tag{22}$$

Where,
$I_{chg_{max}}$ - maximum value of charge current [A]
$I_{dchg_{max}}$ - maximum value of discharge current [A]

From the Thevenin model battery power (P_{bat}) also analysed for the given components. Power balance equation is applied to equivalent circuit[11].

$$P_{bat} = \begin{cases} I_{dchg} \cdot OCV - I_{dchg}^2 \cdot R_{dchg} & \text{– Traction mode} \\ I_{chg} \cdot OCV + I_{chg}^2 \cdot R_{chg} & \text{– Braking mode} \end{cases} \tag{23}$$

The OCV relative to SOC has illustrated in Figure 9a. It can be seen from the graph that the voltage has nearly linear dependence from SOC in the region of interest (0.1 – 0.9). The internal resistances of the battery in charging and discharging phases are shown in Figure 9b and Figure 9c respectively.

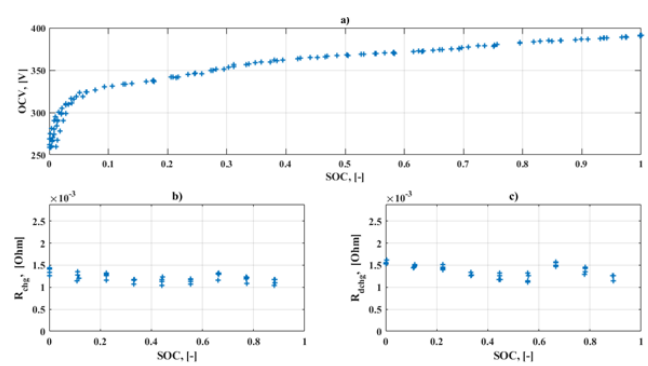

Fig. 9: OCV, R_{dchg} and R_{chg} analysis by SOC

The main purposes are changing values of SOC, current and voltage by time during driving cycle and these can be estimate by the battery model in MATLAB/Simulink. Battery

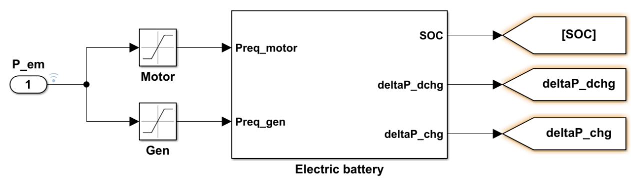

Fig. 10: Battery model

model is illustrated in Figure 10. It can be seen the electric battery can take electric power from the electric machine block and works in charging/discharging mode.

Electric battery part separates charging and braking mode which is shown in Figure 11. Electric battery polynomials used to find OCV and finally get a SOC, these values are calculated by equation 18 and 19 respectively.

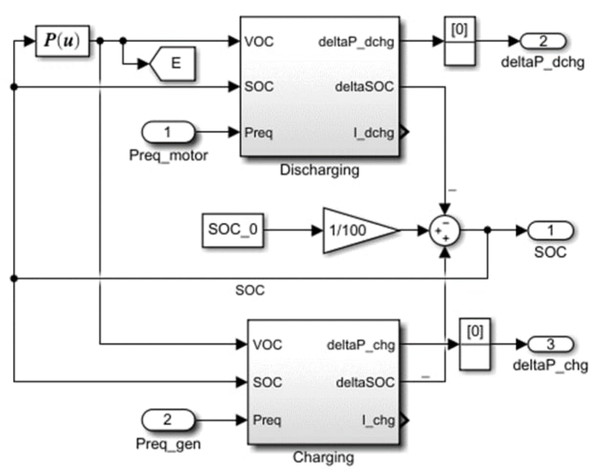

Fig. 11: Working principle of charging/discharging of the battery

III RESULTS

When the model is launched, several results can be obtained. Electrical energy is converted into the mechanical energy to generate mechanical torque and angular velocity on the wheels. Power loss from the battery to the wheels through the gearbox is in the range of 5 - 10 kW. Comparison results between the mechanical and electrical power is shown in Figure 12.

SOC of the battery has been simulated theoretically and illustrated in blue dotted line in Figure 13. This theoretical graph was compared with the result of real experimental data available from [6]. The difference between them is marginal. This may be due to the fact that complete data (i.e., rolling resistance coefficient, aerodynamic drag coefficient, auxiliary

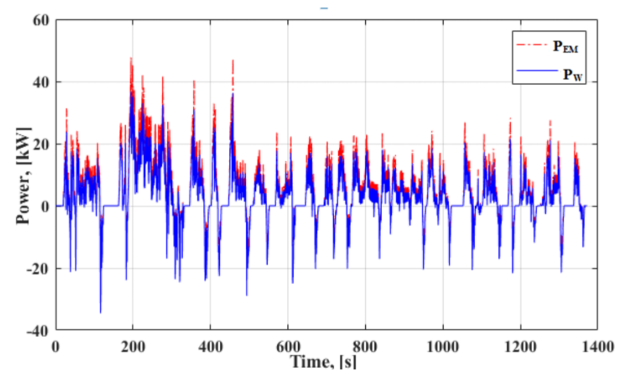

Fig. 12: Comparison of the electric and mechanical power time history over UDDS cycle

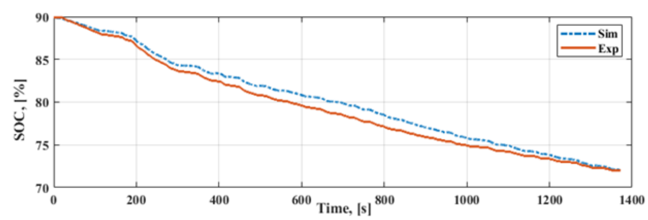

Fig. 13: SOC during the drive cycle

power) are different from these used in experiment.

IV CONCLUSION

The purpose model is a complete model of BEV and consists of several blocks. These blocks include: Driving cycle, vehicle dynamics, gearbox, electric machine and battery blocks. The drive cycle is represented by a data of the changing vehicle speed over time and the UDDS drive cycle was used during the testing of this model. The SOC of the battery was compared with the experimental results.

Mechanical power is slightly less than electric power, where the difference is around 5-10 kW. These losses occur mainly in the motor and gearbox block. The charge level of the car differs by a small amount compared to the experiment. The main reason for this is the lack of data on auxiliary power, rolling resistance, aerodynamic drag coefficients. The model results show good correlation with experiments. The future work will analyse the influence of the motor, battery characteristics on the energy consumption calculation results.

V REFERENCES

[1] Matheus Koengkan, José Alberto Fuinhas, Matheus Belucio, Nooshin Karimi Alavijeh, Nasrin Salehnia, Daniel Machado, Vinícius Silva and Fatemeh Dehdar,

(2022) “The Impact of Battery-Electric Vehicles on Energy Consumption: A Macroeconomic Evidence from 29 European Countries” World Electr., Veh., J., 2022, 13, 36. *https://doi.org/10.3390/wevj13020036*

[2] Ilyès Miri, Abbas Fotouhi and Nathan Ewin, (2020) “Electric vehicle energy consumption modelling and estimation — A case study” 2020 The Authors. International Journal of Energy Research published by John Wiley and Sons Ltd. nt J Energy Res., 2021;45:501–520.

[3] František Synák, Matej Kučera, Tomáš Skrúcaný, (2021) "ASSESSING THE ENERGY EFFICIENCY OF AN ELECTRIC CAR", Department of Road and Urban Transport, Faculty of Operation and Economics of Transport and Communications, University of Zilina, Zilina, Slovakia, pp.A1–A13., *https://doi.org/10.26552/com.C.2021.1.A1-A13*.

[4] Anja Konzept, Benedikt Reick, André Kaufmann, Ralf Hermanutz and Ralf Stetter, (2022) “Battery Electric Vehicle Efficiency Test for Various Velocities” Vehicles 2022, 4, 60–73. *https://doi.org/10.3390/vehicles4010004*

[5] Hakan Suvak and Kemal Erşan, (2016) The Simulation of a Full Electric Vehicle Using the City Cycle. Karabuk University, Vocational High School, Turkey., International Journal of Automotive Engineering and Technologies Vol. 5, Issue 2, pp. 38 – 46, 2016.

[6] Official website of Argonnen National Laboratory. Available online: *https://www.anl.gov/es/*. [Accessed on February 2022]

[7] Guzzella L., Sciarretta A., Vehicle Propulsion Systems, Springer: Berlin/Heidelberg, Germany, 2013. *https://doi.org/10.1007/978-3-642-35913-2*.

[8] Onori S., Serrao L., Rizzoni G., Hybrid Electric Vehicles, Springer: London, UK, 2016. *https://doi.org/10.1007/978-1-4471-6781-5*

[9] Official website Idaho National laboratory., Available online: *https://avt.inl.gov/index.html*. [Accessed on November 2021]

[10] Javier A. Oliva, Christoph Weihrauch and Torsten Bertram, (2013) “Model-Based Remaining Driving Range Prediction in Electric Vehicles by using Particle Filtering and Markov Chains”, Institute of Control Theory and Systems Engineering, Technische Universitat Dortmund, EVS27 International Battery, Hybrid and Fuel Cell Electric Vehicle Symposium.

[11] S.L.Eshkabilov, A.A.Mukhitdinov, S.K.Ruzimov, Optimal control strategies for cvt of the hev during a regenerative process, 2006.

[12] S.K.Ruzimov, J.R.Mavlonov, A.A.Mukhitdinov, Analysis of the Powertrain Component Size of Electrified Vehicles Commercially Available on the Market, Komunikacie, Slovakia, Available online: *https://doi.org/10.26552/com.C.2022.1.B74-B86*.

[13] Branislav Sarkan, Stefania Semanova, Veronika Harantova, Ondrej Stopka, Maria Chovancova and Mirosław Szala, (2019) "Vehicle fuel consumption prediction based on the data record obtained from an engine control unit", Department of Road and Urban Transport, Faculty of Operation and Economics of Transport and Communications, University of Zilina, Univerzitna 1, 010 26 Zilina, Slovak Republic.

[14] Ewelina Sendek-Matysiak, Hubert Rzędowski, (2021), “THE COSTS OF CHARGING ELECTRIC VEHICLES IN POLAND”, Department of Automotive Engineering and Transport, Kielce University of Technology Kielce, Poland, pp.A1–A11, *https://doi.org/10.26552/com.C.2022.1.A1-A11*

[15] Tingting Wang Dongming Zhang Dongchen Qin, Jianjie Li., Modeling and simulating a battery for an electric vehicle based on modelica., Automotive Innovation, 2:169–177, 2019.

[16] Sven Schumacher, Stefan Schmid, Philipp Wieser, Ralf Stetter and Markus Till, (2021) “Design, Simulation and Optimization of an Electrical Drive-Train” Vehicles 2021, 3, 390–405. *https://doi.org/10.3390/vehicles3030024*

[17] MATLAB simulink and development., Available online:*https:// www.matworks.com*. [Accessed on February 2022].

Acta of Turin Polytechnic University in Tashkent, 2022, 31, 14-18
Published Online March 2022 in Acta TTPU (http://www.acta.polito.uz/)
Doi:XX

CONSERVATIVE DIFFERENCE SCHEMES FOR OPTIMAL PLACEMENT OF HEAT SOURCES IN A PARALLELEPIPED

B.Kh.Khayitkulov
National University of Uzbekistan named after Mirzo Ulugbek
Email: b.hayitqulov@mail.ru

Abstract—In this paper, a method and algorithm for solving the non-stationary problem of optimal placement of heat sources of minimum power in the space have been developed. As a result, the temperature in the space is within the specified limits and the value of the functional is minimized. The mathematical model of the process is described by the heat conduction equation with a variable coefficient. The numerical model of the problem is constructed using implicit conservative difference schemes. To solve the problem of thermal conductivity control, a linear programming problem was used. Software for numerical modeling has been developed. The results of a computational experiment are presented.

Keywords—optimal placement; heat sources; integro-interpolation method; conservative schemes; Big M method.

I INTRODUCTION

One of the most common objects in various fields of human activity is the system of heat sources, the heat balance in heated rooms. Mathematical modeling of such systems poses the problem of optimal placement of heat sources in heated rooms, which is associated with resource-saving engineering technologies. The task of optimal placement of heat sources in heated areas has always been relevant in design work in construction, greenhouses and other technical and technological areas.

The heat transfer process can be controlled in different ways. The process is often controlled by the placement of heat sources or changes in ambient temperature. The problems of controlling the process of heat propagation under various conditions were studied by A.G.Butkovsky [1], J.L.Lions [2], Yu.V.Egorov [3], A.I.Egorov [4], as well as by other authors, and important results were obtained. Their work forms the basis of this work. In the work [5] the problem of optimal control of processes described by the heat equation was studied. The control parameter is set in the boundary condition and has reached the minimum of the functional given by the integral quadratic expression. A method for finding an admissible control that gives a minimum to the functional is shown. In the paper [6] the third boundary value problem of parabolic type was considered. The right side of the boundary condition contains controls in additive form. The problem of transferring an object from the initial state to the zero state in a conflict situation is solved.

In the work [7], the differential-difference problem of controlling the diffusion process was studied, an analogue of the maximum principle was obtained, which makes it possible to determine the moments of switching on and off the source of maximum power. The paper [8] proposes a solution to the problem of optimal placement of sources in inhomogeneous media, in which scalar stationary fields are described by elliptic equations. The algorithms for solving the problem are based on methods for estimating the values of the functional on the set of possible locations of sources, which makes it possible to choose the optimal variant by implementing the branch and bound method. The paper [9] considers the problem of optimizing the density of heat sources in stationary processes described by elliptic equations given by the third boundary condition. In the work [10], the minimax problem of the optimal placement of sources in the processes of heat propagation described by equations of elliptic type was numerically solved. To find the extremum of the objective function depending on the location of the sources of the physical field, the minimax method of mathematical modeling was used. The proposed approach made it possible to find a numerical solution to the boundary value problem in terms of the source carrier placement parameters. In works [11, 12, 13], a method for the numerical solution of the non-stationary problem of optimal placement of heat sources with a minimum power in processes described by parabolic type equations is proposed. An algorithm and a set of programs for the numerical solution of non-stationary problems of optimal control of the location of heat sources and visualization of the results obtained have been developed.

In the work [14], the problems of optimal space heating based on the Pontryagin maximum principle are considered. The paper [15] considers the problem of energy-efficient heat supply of a building in a central heating system.

In this paper, we consider the problem of heat conduction control based on the optimization of a linear objective functional, taking into account constraints, which is solved on the basis of approximation and reduction to a linear programming problem. The paper proposes a technique and algorithm for solving the non-stationary problem of maintaining the temperature inside the region within the given limits, by optimally placing heat sources in a parallelepiped. Software was developed for carrying out computational experiments.

II Statement of the problem and its conservative approximation

In the domain $D=\{a\le x\le b,\ c\le y\le d,\ p\le z\le q,\ 0\le t\le T\}$, it is required to find a function $f(x,y,z,t)\ge 0$ such that for any t the linear functional

$$J\{f\}=\int_a^b\int_c^d\int_p^q f(x,y,z,t)dzdydx\to\min, \tag{1}$$

reaches a minimum and satisfies the following conditions:

$$\begin{gathered}\frac{\partial u}{\partial t}=\frac{\partial}{\partial x}\left(\chi\frac{\partial u}{\partial x}\right)+\frac{\partial}{\partial y}\left(\chi\frac{\partial u}{\partial y}\right)+\frac{\partial}{\partial z}\left(\chi\frac{\partial u}{\partial z}\right)+\\ f,\quad x\in(a,b),\ y\in(c,d),\ z\in(p,q),\ t\in(0,T],\\ u(x,y,z,0)=u_0(x,y,z),\\ u(a,y,z,t)=\mu_1(y,z,t),\quad u(b,y,z,t)=\mu_2(y,z,t),\\ u(x,c,z,t)=\mu_3(x,z,t),\quad u(x,d,z,t)=\mu_4(x,z,t),\\ u(x,y,p,t)=\mu_5(x,y,t),\quad u(x,y,q,t)=\mu_6(x,y,t),\end{gathered} \tag{2}$$

$$m(x,y,z,t)\le u(x,y,z,t)\le M(x,y,z,t),\ (x,y,z,t)\in D, \tag{3}$$

where $u=u(x,y,z,t)$ is the temperature at the point (x,y,z) of the parallelepiped at time t; $\chi=\chi(x,y,z)$ is the thermal conductivity coefficient; $u_0(x,y,z)$, $\mu_1(y,z,t)$, $\mu_2(y,z,t)$, $\mu_3(x,z,t)$, $\mu_4(x,z,t)$, $\mu_5(x,y,t)$, $\mu_6(x,y,t)$, $m(x,y,z,t)$, $M(x,y,z,t)$ are given functions. The functions $m(x,y,z,t)$ and $M(x,y,z,t)$ are the minimum and maximum temperatures defined in the domain D. $f=f(x,y,z,t)$ is the heat source defined in the space $L_2(D)$.

Let $Lu=\frac{\partial u}{\partial t}-\frac{\partial}{\partial x}\left(\chi(x,y,z)\frac{\partial u}{\partial x}\right)-\frac{\partial}{\partial y}\left(\chi(x,y,z)\frac{\partial u}{\partial y}\right)-\frac{\partial}{\partial z}\left(\chi(x,y,z)\frac{\partial u}{\partial z}\right)$. The operator L defined in $L_2(D)$ has an inverse L^{-1}. Here L^{-1} is an integral operator with a continuous kernel (Green's function). Using it, we can write problem (1)-(3) in the following form:

$$\begin{gathered}m(x,y,z,t)\le(L^{-1}f)(x,y,z,t)\le M(x,y,z,t),\\ f(\cdot,\cdot,\cdot,\cdot)\in L_2(D),\quad f(x,y,z,t)\ge 0.\end{gathered} \tag{4}$$

We will solve this problem in a complete mathematical formulation by the integro-interpolation method on a uniform grid.

Introduce in D a difference grid uniform in four variables $\overline{\omega}^{\tau}_{h_1h_2h_3}=\overline{\omega}_{h_1}\times\overline{\omega}_{h_2}\times\overline{\omega}_{h_3}\times\overline{\omega}^{\tau}=\{(x_i,y_j,z_k,t_s):\ x_i=ih_1,\ y_j=jh_2,\ z_k=kh_3,\ t_s=s\tau,\ i=\overline{0,N_1},\ j=\overline{0,N_2},\ k=\overline{0,N_3},\ s=\overline{0,N_4}\}$ with steps $h_1=(b-a)/N_1,\ h_2=(d-c)/N_2,\ h_3=(q-p)/N_3,\ \tau=T/N_4$.

To obtain conservative difference schemes, we use the integro-interpolation method. To obtain a difference equation, we write an integral heat balance equation on a parallelepiped $x_{i-1/2}\le x\le x_{i+1/2}$, $y_{j-1/2}\le y\le y_{j+1/2}$, $z_{k-1/2}\le z\le z_{k+1/2}$ for time $t_s\le t\le t_{s+1}$ [16]:

$$\begin{gathered}\int_{x_{i-1/2}}^{x_{i+1/2}}\int_{y_{j-1/2}}^{y_{j+1/2}}\int_{z_{k-1/2}}^{z_{k+1/2}}(u(x,y,z,t_{s+1})-u(x,y,z,t_s))dzdydx=\\ \int_{t_s}^{t_{s+1}}\int_{y_{j-1/2}}^{y_{j+1/2}}\int_{z_{k-1/2}}^{z_{k+1/2}}(W(x_{i-1/2},y,z,t)-W(x_{i+1/2},y,z,t))dzdydt+\\ \int_{t_s}^{t_{s+1}}\int_{x_{i-1/2}}^{x_{i+1/2}}\int_{z_{k-1/2}}^{z_{k+1/2}}(W(x,y_{j-1/2},z,t)-W(x,y_{j+1/2},z,t))dzdxdt+\\ \int_{t_s}^{t_{s+1}}\int_{x_{i-1/2}}^{x_{i+1/2}}\int_{y_{j-1/2}}^{y_{j+1/2}}(W(x,y,z_{k-1/2},t)-W(x,y,z_{k+1/2},t))dydxdt+\\ \int_{t_s}^{t_{s+1}}\int_{x_{i-1/2}}^{x_{i+1/2}}\int_{y_{j-1/2}}^{y_{j+1/2}}\int_{z_{k-1/2}}^{z_{k+1/2}}f(x,y,z,t)dzdydxdt.\end{gathered}$$

Here $W(x,y,z,t)$ is the heat flux, $W(x,y,z,t)=-\chi(x,y,z)\,\mathrm{grad}\,u$.

We approximate the integrals included in the balance equation by approximate formulas

$$\int_{x_{i-1/2}}^{x_{i+1/2}}\int_{y_{j-1/2}}^{y_{j+1/2}}\int_{z_{k-1/2}}^{z_{k+1/2}}u(x,y,z,t_{s+1})dzdydx\approx h_1h_2h_3u^{s+1}_{ijk},$$

$$\int_{t_s}^{t_{s+1}}\int_{y_{j-1/2}}^{y_{j+1/2}}\int_{z_{k-1/2}}^{z_{k+1/2}}W(x_{i-1/2},y,z,t)dzdydt\approx\tau h_2h_3W^{s+1}_{i-1/2jk},$$

$$\int_{t_s}^{t_{s+1}}\int_{x_{i-1/2}}^{x_{i+1/2}}\int_{z_{k-1/2}}^{z_{k+1/2}}W(x,y_{j-1/2},z,t)dzdxdt\approx\tau h_1h_3W^{s+1}_{ij-1/2k},$$

$$\int_{t_s}^{t_{s+1}}\int_{x_{i-1/2}}^{x_{i+1/2}}\int_{y_{j-1/2}}^{y_{j+1/2}} W(x,y,z_{k-1/2},t)dydxdt \approx \tau h_1 h_2 W^{s+1}_{ijk-1/2},$$

$$\int_{t_s}^{t_{s+1}}\int_{x_{i-1/2}}^{x_{i+1/2}}\int_{y_{j-1/2}}^{y_{j+1/2}}\int_{z_{k-1/2}}^{z_{k+1/2}} f(x,y,z,t)dzdydxdt \approx \tau h_1 h_2 h_3 f^{s+1}_{ijk},$$

$$W^{s+1}_{i-1/2jk} = -\chi_{i-1/2jk}\frac{u^{s+1}_{ijk}-u^{s+1}_{i-1jk}}{h_1},$$

$$W^{s+1}_{ij-1/2k} = -\chi_{ij-1/2k}\frac{u^{s+1}_{ijk}-u^{s+1}_{ij-1k}}{h_2},$$

$$W^{s+1}_{ijk-1/2} = -\chi_{ijk-1/2}\frac{u^{s+1}_{ijk}-u^{s+1}_{ijk-1}}{h_3}.$$

In this case, $\chi_{i-1/2jk}$, $\chi_{ij-1/2k}$, $\chi_{ijk-1/2}$ and f^{s+1}_{ijk} are defined by the equalities

$$\chi_{i-1/2jk} = \chi\left(\frac{x_i+x_{i-1}}{2}, y_j, z_k\right),$$

$$\chi_{ij-1/2k} = \chi\left(x_i, \frac{y_j+y_{j-1}}{2}, z_k\right),$$

$$\chi_{ijk-1/2} = \chi\left(x_i, y_j, \frac{z_k+z_{k-1}}{2}\right),$$

$$\chi_{ijk} = \chi(x_i,y_j,z_k), \quad f^{s+1}_{ijk} = f(x_i,y_j,z_k,t_{s+1}).$$

The implicit conservative difference scheme for problem (2) has the form:

$$\begin{cases} \frac{u^{s+1}_{ijk}-u^s_{ijk}}{\tau} = \left[\chi_{i+1/2jk}\frac{u^{s+1}_{i+1jk}-u^{s+1}_{ijk}}{h_1^2} - \right. \\ \left. \chi_{i-1/2jk}\frac{u^{s+1}_{ijk}-u^{s+1}_{i-1jk}}{h_1^2}\right] + \left[\chi_{ij+1/2k}\frac{u^{s+1}_{ij+1k}-u^{s+1}_{ijk}}{h_2^2} - \right. \\ \left. \chi_{ij-1/2k}\frac{u^{s+1}_{ijk}-u^{s+1}_{ij-1k}}{h_2^2}\right] + \left[\chi_{ijk+1/2}\frac{u^{s+1}_{ijk+1}-u^{s+1}_{ijk}}{h_3^2} - \right. \\ \left. \chi_{ijk-1/2}\frac{u^{s+1}_{ijk}-u^{s+1}_{ijk-1}}{h_3^2}\right] + f^{s+1}_{ijk},\ i=\overline{1,N_1-1}, \\ j=\overline{1,N_2-1},\ k=\overline{1,N_3-1},\ s=\overline{0,N_4-1}, \\ u^0_{ijk} = u_0(x_i,y_j,z_k), \\ u^{s+1}_{0jk} = \mu_1(y_j,z_k,t_{s+1}),\ u^{s+1}_{N_1jk} = \mu_2(y_j,z_k,t_{s+1}), \\ u^{s+1}_{i0k} = \mu_3(x_i,z_k,t_{s+1}),\ u^{s+1}_{iN_2k} = \mu_4(x_i,z_k,t_{s+1}), \\ u^{s+1}_{ij0} = \mu_5(x_i,y_j,t_{s+1}),\ u^{s+1}_{ijN_3} = \mu_6(x_i,y_j,t_{s+1}), \\ i=\overline{0,N_1},\ j=\overline{0,N_2},\ k=\overline{0,N_3},\ s=\overline{0,N_4-1}. \end{cases} \tag{5}$$

Let us introduce the notation

$$\overline{XYZ} = \left(\frac{1}{\tau} + \frac{\chi_{i\pm1/2jk}}{h_1^2} + \frac{\chi_{ij\pm1/2k}}{h_2^2} + \frac{\chi_{ijk\pm1/2}}{h_3^2}\right),$$

$$X^+ = -\frac{\chi_{i+1/2jk}}{h_1^2}, \quad X^- = -\frac{\chi_{i-1/2jk}}{h_1^2}, \quad Y^+ = -\frac{\chi_{ij+1/2k}}{h_2^2},$$

$$Y^- = -\frac{\chi_{ij-1/2k}}{h_2^2}, \quad Z^+ = -\frac{\chi_{ijk+1/2}}{h_3^2}, \quad Z^- = -\frac{\chi_{ijk-1/2}}{h_3^2}.$$

Consider the matrix

$$A = \begin{bmatrix} \overline{XYZ} & Z^+ & 0 & \dots & 0 & Y^+ & 0 & \dots & 0 & X^+ & 0 & \dots & \dots & 0 \\ Z^- & \overline{XYZ} & Z^+ & 0 & \dots & 0 & Y^+ & 0 & \dots & 0 & X^+ & 0 & \dots & 0 \\ \dots & \dots & \dots & \dots & \dots & \dots & \dots & \dots & \dots & \dots & \dots & \dots & \dots & \dots \\ 0 & \dots & 0 & X^- & 0 & \dots & 0 & Y^- & 0 & \dots & 0 & Z^- & \overline{XYZ} & Z^+ \\ 0 & \dots & \dots & 0 & X^- & 0 & \dots & 0 & Y^- & 0 & \dots & 0 & Z^- & \overline{XYZ} \end{bmatrix}.$$

We get

$$G = A^{-1}.$$

We approximate problem (1)-(5) in the form of a linear programming problem. We divide the region D by x,y,z,t into N_1, N_2, N_3, N_4 equal parts, respectively: $D = \bigcup_{s=1}^{N_4}\bigcup_{i=1}^{N_1}\bigcup_{j=1}^{N_2}\bigcup_{k=1}^{N_3} D^s_{ijk}$, where $D^s_{ijk} = \{(x,y,z,t),\ x_{i-1}\le x\le x_i,$ $y_{j-1}\le y\le y_j,\ z_{k-1}\le z\le z_k,\ t_{s-1}\le t\le t_s\}$, $i=\overline{1,N_1}$, $j=\overline{1,N_2}$, $k=\overline{1,N_3}$, $s=\overline{1,N_4}$. In the space $L_2(D)$, the functions $f(x,y,z,t) = f^s_{ijk}$, $(x,y,z,t)\in D^s_{ijk}$ $(i=\overline{1,N_1-1}$, $j=\overline{1,N_2-1}$, $k=\overline{1,N_3-1}$, $s=\overline{1,N_4})$ are defined as piecewise constant functions. From here we get $f(x,y,z,t)\approx \sum_{s=1}^{N_4}\sum_{i=1}^{N_1-1}\sum_{j=1}^{N_2-1}\sum_{k=1}^{N_3-1} f^s_{ijk}$.

Let $g_{rw}=G$, $m^s_{ijk}=m(x_i,y_j,z_k,t_s)$, $M^s_{ijk}=M(x_i,y_j,z_k,t_s)$, $\tilde{f}^s_w = f^s_{ijk}$, $r=w$, $w=(i-1)(N_2-1)(N_3-1)+(j-1)(N_3-1)+k$, $N=(N_1-1)(N_2-1)(N_3-1)$, $r=\overline{1,N}$, $i=\overline{1,N_1-1}$, $j=\overline{1,N_2-1}$, $k=\overline{1,N_3-1}$, $s=\overline{1,N_4}$. We substitute the expression $f(x,y,z,t)$ into (1) and replace inequality (4) with grid functions.

After that, we get the following linear programming problem:

$$\begin{gathered} J_s\{f\} = \sum_{i=1}^{N_1-1}\sum_{j=1}^{N_2-1}\sum_{k=1}^{N_3-1}(\text{mes}D^s_{ijk})f^s_{ijk}\to\min, \\ m^s_{ijk}\le\sum_{w=1}^{N} g_{rw}\tilde{f}^s_w\le M^s_{ijk}, \quad r=1,2,...,N, \\ i=\overline{1,N_1-1},\ j=\overline{1,N_2-1},\ k=\overline{1,N_3-1},\ s=\overline{1,N_4}, \\ \tilde{f}^s_w\ge 0, \quad w=1,2,...,N,\ s=1,2,...,N_4. \end{gathered} \tag{6}$$

Problem (6) is solved by the big M method [17, 18]. The numerical solution of problem (2) is found using $u^s_{ijk} = \sum_{w=1}^{N} g_{rw}\tilde{f}^s_w$. The found $\tilde{f}^s_w$ is a function that gives a minimum to the functional (1).

III Description of the algorithm and modeling results

For an approximate solution of problem (1)-(6), software in the *C#* language has been developed. It allows you to represent all the necessary input data: constants, coefficients, grid parameters, as well as temperature functions, initial and boundary conditions, in the form of scripts. Graphical modules have been developed to present the results.

The flowchart (Fig. 1) shows a general algorithm for the numerical solution of the non-stationary problem of controlling the optimal location of heat sources.

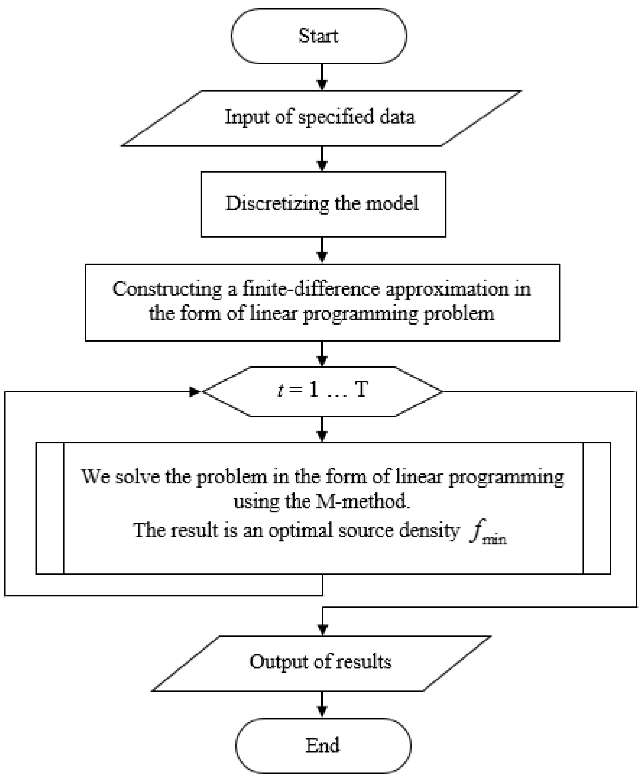

Fig. 1: Flowchart of the general algorithm for solving the problem

Computational experiment. Find the optimal location of heat sources with the minimum power cubed. The problem was solved with the following values of input parameters: $x, y, z \in [0, 1]$, thermal diffusivity $\chi(x,y,z) = x^2y^2z^2$ m^2/s, the initial and boundary conditions are determined by the functions: $u_0(x,y,z) = 2+x^2+y^2+z^2$ m/s, $\mu_1(y,z,t) = 2+y^2+z^2+t^2$ m/s, $\mu_2(y,z,t) = 3+y^2+z^2+t^2$ m/s, $\mu_3(x,z,t) = 2+x^2+z^2+t^2$ m/s, $\mu_4(x,z,t) = 3+x^2+z^2+t^2$ m/s, $\mu_5(x,y,t) = 2+x^2+y^2+t^2$ m/s, $\mu_6(x,y,t) = 3+x^2+y^2+t^2$ m/s, the minimum and maximum temperatures are given by the functions $m(x,y,z,t) = 1+x^2+y^2+z^2+t^2$ K, $M(x,y,z,t) = 4+x^2+y^2+z^2+t^2$ K, end of time $T = 1$. Computational grid with the number of sources $(N_1-1)\times(N_2-1)\times(N_3-1)\times N_4 = 6\times6\times6\times7$. The minimum value of the functional in the numerical solution is $J_{min} = 14.35$ K·m/s. On fig. 2 presents the results of the numerical solution of problem (6). Results are shown with minimum (borders in blue, below), maximum (borders in red, above), and approximate (green, middle) temperature values. On fig. 3 shows the optimal location of heat sources with a minimum power in the form of a bar graph.

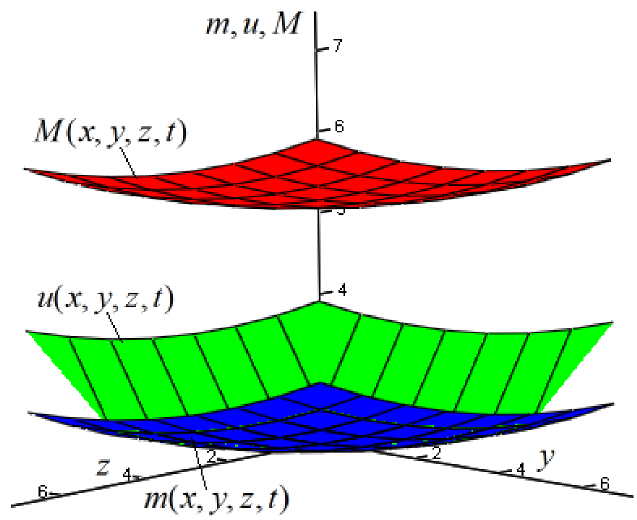

Fig. 2: Graph of the solution of problem (6) at $x = 0.5$, $t = T$

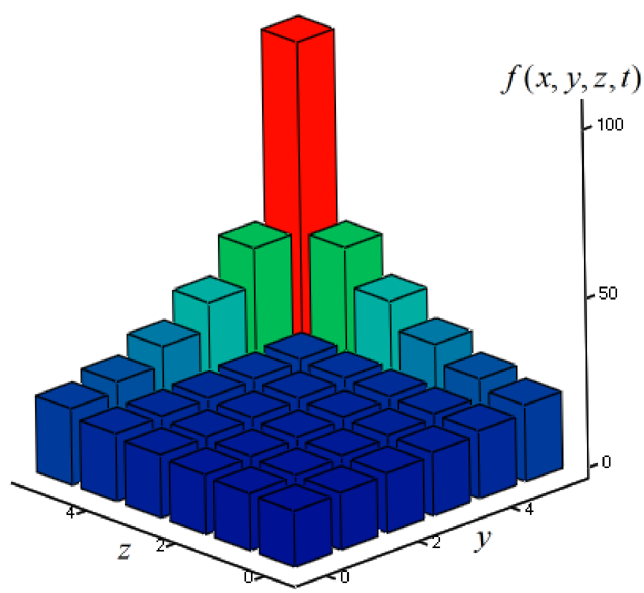

Fig. 3: Optimal placement of heat sources $f(x,y,z,t)$ at $x = 0.5$, $t = T$

IV CONCLUSION

As you know, the construction of the Green's function for problems in partial derivatives, in fact, means finding a solution in an explicit form. When applying numerical methods, the values of the Green's function are presented in the form of a matrix, which is inverse to the matrix composed of the coefficients of the system of linear algebraic equations. Thus, it is possible to indicate the values of the desired function at the nodal points of the partition. After substituting these values for the conditions-restrictions of body temperature, taking into account finding the extremum of the functional, a linear programming problem is obtained, for the solution of which the standard algorithm big M method is used. A technique and algorithm for solving the non-stationary problem of ensuring the temperature inside the region within the given limits by optimal placement of heat sources in a parallelepiped are proposed. The results of this computational experiment show that the functional reaches its minimum.

REFERENCES

[1] A.G. Butkovskii. Nauka, Moscow, 1975.

[2] Lions Zh.L. Lattes, R. Mir, Moscow, 1970.

[3] Yu.V. Egorov. Some problems in the theory of optimal control. *U.S.S.R. Comput. Math. Math. Phys.*, 3(5):1209–1232, 1963.

[4] A.I. Egorov. Nauka, Moscow, 1978.

[5] Znamenskaya L.N. Egorov, A.I. Control of a heat conduction process with a quadratic cost functional. *Comput. Math. Math. Phys.*, 57(12):1209–1232, 2017.

[6] Abduolimova G.M. Khayitkulov B.Kh. Tukhtasinov, M.T. Boundary control of heat propagation in a bounded body. *Bulletin of the Institute of Mathematics*, (1):1–10, 2019.

[7] Kogan Yu.V. Islamov, G.G. The difference-differential problem of control by diffusion process. *The Bulletin of Udmurt University. Mathematics. Mechanics. Computer Science*, (1):121–126, 2008.

[8] Kulibanov V.N. Akhmetzyanov, A.V. Optimal placement of sources for stationary scalar fields. *Automation and telemechanics*, (6):50–58, 1999.

[9] Brusentsev A.G. Osipov, O.V. Optimal location of heat sources inside areas with complex geometric shapes. *Mathematical Models and Computer Simulations*, 11(6):905–913, 2019.

[10] V.B. Kryzhanivskyy. Optimization of placement of discrete sources of physical field described by mixed boundary problem. *Electronic Modeling*, 36(5):81–93, 2014.

[11] B.Kh. Khayitkulov. Conservative difference schemes for the optimal selection of the location of heat sources in the rod. *Mathematical Modeling and Computational Methods*, (3):85–98, 2020.

[12] Khaitkulov B. Kh. Homogeneous different schemes of the problem for optimum selection of the location of heat sources in a rectangular body. *Solid State Technology*, 63(4):583–592, 2020.

[13] B.Kh. Khayitkulov. Finite-difference method for solving non-stationary problems of convection-diffusion control. *Vestnik Tomskogo gosudarstvennogo universiteta. Upravlenie vychislitelnaja tehnika i informatika*, (57):45–52, 2021.

[14] Sidelnikov V.I. Mirskaya, S.Yu. Efficient heating of the room as the optimal control problem. *Technical and technological problems of service*, 30(4):75–78, 2014.

[15] Baitasov T.M. Sabdenov, K.O. Optimal (energy efficient) heat supply to buildings in central heating system. *Bulletin of the Tomsk Polytechnic University. Geo Assets Engineering*, 326(8):53–60, 2015.

[16] Samarskii A.A. Tikhonov, A.N. Nauka, Moscow, 2004.

[17] G.B. Dantzig. Princeton University Press, Princeton, 2016.

[18] Ivanitskii A.Yu. Vasilev, F.P. Faktorial, Moscow, 1998.

Acta of Turin Polytechnic University in Tashkent, 2022, 31, 19-23
Published Online March 2022 in Acta TTPU (http://www.acta.polito.uz/)

LTE NETWORK RELIABILITY ASSESSMENT MODELS AND ANALYTICAL EXPRESSIONS

Davronbekov D.A.[1], Matyokubov U.K.[2] * and Matqurbanov T.A.[3]
Tashkent University of Information Technologies named after Muhammad al-Khwarizmi[1]
Urgench branch of Tashkent University of Information Technologies named after Muhammad al-Khwarizmi[2 3]
*Corresponding author email: otkir_ matyokubov89@mail.ru

Abstract– Broadband networks, especially Long-Term Evolution (LTE)/LTE Advanced (LTE-A), are in high demand due to their high-speed wireless data transmission, the coverage of the base stations used, and the complexity of the protocol software. In such cases, the efficiency of the network depends mainly on two important features, which are the reliability and viability of the network. The LTE architecture and network structure should be taken into account to improve reliability and viability. This paper develops reliability assessment models based on the structure architecture of LTE/LTE-A networks. Analytical expressions of reliability assessment based on the developed models are given. In addition, the LTE network is digitally analyzed using these models and analytical expressions.

Key words– LTE/LTE-A networks, reliability, viability, reliability assessment model.

I Introduction

The advantages of Long-Term Evolution (LTE) and LTE Advanced (LTE-A) technologies are high-speed data transmission, spectral efficiency, and low latency [1]. However, factors such as changes in antenna position, software errors, and changes in the environment, hardware and software failures, and power outages are among the causes of network inefficiency [2]. Improving network reliability and viability in the LTE/LTE-A network, as in all modern systems today, is a key requirement. Understanding the LTE architecture and defining the network structure is important in determining these indicators [3, 4]. [5] presents an analytical model for analyzing the performance of the VANET system for LTE mobile networks. [6] discusses an architecture-based approach to assessing the reliability of software components. This article discusses the processes of component failure, repair, and replacement to analyze the reliability of LTE/LTE-A networks. For LTE/LTE-A networks, reliability attributes such as reliability, availability, and viability were analyzed.

II Materials and Methods

LTE architecture. The LTE network is an Internet Protocol (IP) based network that effectively supports packet transmission. The structure of the LTE architecture is shown in Fig. 1.

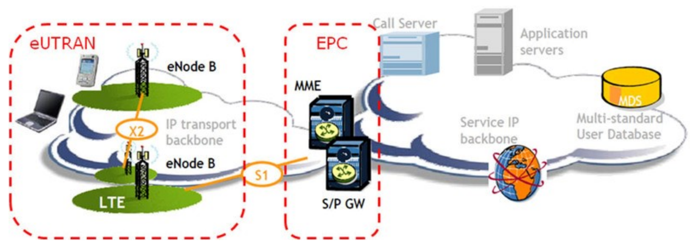

Fig. 1: LTE architecture structure

The LTE system architecture is divided into two parts:

- Evolved Universal Terminal Radio Access Network (E-UTRAN);
- Evolved Packet Core (EPC).

E-UTRAN consists of the following components:

- User equipment (UE). The main function of the UE is to save, add and delete connections, configure the network according to the needs of users;
- NodeB (eNB). eNB is a base station that controls all functions related to radio communication. eNB is distributed across network coverage;
- Mobile main network (Evolved Packet Core - EPC).

Its main functions are to manage mobility and provide security. It consists of the following components:

1. Service Gateway (S-GW). S-GW performs the function of general routing of packets.

2. Mobile Management Entity (MME). Responsible for signaling processes between UE and S-GW.

3. Home Subscriber Server (Mobile Management Entity - HSS).

4. Packet Data Network (PDN) gateway (P-GW). A gateway connects the UE to external packet data networks such as the Internet and IMS4.

To fully describe the reliability attributes of an LTE system, it is important to consider reliability, availability, and viability models simultaneously. To study the reliability attributes based on the LTE architecture, it is necessary to analyze the following features of the system:

- Software architecture;
- Equipment architecture;
- Failure and repair process.

In this study, component failure is considered in terms of reliability or failure rate, the failure of all components is considered independent of each other, and the failure rate and repair rate of the same type of components are the same.

Here are some definitions of the concepts used in the work. Reliability is the ability of a component or network to perform a set of functions under certain conditions for a specific operating time. Mathematically, reliability can be expressed as the probability that a component or system failure time is greater than or equal to the specified time (t):

$$R(t) = P[T \geq t] \quad (1)$$

To model the reliability of the system, it is necessary to determine the probability of failure of components and the state of interconnection of system components [14-16].

Survival is the ability of system components to perform their functions at any time under certain conditions.

We express viability through the following function:

$$X(t) = \begin{cases} 1, & t - time \quad system \quad functions \\ 0, & otherwise \end{cases} \quad (2)$$

In $t > 0$, existence is represented by $A(t)$:

$$A(t) = Pr[X(t) = 1] = E[X(t)]. \quad (3)$$

III Results and Discussions

Defects occur in the LTE system due to the implementation of the handover process, connection errors, failure to ensure uninterrupted power supply [7, 8], and component failure [17-19] [9-13].

The LTE network system consists of two main parts: E-UTRAN and EPC. E-UTRAN consists of eNBs connected to each other via an X2 interface. Each eNB consists of up to three RRHs (Radio Heads) and one BBU (Baseband Unit). RRH is used to transmit and receive wireless signals. The simple structural structure of eNB is shown in Fig. 2 and the relationship between RRH and BBU is shown in Fig. 3.

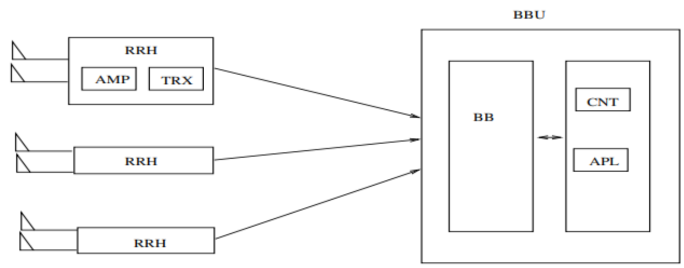

Fig. 2: The simple structural structure of eNB

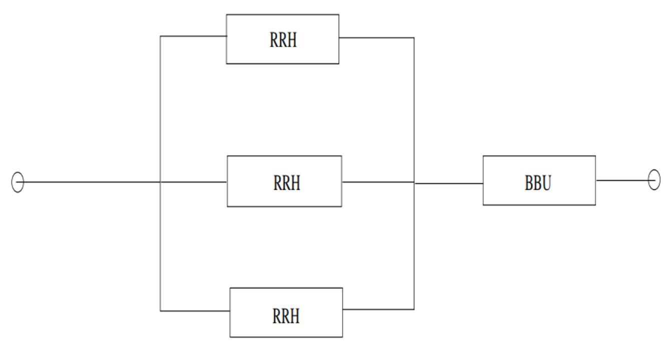

Fig. 3: Structural model of connection of elements on reliability of RRH and BBU system

The total reliability value of the eNB system shown in Fig. 3 is determined by the following expression:

$$R_{eNB}(t) = [1 - [1 - R_{RRH}(t) \cdot R_{BBU}(t)]] =$$
$$= [1 - [1 - e^{(-\lambda_{RRH} \cdot t)}]^3] \cdot e^{(-\lambda_{BBU} \cdot t)}. \quad (4)$$

Here $R_{RRH}(t)$ – is the reliability of RRH, $R_{BBU}(t)$ – is the reliability of BBU, λ_{RRH} – is the failure rate of RRH, λ_{BBU} – BBU is the failure rate of BBU.

EPC (Enveloped Packet Core) consists of MME, S-GW and P-GW. These components can be interconnected in various combinations:

- The relationship between MME, S-GW as a single component and P-GW as a separate component. This connection is especially useful on 3G networks;
- Bind MME, S-GW and P-GW as separate components. Fig. 4 shows a structural model of the connection of the elements of the system under consideration for this case in terms of reliability.

Fig. 4: Structural model of element connection of MME, S-GW and P-GW in terms of reliability

We enter the following definitions and determine the reliability of the system in Fig. 4 using formula (5). In this case, $R_{MME}(t)$ – MME reliability, $R_{(S-GW)}(t)$ – S-GW reliability, $R_{(P-GW)}(t)$ – P-GW reliability, λ_{MME} – MME failure intensity, $\lambda_{(S-GW)}$ – S-GW failure intensity and $\lambda_{(P-GW)}$ – P-GW failure intensity.

$$R_{ePG}(t) = R_{MME}(t) \cdot R_{S-GW}(t) \cdot R_{P-GW}(t) = \\ = e^{(-\lambda_{MME} \cdot t)} \cdot e^{(-\lambda_{S-GW} \cdot t)} \cdot e^{(-\lambda_{P-GW} \cdot t)}. \quad (5)$$

The reliability of an LTE network depends on the likelihood that the network will support the required functions in the event of a random component failure. Communication between eNBs is important for the reliability of the LTE network.

The viability of an LTE network is the total network bandwidth available to route traffic.

If we assume that all eNBs are the same and their faults differ from each other, the reliability of the LTE network depends on the number of eNBs. Therefore, the more eNBs in a network, the more reliable the network is.

The reliability of an LTE network connected on the basis of a mesh topology, consisting of K eNBs and in the K/2 eNB state, is determined by expression (6).

$$R_{network}(t) = [1 - [1 - (R_{eNB}(t))^2]^{\frac{K}{2}}] = \\ [1 - [1 - e^{(-2\lambda_{eNB} \cdot t)}]^{\frac{K}{2}}] \quad (6)$$

The average LTE network downtime (MTTF) (7) and network downtime (8) are determined by the expressions:

$$MTTF_{network} = \int_0^\infty R_{network}(t)dt \quad (7)$$

$$\lambda_{network} = \frac{1}{MTTF_{network}} \quad (8)$$

IV CONCLUSION

The reliability of the eNB and LTE / LTE-A network is shown in Fig. 5 and Fig. 6, respectively. These results were obtained on the basis of expressions (4) and (6).

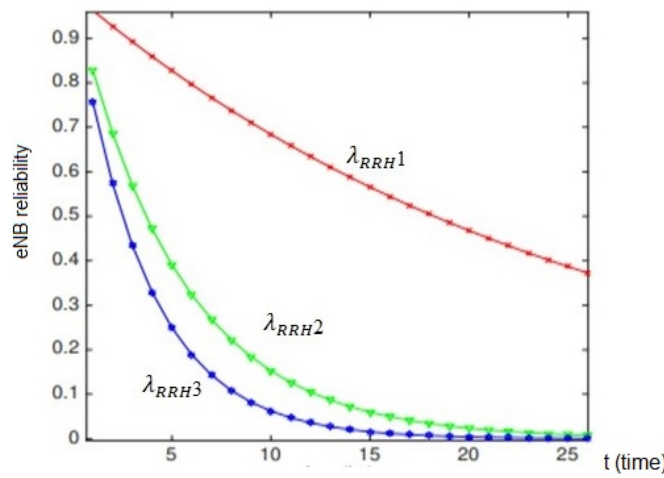

Fig. 5: eNB reliability

$$\lambda_{BBU} = 0.008\frac{1}{hour}, \quad \lambda_{RRH1} = 0.01\frac{1}{hour},$$
$$\lambda_{RRH2} = 0.06\frac{1}{hour}, \quad \lambda_{RRH3} = 0.09\frac{1}{hour}.$$

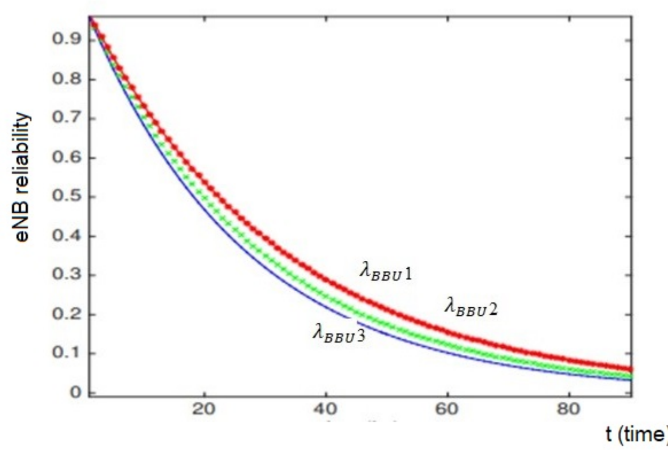

Fig. 6: eNB reliability

$$\lambda_{RRH} = 0.01\frac{1}{hour}, \quad \lambda_{BBU1} = 0.008\frac{1}{hour},$$
$$\lambda_{BBU2} = 0.005\frac{1}{hour}, \quad \lambda_{BBU3} = 0.001\frac{1}{hour}.$$

As can be seen from Fig. 5 and Fig. 6, the reliability of eNB decreases at different values of λ_{RRH} and λ_{BBU} over time.

As can be seen from Fig. 7 and Fig. 8, the reliability decreases as the component failure rate increases. It should be noted that the reliability of the LTE / LTE-A network is significantly affected by changes in the failure rate of the eNB component.

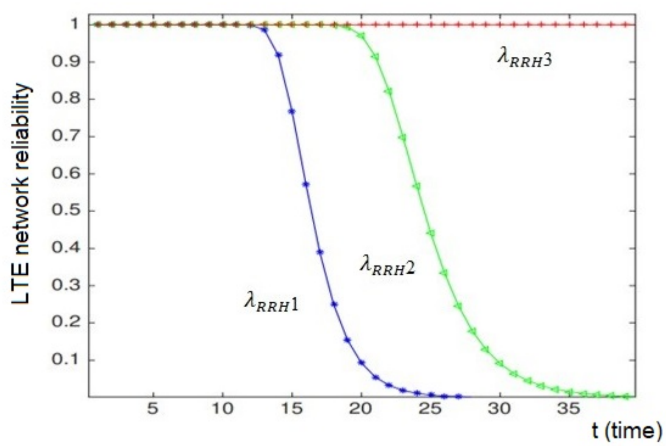

Fig. 7: LTE network reliability

$$\lambda_{BBU} = 0.008\frac{1}{hour}, \quad \lambda_{RRH1} = 0.09\frac{1}{hour},$$
$$\lambda_{RRH2} = 0.06\frac{1}{hour}, \quad \lambda_{RRH3} = 0.01\frac{1}{hour}.$$

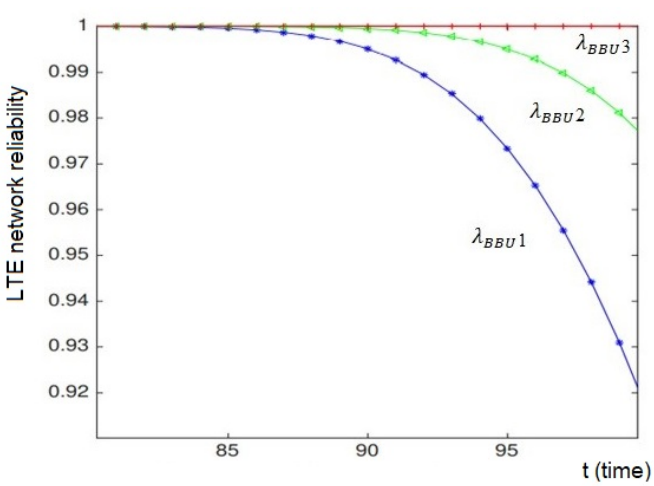

Fig. 8: LTE network reliability

$$\lambda_{RRH} = 0.01\frac{1}{hour}, \quad \lambda_{BBU1} = 0.008\frac{1}{hour},$$
$$\lambda_{BBH2} = 0.005\frac{1}{hour}, \quad \lambda_{BBH3} = 0.001\frac{1}{hour}.$$

V References

[1] I. F. Akyildiz, D. M. Gutierrez-Estevez, E.C. Reyes,“The evolution to 4G cellular systems: LTE-Advanced”, Physical Communication, 3(4), 217-244 (2010).

[2] D. Wu, J. Eilert, R. Asghar, D. Liu, A. Nilsson, E. Tell and E. Alfredsson,“ System architecture for 3GPP-LTE modem using a programmable baseband processor”. International Journal of Embedded and Real-Time Communication Systems (IJERTCS), 1(3), 44-64 (2010).

[3] A. Saxena and R. Sindal, “LTE channel throughput assessment and comparison under different terrain”, International Journal of Communication Systems, 31(10), *doi:https://doi.org/10.1002/dac.3586* (2018).

[4] I. Ahmad, R. Md Noor, and M. Reza Z0 aba, “LTE efficiency when used in traffic information systems: A stable interest aware clustering”, International Journal of Communication Systems, 32(2), *doi: https://doi.org/10.1002/dac.3853* (2019).

[5] W. Li, M. A. Xiaomin, J. Wu, K. S. Trivedi, X.L. Huang, Q. Liu,“Analytical model and performance evaluation of long term evolution for vehicle safety services”, IEEE Transactions on Vehicular Technology, 66(3), 1926-1939 (2017).

[6] K. Goseva-Popstojanova, K. S. Trivedi, “Architecture-based approach to reliability assessment of software systems”. Performance Evaluation, 45(2), 179-204 (2001).

[7] Matyokubov U. K. and Davronbekov D.A., (2021) "Calculate the reliability of the BTS-BSC network with the reserved line connection," Chemical Technology, Control and Management: Vol. 2021: Iss.1, Article11. *doi: https://doi.org/10.34920/2021.1.76-84*.

[8] Matyokubov U. K. and Davronbekov D.A., (2021) "The use of supercapacitors to stabilize the power supply system of the base station of mobile communication" Scientific-technical journal: Vol. 25: Iss.1, Article 1.

[9] Matyokubov U. K. and Davronbekov D.A., and Abdullaeva M.I., “Evaluation of reliability indicators of mobile communication system bases”, Bulletin of TUIT: Management and Communication Technologies, vol. 3, Article 1, 2020.

[10] Matyokubov U. K. and Davronbekov D.A., “Reliability of the BTS-BSC System with Different Types of Communication Lines Between Them”, International Journal of Advanced Trends in Computer Science and Engineering, vol. 9, no. 4, pp. 6684 – 6689, 2020.

[11] Matyokubov U. K. and Davronbekov D.A., “The effect of the number of backup communication lines in the BTS-BSC system on reliability”, Scientific Collection «InterConf», №40. Proceedings of the 2nd International Scientific and Practical Conference «Scientific community: interdisciplinary research», January 26-28, 2021, Hamburg, Germany: 2021, pp. 679-684, 2021.

[12] Matyokubov U. K. and Davronbekov D.A., “The Impact of Mobile Communication Power Supply Systems on Communication Reliability and Viability and Their Solutions”, International Journal of Advanced Science and Technology. vol. 29, no. 5, pp. 3374 – 3385, 2020.

[13] Matyokubov U. K. and Davronbekov D.A., “Approaches to the organization of disaster resistant mobile network architecture in Uzbekistan”, Acta of Turin Polytechnic University in Tashkent, no. 10(2):10, pp. 34-42, 2020.

[14] Matyokubov U. K. and Davronbekov D.A., “Increasing energy efficiency of base stations in mobile communication systems”, Acta of Turin Polytechnic University in Tashkent, no. 10(1):19, pp. 22-27, 2020.

[15] Matyokubov U. K. and Davronbekov D.A., “Some issues of improving the survivability of mobile communication systems in emergency situations”, Central Asian Problems of Modern Science and Education, no.3, pp. 197-215, 2020.

[16] Davronbekov D.A. and Matyokubov U.K., “The role of network components in improving the reliability and survivability of mobile communication networks”, Acta of Turin Polytechnic University in Tashkent, no.10(3):2, pp. 7-14, 2020.

[17] Davronbekov D.A. and Matyokubov U.K., “Mobil aloqa tizimi elementlaridagi buzilishlarni prognozlash orqali tizim yashovchanligini oshirish”, Muhammad al-Xorazmiy avlodlari, no.1, pp.85-89, 2020.

[18] Davronbekov D.A. and Matyokubov U.K., “Telekommunikasiya tarmoqlari yashovchanligini ta’minlashning ba’zi masalalari”, Axborot-kommunikasiyalar: tarmoqlar, texnologiyalar, yechimlar, vol. (54) 2020, no.2, pp. 25-32, 2020.

[19] Matyokubov U.K., Mobil aloqa tizimlari ishonchliligini baholash model va algoritmlarini ishlab chiqish // texnika fanlari bo’yicha falsafa doktori darajasini olish uchun dissertatsiya, Toshkent, 2021.

Acta of Turin Polytechnic University in Tashkent, 2022, 31, 24-27
Published Online March 2022 in Acta TTPU (http://www.acta.polito.uz/)

NEURAL NETWORKS PERFORMANCE IMPROVEMENT WITH GAUSSIAN WHITE NOISE AUGMENTATION

Abdurashitova Muniskhon
Department of Control and Computer Engineering, Turin Polytechnic University in Tashkent, Uzbekistan
Email: abdurashitova.munisxon@gmail.com

Abstract– Data augmentation is a strategy for creating synthetic data from existing data by adding slightly changed copies of current data to expand the amount of available data. When training a machine learning model, it functions as a regularizer and helps to reduce overfitting. This work will discuss the improved neural network performance with the data augmentation method employing Gaussian white noise.

Key words– Gaussian White Noise, Neural Networks, Data Augmentation Techniques

I OBJECTIVE

Training neural network models on additional data can enhance their capacity to generalize what they have learned to new data. Augmentation techniques can provide variations of datasets that can improve the fit models' ability to generalize what they've learned to new unseen data. We will use data augmentation strategies to improve model inference generalization robustness when training neural networks in this paper.

II INTRODUCTION

Data augmentation refers to a set of strategies for creating new training samples from existing ones by introducing random variations and disturbances, ensuring that the data is not destroyed. Our purpose is to boost the model generalizability using data augmentation. We discuss the generation of augmented sets with the addition of Gaussian white noise to original data. We are exploring human indoor localization in a restricted area because it is trendy in the fields like energy management, health monitoring, and security. The purpose is to explore cheap but efficient techniques for indoor localization because for outdoors person tracking, there exists GPS technology that can quickly determine a person location through the wearable tag or cell phone. At home or inside a room, a person is not always carrying a phone; that is why we should search approaches for tagless localization. Four sets of experimental data are collected in a 3x3 meter room for a short period. A 4x4 pixel Omron D6T-44L-06 thermopile infrared sensor is installed on the ceiling of a room, and the person reference location is collected with an ultrasound-based tag of the Marvelmind Starter Set HW v4.9. Each tuple of experimental data has 18 elements: 16 pixels of the infrared sensor (IR) plus the X and Y coordinates of the person representing the label.

III MAIN PART

The first set of experimental data is used for the model training in a 60/20/20 ratio representing training/validation/test sets. The other three sets are used only for inference because our purpose is to improve the model generalization, which refers to model performance for unseen data. Since the amount of training data is small, we generate synthetic data by adding Gaussian white noise. Noise has a normal distribution with zero mean and finite variance

$$f(x) = \frac{1}{\sigma\sqrt{2\pi}} e^{-\frac{1}{2}\left(\frac{x-\mu}{\sigma}\right)^2}. \quad (1)$$

Function *f(x)* is the probability density, σ is the standard deviation, μ is the mean.

Experimental analysis

For the Gaussian white noise, the standard deviation parameter allows modulating the noise amplitude. That is why the first experiment trains the model with the following values {0.01, 0.11, 0.21, 0.31, 0.41, 0.51, 0.61}. Table 1 represents the output of the model for each white noise parameter. For each white noise amplitude in the range {0.01, 0.11, 0.21, 0.31, 0.41, 0.51, 0.61}, based on the best training giving the smallest Overall_Performance, obtained MSE metrics for sets A, B, C and D are given in the table 1.

Now we can compare the model results trained on augmented data with our baseline. Let us represent the model

Noise Amplitude	MSE_A	MSE_B	MSE_C	MSE_D
Baseline	0.001565	0.040742	0.113454	0.080686
0.01	0.001904	0.037636	0.033084	0.062054
0.11	0.002187	0.055132	0.053950	0.068099
0.21	0.001810	0.052376	0.054861	0.075765
0.31	0.001577	0.055950	0.075206	0.090898
0.41	0.002161	0.070060	0.051307	0.077119
0.51	0.002728	0.068208	0.040365	0.085448
0.61	0.002427	0.076800	0.035568	0.093364

TABLE 1: MODEL TRAINING RESULTS AT DIFFERENT WHITE NOISE AMPLITUDES ARE COMPARED TO THE BASELINE. FOR EACH NOISE PARAMETER CORRESPONDING MSE METRICS FOR SETS A, B, C, D ARE SHOWN.

results in a graphical way so that we can easily extract the features. Figure 1 shows that for set A, the model behavior fluctuates in an interval. For smaller values of the noise amplitude, the model output seems to have smaller MSE values, while for higher noise values, MSE is also increasing. Overall results show that model training with augmented sets does not improve with respect to the baseline. The model shows a more coherent behavior for the set B. The MSE is steadily rising for increasing amounts of noise, showing improvements in a neighborhood of 0.01 noise standard deviation. Set C is the only one fully improved by the training with augmented data. It has smaller MSE values compared to baseline over the whole noise range. Finally, set D expresses better model improvement up to noise standard deviation 0.5 except for the peak around a point 0.3 and increasing MSE for higher noise standard deviations. Since we are interested in overall model generalization quality, we should merge all independent results of the four sets. In the noise amplitude under the exploration, all sets show different characteristics, one showing very significant improvement while others without any improvements. When we sum MSE metrics, significant improvements of one or two sets could exceed losses in other sets, so it could be a misleading point to decide as a better model generalization. To avoid these kinds of "misleading" points after generating the overall sum of MSEs, we extract the areas with smaller MSE sum values with respect to the baseline(obtained without augmentation). We should further inspect extracted areas for each set independently. If at least three sets have improvements in these intervals, we can decide that the model has improved generalization for all sets. Suppose less than three sets show more extensive improvements that surpass the unsatisfactory results of other sets. In that case, these noise intervals are not considered as a noise range with better generalization quality. Going back to our results in the figure 2, we have overall model results for all sets. It is showing improvement in a total interval of investigated noise standard deviation. However, it is not enough to decide on the improved generalization. We go back to independent plots of sets and search for the areas with more than two sets showing smaller MSEs than the baseline. It gives the range roughly around zero.

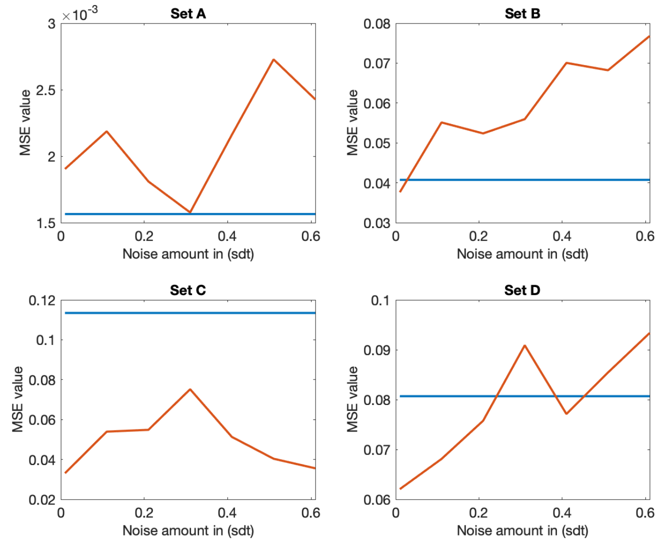

Fig. 1: Model output MSE values(red line) obtained by augmentation with white noise amplitude range [0; 0.6], for data sets A, B, C and D. Blue line represents the model MSE baseline obtained without augmented data.

We perform another experiment in the same interval, but with a higher resolution. White noise standard deviations, which are directly proportional to white noise amplitudes, are chosen as follows: {0.01 0.06 0.11 0.16 0.21 0.26 0.31 0.36 0.41 0.46 0.51 0.56 0.61}. When we analyze the results for every 30 trainings best model is chosen near to 200 epochs, which means that the model was still able to learn. According to the second experiment, model training with specified noise parameters (by performing 30 trainings for each noise value and choosing the best one) generates the following results given in Table 2. Since the resolution of the given interval is higher than the previous experiment, we can precisely extract the sections of the range with better model generalization. Let us visually analyze the model output with graphs to determine the most promising areas in Figure 3.

Mean square error loss function values for set A show smoother behavior in this experiment. MSE value is slightly higher than the baseline at the beginning of the noise range. Then it gradually decreases below the baseline, demonstrating model improvement until around 0.3. After that, it continuously increases with increasing noise amplitude. It is evident that more significant noise amounts does not help the training generate improvements for set A. Analyzing the plot of set B, we can say that set B is less resistant to noisy data

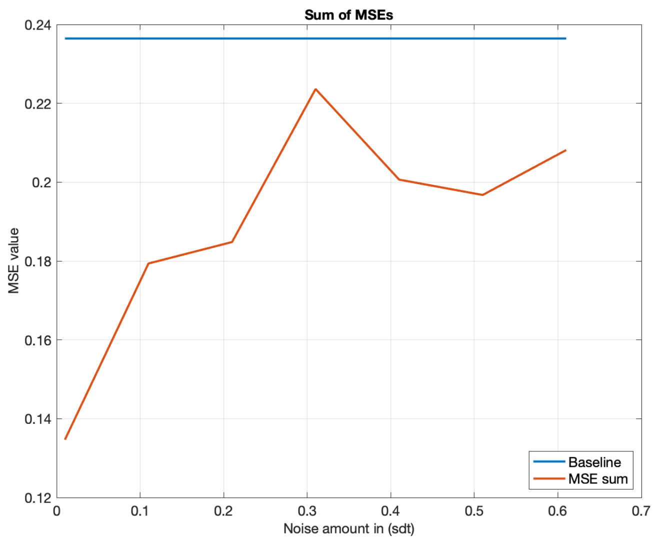

Fig. 2: The model overall inference generalization obtained by white noise augmentation.

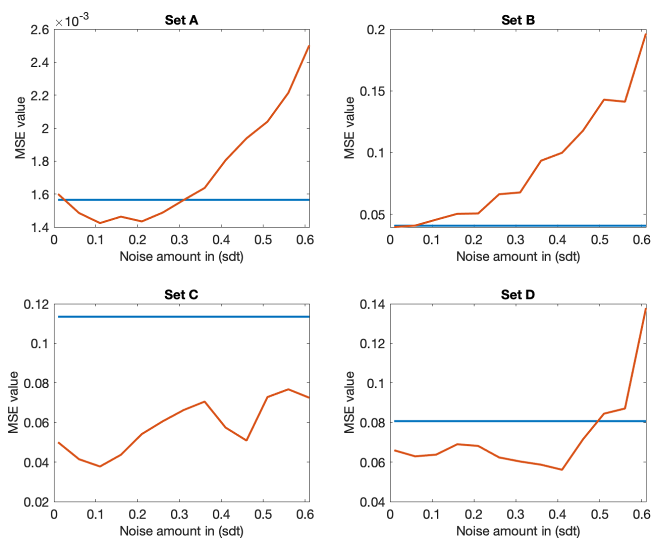

Fig. 3: The second experiment. Model output MSE values(red line) with augmented data generated in white noise amplitude range [0; 0.6], for data sets A, B, C and D. Blue line represents the model MSE baseline obtained without augmented data.

Noise Amplitude	MSE_A	MSE_B	MSE_C	MSE_D
Baseline	0.001565	0.040742	0.113454	0.080686
0.01	0.0016	0.039653	0.049996	0.065936
0.06	0.001485	0.040832	0.041435	0.062892
0.11	0.001424	0.04568	0.037765	0.063757
0.16	0.001463	0.050361	0.043676	0.069003
0.21	0.001434	0.05065	0.05417	0.068153
0.26	0.001488	0.066244	0.060627	0.062341
0.31	0.001564	0.067676	0.066316	0.06029
0.36	0.001637	0.093435	0.070558	0.05868
0.41	0.001805	0.099847	0.057439	0.056119
0.46	0.001938	0.117797	0.050876	0.071523
0.51	0.002039	0.142877	0.072843	0.084473
0.56	0.002214	0.141222	0.076763	0.087068
0.61	0.002502	0.196399	0.072507	0.137806

Table 2: Result of the model trainings at different white noise amplitudes. For each noise parameter corresponding MSE metrics for sets A, B, C, D and best training are shown.

showing slight improvement of the model for small amounts of noise approximately up to 0.05. After that point, the model MSE value starts to increase gradually as for set A. Set C has total improvement in this range, as in the previous experiment. Considering the graph of set D, we can say that we could generate more stable and understandable behavior with respect to the previous experiment. It shows model improvement in a noise range of [0; 0.5], which is the same as the initial results. After noise amplitude 0.5, the MSE starts to increase abruptly.

Now we can generate a plot to check model overall improvement. The sum of the MSE values for all sets is represented on the vertical axis in Figure 4, while on the horizontal axis, noise amplitudes are described. Overall model behavior shows a gradual MSE increase for increasing amounts of noise amplitude. Up to 0.45, MSE is below the baseline, which means the model has overall improvement. However, Figure 4 is not enough factor to decide on model generalization quality because we should further check the plots of each set to avoid points in which improvements of one or two sets are big so that it surpasses the destructive results of other sets. At the upper end of the noise interval, the overall model characteristic shows higher MSE values than the baseline, which means the model has poor performance.

IV Conclusion

The model overall generalization quality is determined both by the improved MSE sum of all sets and individual improvements of at least three sets. Based on Figure 4, it is ob-

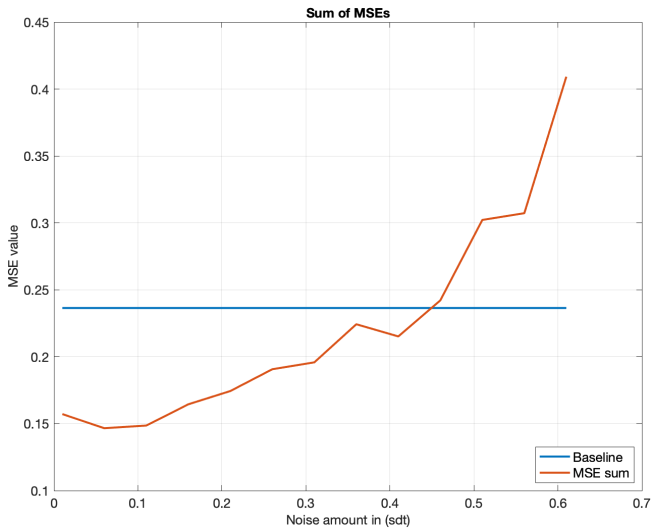

Fig. 4: The model overall inference generalization obtained by white noise augmentation (the second experiment).

vious that MSE sum is below the baseline in a noise range of [0; 0.45]. In this range sets C and D have total improvement. Fields of improvement for sets A and D are smaller than [0; 0.45]. Set A starts to go above the baseline after point 0.3, which means that we should reduce our initial range from [0; 0.45] to [0; 0.3] to have at least three sets with individual improvements. For set B, noise amounts in the range [0; 0.3] could result in MSE values above and below the baseline. However, we can accept this range as a reasonable interval giving better model generalization quality since at least sets A, C, D are performing adequately. The last experiment is accomplished to precisely determine the noise amplitude. All the sets have simultaneous improvement concerning the corresponding baselines and improved overall model generalization. We will not explicitly state the resulting table and plots here. The noise amplitude in the interval [0; 0.046] gives the best model inference generalization quality with all sets individual improvements.

REFERENCES

1. Tariq, Osama Bin and Lazarescu, Mihai Teodor and Lavagno, Luciano(2021). Neural networks for indoor person tracking with infrared sensors

2. Carter, Mancini, Bruce, Ron (2009). Op Amps for Everyone. Texas Instruments. pp. 10–11

3. https://onlinelibrary.wiley.com/doi/pdf/10.1002/9780471679370.app2

4. https://en.wikipedia.org/wiki/Whitenoise

Acta of Turin Polytechnic University in Tashkent, 2022, 31, 28-33
Published Online March 2022 in Acta TTPU (http://www.acta.polito.uz/)

ON SOME PROPERTIES OF CONTINUED FRACTIONS AND RETURN TIME FOR CIRCLE HOMEOMORPHISMS

J.J.Karimov[1], A.N.Qodiriy[2] and S.J.Jahongirov[3]
Turin Polytechnic University in Tashkent
[1]Email: jkarimov0702@gmail.com
[2]Email: abduraufqodiriy@gmail.com
[3]Email: samandarjahongirov574@gmail.com

Abstract—In present work we study general properties of continued fractions and the return times for circle homeomorphisms with irrational rotation number. Consider the set X of all orientation preserving circle homeomorphisms T with one break point and irrational rotation number. There are given proof of the main theorem for return time using visualizations and constructed example to computing return time for irrational rotation number.

Keywords—circle homeomorphism, break point, rotation number, continued fractions, return time.

I Introduction

This paper is devoted to study general properties of continued fractions and return times for circle homeomorphisms with irrational rotation number in dynamical partitions. Continued Fractions are important in many branches of mathematics. They arise naturally in long division and in the theory of approximation to real numbers by rationals. These objects that are related to number theory help us find good approximations for real life constants. In A. Khinchin's classic book on continued fractions [1], he defines two notions of being a "best approximation" to a number. The first is the easier one to describe: a fraction c/d is a best approximation to a number a if c/d is closer to a than any number with a smaller denominator. That is, if $|a-c/d| < |a-p/q|$ for any other fraction p/q where $q < d$. Khinchin calls this a *best approximation of the first kind*. The fraction c/d is a *best approximation of the second kind* for a number a if for every other fraction p/q with $q < d$, $|da-c| < |qa-p|$. It's a similar relation as the first kind, but we multiply through by the denominator on both sides. All best approximations of the second kind are best approximations of the first kind, but not all best approximations of the first kind are best approximations of the second kind. Convergents of the continued fraction for a number are best approximations of the second kind, and they're the only numbers that are best approximations of the second kind.

One of the important problems of ergodic theory is to study the behaviour of return times. D.H.Kim and B.K.Seo in [2] investigated return time and waiting time for partition Q_n of same first n digits in binary expansion, i.e. $Q_n = \{[0,2^{-n}),\dots,[1-2^{-n},1)\}$. We consider return time in more general partition, which is called *dynamical partition* (See Section 3). Let $(X,\mathbb{B},\mu)$ be a probability measure space and $T: X > X$ be be an orientation preserving homeomorphism of the circle $S^1 = \mathbb{R}^1/\mathbb{Z}^1 \simeq [0,1)$ with irrational rotation number θ. Let μ be the unique invariant probability measure of T. Consider the measurable subset $E \subset X$, $\mu(E) > 0$ and a point $x \in X$ which returns to E under iterations by T, we define first return time R_E on E by the following way:

$$R_E(x) = min\{j \geq 1 : T^j x \in E\}.$$

Kac's lemma [3] states that $\int_E R_E(x)d\mu \leq 1$. If T is ergodic, then the equality holds.

A.Dzhalilov and J.Karimov studied the entrance times for circle homeomorphisms with one break point and "golden mean" rotation number ($\rho = [1,1,\dots,1,\dots] = \frac{\sqrt{5}-1}{2}$) and universal renormalization properties [4].

II Continued Fractions. Proof of general properties

In this section we prove the general properties of continued fractions for irrational number.

1. Let

$$\theta = [a_0,a_1,a_2,\dots,a_n] = a_0 + \cfrac{1}{a_1+\cfrac{1}{a_2+\cfrac{1}{\dots+\frac{1}{a_n}}}},\ n \in N$$

and
$$\frac{p_k}{q_k} = [a_0, a_1, a_2, \dots, a_k],\ 0 \le k \le n,\ k \in N.$$

The following equations are satisfied for all i such that $0 \le i \le n$, $i \in N$:

$$p_i = a_i p_{i-1} + p_{i-2},\ q_i = a_i q_{i-1} + q_{i-2}.$$

We also have $p_{-2} = 0, p_{-1} = 1, q_{-2} = 1, q_{-1} = 0$.

Proof. Let $S_{-1} = 1$ and $S_0 = a_n$:

$$[a_{n-1}, a_n] = a_{n-1} + \frac{1}{a_n} = \frac{a_{n-1}a_n + 1}{a_n} = \frac{a_{n-1}S_0 + S_{-1}}{S_0}.$$

Let $S_1 = a_{n-1}S_0 + S_{-1}$. Then we will have

$$[a_{n-1}, a_n] = \frac{S_1}{S_0}.$$

We can see that

$$S_k = a_{n-k}S_{k-1} + S_{k-2}, \tag{1}$$

and
$$[a_{n-k}, a_{n-k+1}, \dots, a_n] = \frac{S_k}{S_{k-1}}.$$

We have $\theta = [a_0, a_1, \dots, a_n] = [a_{n-n}, a_{n-n+1}, \dots, a_n]$. Thus we obtain $k = n$. Then $\theta = \frac{S_n}{S_{n-1}}$. We know that $\theta = \frac{p_n}{q_n}$. From that
$$\frac{p_n}{q_n} = \frac{S_n}{S_{n-1}}$$

We cannot say p_n is the same as S_n because of $S_0 = a_n$ and $p_0 = a_0$ are not equal at the all time.

Let's do some substitutions on S_n. From the equation (1) we obtain

$$S_n = a_0 S_{n-1} + S_{n-2} = a_0(a_1 S_{n-2} + S_{n-3}) + S_{n-2} =$$

$$= (a_1 a_0 + 1)S_{n-2} + a_0 S_{n-3}$$

Let $T_{-1} = 1$ and $T_0 = a_0$. Then

$$S_n = (a_1 T_0 + T_{-1})S_{n-2} + T_0 S_{n-3}$$

Let $T_1 = a_1 T_0 + T_{-1}$. Then

$$S_n = T_1 S_{n-2} + T_0 S_{n-3}$$

Therefore

$$S_n = T_1(a_2 S_{n-3} + S_{n-4}) + T_0 S_{n-3} = (a_2 T_1 + T_0)S_{n-3} + T_1 S_{n-4}$$

Similarly consider $T_2 = a_2 T_1 + T_0$, then:

$$S_n = T_2 S_{n-3} + T_1 S_{n-4}$$

We can see that
$$T_k = a_k T_{k-1} + T_{k-2}$$

and
$$S_n = T_{k-1} S_{n-k} + T_{k-2} S_{n-k-1}.$$

If $n = k$ then

$$S_n = T_{n-1} S_0 + T_{n-2} S_{-1} = T_{n-1} a_n + T_{n-2}$$

But it is known that $T_n = a_n T_{n-1} + T_{n-2}$. Thus $S_n = T_n$. Therefore $p_n = T_n$. If we look at $p_0 = a_0$ and $T_0 = a_0$, we can obtain that they are equal. So, p_n is the sequence as same as the sequence T_n. Then we can conclude that p_n also has the same recurrence equation:

$$p_i = a_i p_{i-1} + p_{i-2}$$

We can prove $q_i = a_i q_{i-1} + q_{i-2}$ using above method. In this case, we should substitute S_1 instead of S_0.

2. For all $n \in N$, following equality holds:

$$p_n q_{n-1} - p_{n-1} q_n = (-1)^{n-1}$$

Proof. We use the 1st property and obtain

$$p_n q_{n-1} - p_{n-1} q_n = (a_n p_{n-1} + p_{n-2}) q_{n-1} - p_{n-1}(a_n q_{n-1} + q_{n-2}) =$$

$$= a_n p_{n-1} q_{n-1} + p_{n-2} q_{n-1} - a_n p_{n-1} q_{n-1} - p_{n-1} q_{n-2} =$$

$$= p_{n-2} q_{n-1} - p_{n-1} q_{n-2} = (-1)(p_{n-1} q_{n-2} - p_{n-2} q_{n-1}).$$

We obtain

$$p_n q_{n-1} - p_{n-1} q_n = (-1)^k (p_{n-k} q_{n-k-1} - p_{n-k-1} q_{n-k}).$$

Let $k = n + 1$.

$$p_n q_{n-1} - p_{n-1} q_n = (-1)^{n+1} (p_{-1} q_{-2} - p_{-2} q_{-1}).$$

It is known that $p_{-2} = 0,\ p_{-1} = 1,\ q_{-2} = 1,\ q_{-1} = 0$. Thus

$$p_n q_{n-1} - p_{n-1} q_n = (-1)^{n-1}.$$

3. For all $n \in N$ the following equality holds:

$$p_n q_{n-2} - p_{n-2} q_n = (-1)^n a_n.$$

Proof.

$$p_n q_{n-2} - p_{n-2} q_n = (a_n p_{n-1} + p_{n-2}) q_{n-2} - p_{n-2}(a_n q_{n-1} + q_{n-2}) =$$

$$= a_n p_{n-1} q_{n-2} + p_{n-2} q_{n-2} - a_n p_{n-2} q_{n-1} - p_{n-2} q_{n-2} =$$

$$= a_n p_{n-1} q_{n-2} - a_n p_{n-2} q_{n-2} = a_n (p_{n-1} q_{n-2} - p_{n-2} q_{n-2}).$$

From the 2nd property, it is known that

$$p_{n-1} q_{n-2} - p_{n-2} q_{n-2} = (-1)^{n-2} = (-1)^n$$

So,

$$p_nq_{n-2} - p_{n-2}q_n = (-1)^n a_n$$

Before starting the proof of the next properties, consider some important notations:

a) Let k be non-negative number such that $0 \leq k \leq n$:

$$a'_k = [a_k, a_{k+1}, \dots, a_n]$$

So, we can easily see that

$$\theta = [a_0, a_1, \dots, a_{k-1}, a'_k]$$

Also, it is necessary to show the following equations:

$$p'_k = a'_k p_{k-1} + p_{k-2} \quad (2)$$

$$q'_k = a'_k q_{k-1} + q_{k-2} \quad (3)$$

Thus, we can write θ as:

$$\theta = \frac{p'_k}{q'_k}$$

b) For all $x \in R$, we define the distance to the nearest integer as following:

$$\|x\| = \min_{n \in Z} |x - n|$$

From that we can say that $\|x\| \in [0; 0.5]$

4. For all $i \in N$ such that $0 \leq i \leq n$:

$$\theta - \frac{p_i}{q_i} = \frac{(-1)^i}{q_i q'_{i+1}}$$

Proof. Let

$$\theta = \frac{p'_{i+1}}{q'_{i+1}}$$

Thus,

$$\theta - \frac{p_i}{q_i} = \frac{p'_{i+1}}{q'_{i+1}} - \frac{p_i}{q_i} = \frac{p'_{i+1}q_i - p_i q'_{i+1}}{q_i q'_{i+1}}$$

By the equations (2) and (3), we can write the equality above as following:

$$\theta - \frac{p_i}{q_i} = \frac{(a'_{i+1}p_i + p_{i-1})q_i - p_i(a'_{i+1}q_i + q_{i-1})}{q_i q'_(i+1)} =$$

$$= \frac{a'_{i+1}p_iq_i + p_{i-1}q_i - a'_{i+1}p_iq_i - p_iq_{i-1}}{q_iq'_{i+1}} = -\frac{p_iq_{i-1} - p_{i-1}q_i}{q_iq'_{i+1}}$$

We use the 2nd property:

$$\theta - \frac{p_i}{q_i} = -\frac{(-1)^{i-1}}{q_iq'_{i+1}} = \frac{(-1)^i}{q_iq'_{i+1}}$$

So,

$$\theta - \frac{p_i}{q_i} = \frac{(-1)^i}{q_iq'_{i+1}}$$

We can conclude that the signs of the sequence $\{\theta - p_i/q_i\}_{i=0}^{\infty}$ alternate.

5. For all $i \in N$ such that $1 \leq i \leq n$:

$$\frac{1}{q_{i+1} + q_i} < \|q_i\theta\| < \frac{1}{q_{i+1}}$$

Proof. Let's consider previous property:

$$\theta - \frac{p_i}{q_i} = \frac{(-1)^i}{q_iq'_{i+1}} \Longrightarrow |\theta - \frac{p_i}{q_i}| = \frac{1}{q_iq'_{i+1}}$$

We know $q'_{i+1} > q_{i+1}$ and if $i \geq 2$, then $q_i \geq 2$. Then

$$|\theta - \frac{p_i}{q_i}| < \frac{1}{q_iq_{i+1}} \Longrightarrow |q_i\theta - p_i| < \frac{1}{q_{i+1}} \leq 1/2$$

Because of that, we can say $|q_i\theta - p_i| = \|q_i\theta\|$. Thus

$$\|q_i\theta\| < \frac{1}{q_{i+1}}$$

It is known $|q_i\theta - p_i| = 1/q'_{i+1}$. Now we prove that

$$\frac{1}{q'_{i+1}} > \frac{1}{q_{i+1} + q_i}$$

Then

$$\frac{1}{q'_{i+1}} > \frac{1}{q_{i+1} + q_i} \Longrightarrow q'_{i+1} < q_{i+1} + q_i \Longrightarrow$$

$$\Longrightarrow a'_{i+1}q_i + q_{i-1} < a_{i+1}q_i + q_{i-1} + q_i \Longrightarrow a'_{i+1} < a_{i+1} + 1$$

We have

$$a'_{i+1} = a_{i+1} + \frac{1}{a'_{i+2}}$$

Thus

$$a'_{i+1} < a_{i+1} + 1 \Longrightarrow a_{i+1} + \frac{1}{a'_{i+2}} < a_{i+1} + 1 \Longrightarrow a'_{i+2} > 1.$$

The last inequality is true for all $1 \leq i < n$.

6. For all $i \in N$ such that $1 \leq i < n$, if $k \in N$ such that $0 < k < q_{i+1}$, then:

$$\|k\theta\| > \|q_i\theta\|$$

Proof. Let $\|k\theta\| = |k\theta - l|$. Then we have:

$$|k\theta - l| > |q_i\theta - p_i|$$

We can set up the following equation system [5]. Here, x and y are some variables:

$$\begin{cases} p_{i+1}x + p_i y = l \\ q_{i+1}x + q_i y = k \end{cases} \implies \begin{cases} x = \frac{lq_i - kp_i}{p_{i+1}q_i - p_i q_{i+1}} \\ y = \frac{lq_{i+1} - kp_{i+1}}{p_{i+1}q_i - p_{i+1}q_i} \end{cases}$$

By the 2nd property:

$$\begin{cases} x = (-1)^i (lq_i - kp_i) \\ y = (-1)^i (lq_{i+1} - kp_{i+1}) \end{cases}$$

x and y cannot be zero. Since l,k are natural numbers then x and y are integer numbers. Thus $|x|, |y| \geq 1$. We have $q_{i+1} > k$. Then x and y should have opposite signs. Also using the 4th property, $\theta - p_i/q_i$ and $\theta - p_{i+1}/q_{i+1}$ have opposite signs. Thus, $x(q_{i+1}\theta - p_{i+1})$ and $y(q_i\theta - p_i)$ have same sign. Then

$$k\theta - l = (q_{i+1}x + q_i y)\theta - (p_{i+1}x + p_i y) =$$

$$= x(q_{i+1}\theta - p_{i+1}) + y(q_i\theta - p_i) \implies$$

$$\implies |k\theta - l| = |x(q_{i+1}\theta - p_{i+1}) + y(q_i\theta - p_i)| =$$

$$= |x(q_{i+1}\theta - p_{i+1})| + |y(q_i\theta - p_i)| > |y(q_i\theta - p_i)| =$$

$$= |y||q_i\theta - p_i| \geq |q_i\theta - p_i|$$

The last inequality above implies the following:

$$|k\theta - l| > |q_i\theta - p_i|$$

or

$$\|k\theta\| > \|q_i\theta\|.$$

III Dynamic Partition. Return Time

Let $T(x) = \{x + \theta\}$ and θ is any irrational number on the interval $(0;1)$. We can write θ as continued fraction:

$$\theta = \cfrac{1}{a_1 + \cfrac{1}{a_2 + \cfrac{1}{a_3 + \dots}}}$$

Let x_0 is any real number on $(0;1)$ and $T(x_0) = x_1, T^2(x_0) = T(T(x_0)) = x_2, \dots, T^n(x_0) = T(T^{n-1}(x_0)) = x_n$.

Properties:

1. x_{q_n} is located nearer to x_0 than any x_i such that $q_n > i$. If n is even, x_{q_n} is located on the right side of x_0, else x_{q_n} is located on the left side of x_0
2. Small distance between x_0 and x_{q_n} is $\|q_n\theta\|$
3. The following equality holds:

$$\|x_m - x_n\| = \|x_k - x_l\|$$

if $m - n = k - l$.

Now we consider "dynamic partition" of $T(x) = \{x + \theta\}$.

Consider the right neighborhood of x_0 and let there be some x_{q_n}:

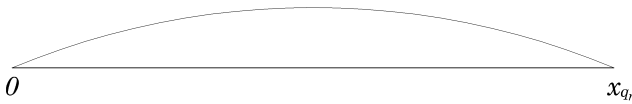

According to our condition, x_{q_n} is located on the right side of x_0. By the 1st property, $x_{q_{n+2}}$ is also located on the right side of x_0. Main thing is that $x_{q_{n+2}}$ creates the interval $(x_0; x_{q_{n+2}})$ with a new length which is smaller than length of previous intervals:

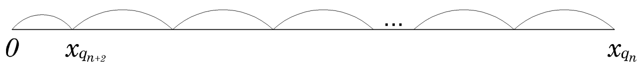

Now define number of intervals which is formed between $x_{q_{n+2}}$ and x_{q_n}. $x_{q_{n+1}}$ also creates smaller interval than previous ones. Thus the intervals created by $x_{q_{n+1}}, x_{q_{n+1}+1}, \dots, x_{q_{n+2}-1}$ are smallest until $x_{q_{n+2}}$ creates a new interval. Using the 2nd and 3rd property:

$$\|x_{q_{n+1}} - x_0\| = \|x_{q_{n+2}} - x_{q_{n+2}-q_{n+1}}\|.$$

Then the point on the right side of $x_{q_{n+2}}$ is $x_{q_{n+2}-q_{n+1}}$:

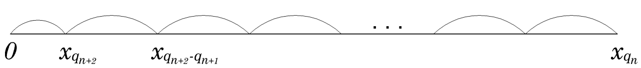

We can continue by this way:

$$\|x_{q_{n+1}} - x_0\| = \|x_{q_{n+2}} - x_{q_{n+2}-q_{n+1}}\| = \|x_{q_{n+2}-q_{n+1}} - x_{q_{n+2}-2q_{n+1}}\|$$

$$= \|x_{q_{n+2}-(a_{n+2}-1)q_{n+1}} - x_{q_{n+2}-a_{n+2}q_{n+1}}\|$$

But $q_{n+2} - a_{n+2}q_{n+1} = q_n$. There is a_{n+2} point between $x_{q_{n+2}}$ and x_{q_n}. The graph is the following:

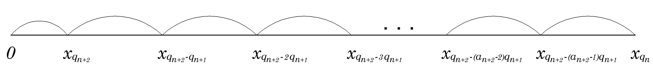

We can illustrate whole graph by that rule.

Now we formulate the theorem on "return time" for circle homeomorphisms with irrational rotation number in dynamical partitions. It is known that the first return time R_E of an irrational rotation T has at most three values if E is an interval ([6], [7]). We present a proof using illustrations of dynamical partitions. Since T is invariant translation, we may assume $E = [0, b)$.

Theorem. Let $T(x) = \{x+\theta\}$ and $b \in (0;\|\theta\|]$. Let $i \geq 0$ be an integer such that $\|q_i\theta\| < b \leq \|q_{i-1}\theta\|$ and K an integer which satisfies

$$K = max\{k \geq 0\colon\, k\|q_i\theta\| + \|q_{i+1}\theta\| < b\}$$

If i is even, then

$$R_{[0;b]}(x) = \begin{cases} q_i, \\ \text{if } 0 \leq x < b - \|q_i\theta\|, \\ q_{i+1} - (K-1)q_i, \\ \text{if } b - \|q_i\theta\| \leq x < K\|q_i\theta\| + \|q_{i+1}\theta\|, \\ q_{i+1} - Kq_i, \\ \text{if } K\|q_i\theta\| + \|q_{i+1}\theta\| \leq x \leq b. \end{cases}$$

If i is odd, then

$$R_{[0;b]}(x) = \begin{cases} q_{i+1} - Kq_i, \\ \text{if } 0 \leq x < b - K\|q_i\theta\| - \|q_{i+1}\theta\|, \\ q_{i+1} - (K-1)q_i, \\ \text{if } b - K\|q_i\theta\| - \|q_{i+1}\theta\| \leq x < \|q_i\theta\|, \\ q_i, \\ \text{if } \|q_i\theta\| \leq x \leq b. \end{cases}$$

Proof with illustrations.
Let $x_0 = 0$ and i be even. Let's consider the interval $[0; x_{q_{i-2}})$. We know that x_{q_i} is nearer to x_0 than $x_{q_{i-2}}$ and $x_{q_i - q_{i-1}}$ is the nearest point to x_{q_i} and the length of the interval $(x_{q_i}; x_{q_i - q_{i-1}})$ is $\|q_{i-1}\theta\|$. Also, we have a_i intervals between x_{q_i} and $x_{q_{i-2}}$ that their length is also $\|q_{i-1}\theta\|$:

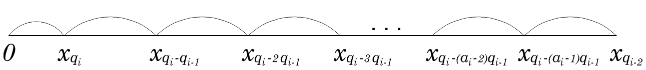

Let's consider the interval $[0; x_{q_i - q_{i-1}})$ only. The point $x_{q_{i+1}+q_i-q_{i-1}}$ takes the place that nearer to $x_{q_i - q_{i-1}}$. So, there will be a_{i+1} intervals between x_{q_i} and $x_{q_{i+1}+q_i-q_{i-1}}$ that their length is $\|q_i\theta\|$ which is the same as distance between x_0 and x_{q_i}:

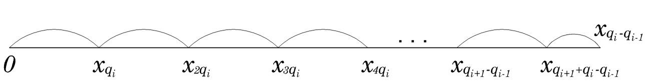

We know that smallest interval here is $(x_{q_{i+1}+q_i-q_{i-1}}; x_{q_i - q_{i-1}})$ and its length is $\|q_{i+1}\theta\|$. Let's take the point b that is located on $(0; x_{q_i - q_{i-1}})$:

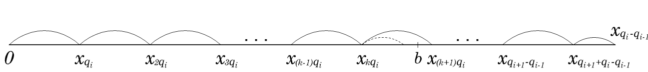

Important note is that b is not on $(x_{q_i - q_{i-1}} - \|q_{i+1}\theta\|; x_{q_i - q_{i-1}})$ because in this case K will be a_{i+1}. If $K = a_{i+1}$, then:

$$a_{i+1}\|q_i\theta\| + \|q_{i+1}\| < b \Longrightarrow \|q_{i-1}\theta\| < b$$

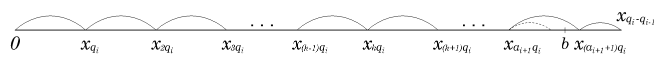

since $a_{i+1}\|q_i\theta\| + \|q_{i+1}\theta\| = \|q_{i-1}\theta\|$. But we have the condition

$$\|q_i\theta\| < b \leq \|q_{i-1}\theta\|.$$

In this case, we should say that $q_{i+1} + q_i - q_{i-1} = (a_{i+1} + 1)q_i$. Also, b cannot be located on $[0; x_{q_i})$, because of the condition above. Then $0 \leq K \leq a_{i+1} - 1$.

Now consider case when $x_0 \in [0; b]$. Let's consider the interval $[0; b - \|q_i\theta\|)$ first. If x_0 is on this interval, x_{q_i} is the 1st point located on $[0; b]$:

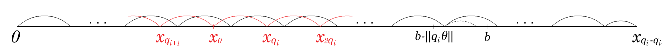

Let's illustrate the graph of $(x_{q_{i-1}}; 1]$ for $x_0 = 0$:

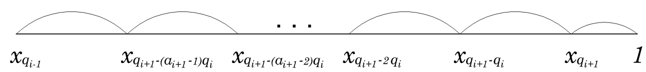

Let $x_0 \in [b - \|q_i\theta\|; K\|q_i\theta\| + \|q_{i+1}\theta\|)$. In this case, the 1st point located on $[0; b]$ is $x_{q_{i+1}-(K-1)q_i}$. We use the previous graph to illustrate it:

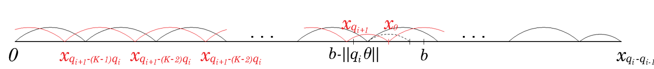

Let $x_0 \in [K\|q_i\theta\| + \|q_{i+1}\theta\|; b]$. In this case, the 1st point located on $[0; b]$ is $x_{q_{i+1}-Kq_i}$:

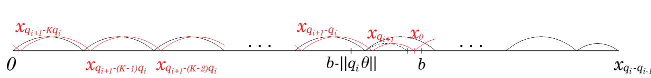

We state that the formula is true for $K = 0$. Let $K = 0$. b will be on the interval $(x_{q_i}; x_{q_i} + \|q_{i+1}\theta\|)$. If $x_0 \in [0; b - \|q_i\theta\|)$ or $x_0 \in [K\|q_i\theta\| + \|q_{i+1}\theta\|; b]$, it's easy to see that $R_{[0;b]} = q_i$ or $R_{[0;b]} = q_i - q_{i-1}$. We should proof that $R_{[0;b]} = q_{i+1} + q_i$, if $x_0 \in [b - \|q_i\theta\|;\, K\|q_i\theta\| + \|q_{i+1}\theta\|)$. Let's draw the graph and fill it with other points:

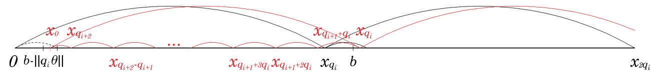

From the graph, you can see that $x_{q_{i+1}+q_i}$ is the 1st point located on

$$[b-\|q_i\theta\|;K\|q_i\theta\|+\|q_{i+1}\theta\|).$$

The theorem is proved for even i.

Let i be odd. Let's move the main graph by 1 to the left side. Then we have the interval $(x_{q_{i-1}}-1;0]$ and let $-b$ be located on that interval but $b\neq 0$ and $\|q_i\theta\|<b\leq\|q_{i-1}\theta\|$. For this condition, we have following return time:

$$R_{[-b;0]}(x)=\begin{cases} q_{i+1}-Kq_i, \\ \text{if } -b\leq x<-K\|q_i\theta\|-\|q_{i+1}\theta\|, \\ q_{i+1}-(K-1)q_i, \\ \text{if } -K\|q_i\theta\|-\|q_{i+1}\theta\|\leq x<-b+\|q_i\theta\|, \\ q_i, \\ \text{if } -b+\|q_i\theta\|\leq x\leq 0. \end{cases}$$

If we shift the interval by b to the right side, then we have:

$$R_{[0;b]}(x)=\begin{cases} q_{i+1}-Kq_i, \\ \text{if } 0\leq x<b-K\|q_i\theta\|-\|q_{i+1}\theta\|, \\ q_{i+1}-(K-1)q_i, \\ \text{if } b-K\|q_i\theta\|-\|q_{i+1}\theta\|\leq x<\|q_i\theta\|, \\ q_i, \\ \text{if } \|q_i\theta\|\leq x\leq b. \end{cases}$$

The proof has completed.

Now we compute return time of circle homeomorphisms using above theorem for exact irrational rotation number.

Let $\theta=\sqrt{2}-1$. Its continued fraction form is the following:

$$\theta=[2,2,\dots,2,\dots]=\cfrac{1}{2+\cfrac{1}{2+\cfrac{1}{2+\dots}}}$$

Let's calculate return time for it:
Let $\|q_i\theta\|<b\leq\|q_{i-1}\theta\|$. Consider the interval $[0;b]$:
We know that

$$0\leq K\leq a_{i+1}-1$$

but have $a_k=2$ for any $k\in[1;\infty)$. So $a_{i+1}=1$. Thus, K can be 0 or 1.
Let $K=0$:

In this case, b cannot be greater than $\|q_{i+1}\theta\|+\|q_i\theta\|$ since K will be 1. Then $b\in(\|q_i\theta\|;\|q_{i+1}\theta\|+\|q_i\theta\|]$.
If i is even:

$$R_{[0;b]}(x)=\begin{cases} q_i, & 0\leq x<b-\|q_i\theta\|, \\ q_{i+1}+q_i, & b-\|q_i\theta\|\leq x<\|q_{i+1}\theta\|, \\ q_{i+1}, & \|q_{i+1}\theta\|\leq x\leq b. \end{cases}$$

If i is odd:

$$R_{[0;b]}(x)=\begin{cases} q_{i+1}, & 0\leq x<b-\|q_{i+1}\theta\|, \\ q_{i+1}+q_i, & b-\|q_{i+1}\theta\|\leq x<\|q_i\theta\|, \\ q_i, & \|q_i\theta\|\leq x\leq b. \end{cases}$$

Let $K=1$. Then $b\in(\|q_{i+1}\theta\|+\|q_i\theta\|;\|q_{i-1}\theta\|]$.
If i is even:

$$R_{[0;b]}(x)=\begin{cases} q_i, & 0\leq x<b-\|q_i\theta\|, \\ q_{i+1}, & b-\|q_i\theta\|\leq x<\|q_i\theta\|+\|q_{i+1}\theta\|, \\ q_{i+1}-q_i, & \|q_i\theta\|+\|q_{i+1}\theta\|\leq x\leq b. \end{cases}$$

If i is odd:

$$R_{[0;b]}(x)=\begin{cases} q_{i+1}-q_i, & 0\leq x<b-\|q_i\theta\|-\|q_{i+1}\theta\|, \\ q_{i+1}, & b-\|q_i\theta\|-\|q_{i+1}\theta\|\leq x<\|q_i\theta\| \\ q_i, & \|q_i\theta\|\leq x\leq b. \end{cases}$$

References

[1] A. Khinchin. *Continued fractions*. 1964.

[2] Seo B.K. Kim, D.H. The waiting time for irrational rotations. *Nonlinearity 16 (5)*, pages 1861–1868, 2003.

[3] M. Kac. On the notion of recurrence in discrete stochastic processes. *Bull. Am. Math. Soc., 53*, pages 1002–10, 1947.

[4] Karimov J. Dzhalilov, A. The entrance times for circle maps with a break. *Bulletin of National University of Uzbekistan: Mathematics and Natural Sciences: Vol. 3 : Iss. 2*, page Article 10, 2020.

[5] S.H. Yang. *Continued fractions and Pell's equation*. 2008.

[6] Berthe V. Alessandri, P. Three distance theorems and combinatorics on words. *Enseign. Math., 44*, pages 103–32, 1998.

[7] N. Slater. Gaps and steps for the sequence $n\theta(mod 1)$. *Proc. Camb. Phil. Soc., 63*, pages 1115–23, 1967.

Acta of Turin Polytechnic University in Tashkent, 2022, 31, 34-38
Published Online March 2022 in Acta TTPU (http://www.acta.polito.uz/)

EXPERIMENTAL DEHYDRATION OF WET SEMI-FINISHED LEATHER PRODUCTS ON A CERAMIC-METAL BASE PLATE

Bahadirov G.A., Tsoy G.N., Nabiev A.M.* and Rakhimova Z.A.
Institute of Mechanics and Seismic Stability of Structures of the Academy of Sciences of the Republic of Uzbekistan
*Email: a.nabiev@mail.ru

Abstract– The article presents the results of an experimental study to determine the influence of such factors as the feed speed, the pressing force of the squeezing rollers on the amount of residual moisture content in the semi-finished leather product after the liquid chrome tanning operation. The experiments were conducted using a cermet base plate, on which one layer of the folded wet leather semi-finished product was previously put and fed vertically between rotating squeezing rollers. The D-optimal method of mathematical planning of the experiment with the K. Kano design matrix was used to conduct experiments. As a result of the study, a mathematical model was obtained for the dependence of the feed speed and the pressing force of the squeezing rollers on the amount of moisture extracted from a wet leather semi-finished product. The analysis of the results of experimental study showed that the use of a base plate made of cermet during squeezing a wet leather semi-finished product increases the efficiency of moisture extraction in comparison with a metal base plate.

Key words– experiment planning; wet leather semi-finished product; ceramic-metal base plate; squeezing rollers; pressure; speed; experiment.

I Introduction

The quality of the finished leather is influenced by all technological stages of processing, therefore, after the realization of each of them, it is necessary to analyze the condition of the leather semi-finished product [1,2,3]. In [4], the influence of the number of layers of leather and moisture-removing materials on the process of extracting moisture during their feed to a metal base plate made of steel 3 was investigated.

Experimental research in the leather industry is aimed at solving complex multifactorial problems, the result of which is determined by rational modes of technological processes for treating leather raw materials. The physical and mechanical properties of semi-finished leather products vary depending on their moisture content. Consequently, the process of extracting excess moisture from a semi-finished leather product after liquid processing substantially affects the quality of subsequent technological processes, for example, planing, splitting, drying [5-8].

This article is devoted to an experimental study of the effect of a cermet base plate on the efficiency of extracting moisture from a wet leather semi-finished product.

II Methods and results of experimental research

The experiment was conducted on a special test bench, where the squeezing rollers were installed horizontally, and the base plate was made of porous cermet material PP64S-250-25-76-40, 0.015 m thick, mounted on a metal guide rod, 0.1 m wide and 0.3 m long (Fig. 1). In the present study, a base plate made of porous cermet material was used. The base plate was turned from an abrasive wheel of the PP64S-250-25-76-40 brand of a universal, straight profile, based on silicon carbide. The percentage of the volume of abrasive grains per unit volume of the wheel is 40. The used material has a 20% porosity, which, at a certain feed rate is sufficient to extract moisture from the inner side of wet leather.

For engineering reasons, the minimum thickness of the base plate was calculated and chosen to be 0.015 m to ensure the required strength under the high pressure of the squeeze rollers. It should be noted that in industrial conditions, after each work shift, the cermet base plate should be rinsed with a pressure of warm water, just as the permeable coatings of the squeezing rollers are washed.

For the experiment, we took a bovine hide of medium weight, splitted, after chrome tanning. According to the International Standard ISO 2588-85, the required size of a leather semi-finished product was selected by the following formula

$$n = 0,2\sqrt{x} \qquad (1)$$

where x is the number of semi-finished leather products for the experiment; 2500 pieces were taken from the batch, so, n=10 pieces. From these 10 samples, 0.05×0.25 m strips were cut out with a cutter across the spine line; the numbered strips were assembled into groups of 5 pieces according to the scheme given in [9].

During the experiment, a wet leather semi-finished product 0.004 m thick was hung folded on a cermet base plate. Before and after squeezing, the samples were weighed on a VLTE-500 laboratory balance with discreteness of 0.01 g (ISO-9001).

The second-order D-optimal planning method with the K. Kano design matrix [10] was used.

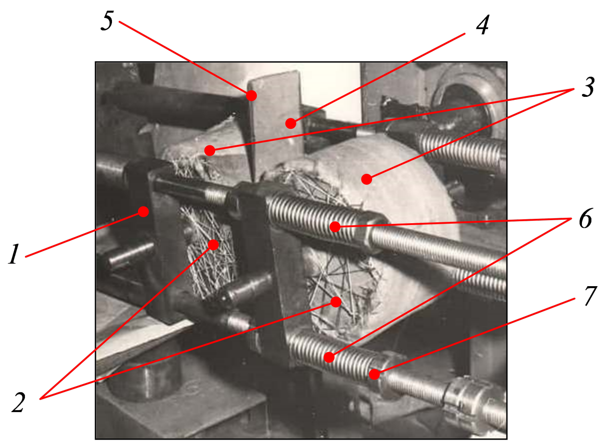

Fig. 1: Fragment of pressing machine for a semi-finished leather product on an experimental test bench: 1 – bed frame, 2 - squeezing rollers, 3 - roller coatings (monchon BM), 4 - semi-finished leather, 5 - cermet base plate, 6 - springs, 7 - tension nuts

On the basis of prior information, the process of moisture extraction was studied considering the following factors:x_1 - pressure intensity P, kN/m; x_2 - feeding speed V, m/s. Based on the analysis of various squeezing machines, the pressure range was selected from 32 to 96 kN/m; the rotation speed of the squeezing rollers was taken from 0.17 to 0.34 m/s; the number of semi-finished leather products was one.

The diameter of the squeezing rollers was 0.2 m and they were coated with 0.01 m thick moisture-removing material made of BM brand felt. Before conducting the experiment, the required number of measurements (the number of replicates) was selected by the methods of mathematical statistics, which ensured the required accuracy.

The working matrix was drawn up according to the K. Kano plan matrix for a two-factor experiment. Factors were encoded according to the formula

$$x_i = \frac{c_i - c_{i0}}{t_0} \tag{2}$$

where x_i is the coding of the factor values; c_i, c_{i0} are the natural values of the factor at the current and zero levels; t_0 is the natural value of the factor variation interval. The levels and intervals of variation of experiment factors are shown in **Table 1**.

Index	Coded value of factors	Natural values of factors	
		x_1, kN/m	x_2, m/s
Upper level	+	96	0.340
Zero level	0	64	0.255
Lower level	-	32	0.170
Variation interval		32	0.085

TABLE 1: LEVELS AND INTERVALS OF VARIATION OF EXPERIMENT FACTORS

Target functions are approximated by a polynomial

$$y = b_0 + \sum_{i=1}^{k} b_i x_i + \sum_{i,j=1}^{k} b_{ij} x_i x_j + \sum_{i=1}^{k} b_{ii} x_i^2 \tag{3}$$

where y is the amount of removed moisture in coded form; b_0, b_i, b_{ij}, b_{ii} are the regression coefficients.

The homogeneity of the variance was realized using the Cochran test [10-12] at a confidence level of $\alpha = 0.95$. Knowing the total number of variances estimates N and the number of degrees of freedom f=k–1 from Table 3 [10], we determine $G_T = 0.358$, for N=9; f=k–1=5–1=4; k is the number of parallel experiments.

$$S_{er}^2 = \frac{\sum_1^n (y - \bar{y})^2}{n-1} \tag{4}$$

$$\sum_1^N S_i^2 = \frac{\sum_1^N \sum_1^n (y - \bar{y})^2}{N(n-1)} \tag{5}$$

$$G_{cal} = \frac{S_{max}^2}{\sum_1^N S_i^2} = \frac{0.4153}{1.7555} = 0.2365 < G_T = 0.358 \tag{6}$$

Consequently, the study results are reproducible.

We determine the regression coefficients b_0, b_i, b_{ij}, b_{ii} from Table 4 [10].

For a semi-finished leather product in coded form they are $b_0 = 18.3372$; $b_{11} = 1.0867$; $b_{22} =$ ˇ0.8083; $b_1 = 3.7063$; $b_2 =$ ˇ2.7359; $b_{12} =$ ˇ0.3. We get the following coded regression equations: for semi-finished leather

$$y = 18.34 + 1.0867 x_1^2 - 0.8083 x_2^2 + \\ + 3.7063 x_1 - 2.7359 x_2 - 0.3 x_1 x_2 \tag{7}$$

TABLE 2: EXPERIMENT PLANNING MATRIX

№	P, x_1	V, x_2	Measurement results, in %						$\sum_1^n (y-\bar{y})^2$	S_{er}^2	y_{cal}	$\bar{y}$-y_{cal}	$(\bar{y}$-$y_{cal})^2$
			y_1	y_2	y_3	y_4	y_5	$\bar{y}$					
1	0	0	18.53	18.61	18.36	18.20	18.55	18.50	0.1311	0.0327	18.34	0.16	0.0256
2	+	+	19.39	18.77	18.78	20.11	19.47	19.30	1.2444	0.3111	19.29	0.01	0.0001
3	-	+	11.65	13.13	13.02	12.26	12.45	12.50	0.4499	0.1124	12.48	0.02	0.0004
4	-	-	17.15	17.5	17.53	16.95	17.86	17.40	0.6035	0.1508	17.30	0.1	0.001
5	+	-	26.33	25.55	25.26	24.98	24.89	25.40	1.3435	0.3358	25.36	0.04	0.0016
6	+	0	22.62	23.23	23.36	23.10	22.98	23.06	0.3205	0.0801	23.13	0.07	0.0049
7	0	+	14.16	15.60	14.46	14.86	14.68	14.75	1.1563	0.2891	14.80	0.05	0.0025
8	-	0	15.60	15.63	15.80	15.43	15.44	15.60	0.1114	0.0278	15.72	0.12	0.0144
9	0	-	20.74	20.18	20.57	19.09	20.02	20.12	1.6614	0.4153	20.27	0.15	0.0225
									$\sum 7.022$	$\sum 1.755$			$\sum 0.082$

Substituting $x_1 = \frac{P-64}{32}$, where$P$ is the pressing force of the squeezing rollers and $x_2 = \frac{V-0.255}{0.085}$, where V is the feed speed of wet leather semi-finished products between the rotating squeezing rollers, we obtain the equations for the amount of moisture removed from wet leather semi-finished products between the rotating squeezing rollers in a natural form.

After the implementation of the working matrix, the arithmetic mean values were obtained (Table 2).

III ANALYSIS OF THE RESULTS

The hypothesis of the adequacy of the equations obtained was tested using Fisher's variance ratio at a confidence level of $\alpha = 0.95$ [10-14].

$$F_{cal} = \frac{S_{ad}^2}{S^2\{y\}} < F_T \tag{8}$$

where S_{ad}^2 is the residual variance or the variance of adequacy; $S^2\{y\}$ - is the variance of reproducibility.

S_{ad}^2 and $S^2\{y\}$ are defined from **Tables 1, 2,** and **3**.

$$S_{ad}^2 = \frac{\sum_1^N n(\bar{y}-y)^2}{\frac{N-(x+2)(x+1)}{2}} = \frac{5 \cdot 0.082}{3} = 0.1366 \tag{9}$$

$$S_{\{y\}}^2 = \frac{\sum_1^N \sum_1^n (y-\bar{y})^2}{N(n-1)} = \frac{7.022}{36} = 0.1950 \tag{10}$$

Fisher's variance ratio of the model adequacy is:

$$F_{cal} = \frac{S_{ad}^2}{S^2\{y\}} = \frac{0.1366}{0.1950} = 0.70 < F_T = 2.880 \tag{11}$$

where N – is the total number of experiments; k is the number of factors; n is the number of experiment repetitions; y_i is the result of a separate observation; $\bar{y}$ is the arithmetic mean of the results of the experiment; y_p is the calculated values of the criterion according to the regression equation.

So, the regression equation can be considered suitable with a 95% confidence level, which in the named form after decoding has the following form: for semi-finished leather:

$$\triangle W = 10.006 + 0.001P^2 - 111.875V^2 - 0.0403P + \\ +17.8165V - 0.1102PV \tag{12}$$

A dependence graph of the amount of extracted moisture $\triangle W$ (12) from a wet leather semi-finished product in percentage at different feed speeds V and pressing forces P (Fig. 2) is built.

Comparative analysis of the efficiency of pressing a wet leather semi-finished product on a porous cermet base plate versus a metal base plate showed the difference in the amount of removed moisture $\triangle W$ by an average of 7%.

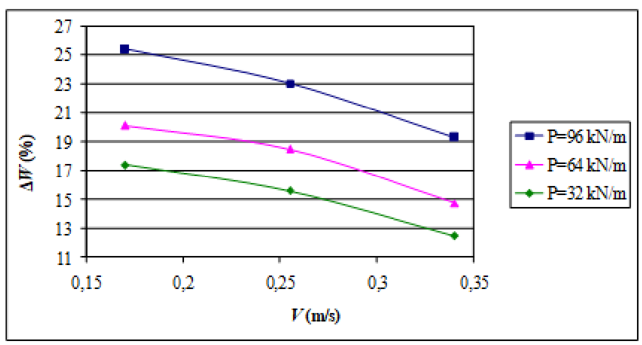

Fig. 2: Dependence of the amount of extracted moisture $\triangle W$ on the feed speed V of the semi-finished leather product with the following values of the pressing force of the squeezing rollers: P=32 kN/m, P=64 kN/m, P=96 kN/m

Consequently, in this case, it is possible to reduce the values of the pressing force between the squeezing rollers and it is recommended in vertical squeezing roller machines to use base plates made of hard porous materials in order to increase the productivity of the technological process.

TABLE 3: DETERMINATION OF REGRESSION COEFFICIENTS

№	P, x_1	V, x_2	Coefficient multipliers						
			b_0	b_{11}	b_{22}	b_1	b_2	b_{12}	$\bar{y}$
1	0	0	0.5772	-0.3234	-0.3234	0	0	0	18.50
2	+	+	-0.1057	0.1691	0.1691	0.1961	0.1961	0.25	19.30
3	-	+	-0.1057	0.1691	0.1691	-0.1961	0.1961	-0.25	12.50
4	-	-	-0.1057	0.1691	0.1691	-0.1961	-0.1961	0.25	17.40
5	+	-	-0.1057	0.1691	0.1691	0.1961	-0.1961	-0.25	25.40
6	+	0	0.2114	0.1617	-0.3383	0.1078	0	0	23.062
7	0	+	0.2114	-0.3383	0.1617	0	0.1078	0	14.750
8	-	0	0.2114	0.1617	-0.3383	-0.1078	0	0	15.60
9	0	-	0.2114	-0.3383	0.1617	0	-0.1078	0	20.12

IV CONCLUSIONS

Analysis of the experimental results (Fig. 2) shows that it is possible to increase the productivity of moisture extraction from semi-finished leather products by increasing the extraction speed on a base plate made of porous cermet material PP64S-250-25-76-40. The results of the experiments show that the removal of moisture at the pressing force P=32 kN/m of the squeezing rollers, the maximum feed speed is slightly less than V=0.34 m/s. At the pressure of the squeezing rollers P=64 kN/m, the maximum feed speed is more than V=0.34 m/s. At the pressure of the squeezing rollers of a roller machine P=96 kN/m, the feed speed is substantially higher than 0.34 m/s. The experiment showed that the moisture removed in excess of the required 13% is from 6 to 1.75% of the initial weight of the leather semi-finished product. Consequently, it will be possible to squeeze out moisture from wet leather semi-finished products at the feed speed of more than 0.34 m/s with the pressing force of the squeezing rollers from 64 to 96 kN/m.

In the future, the maximum speed of moisture extraction from semi-finished leather products of more than 0.34 m/s will be experimentally determined with the proposed design of the base plate in the form of a cermet material PP64-250-25-76-40 with a thickness of 0.015 m and at pressing forces from 64 to 96 kN/m.

The use of the proposed structure as a base plate made of porous cermet material provides moisture removal without fibrous porous materials that wear out quickly. This will increase the efficiency of the technological operation of extracting excess moisture from the wet leather semi-finished product.

V REFERENCES

[1] Burmistrov AG Equipment of enterprises for the leather and fur production: Textbook/M.: Light and food industry, 1981, pp. 416.

[2] Patent RUz №IAP 04451 Method of extracting moisture from wet leather. Authors: Amanov T.Yu., Bahadirov G.A., Tsoi G.N., Nabiev A.M. Official Bulletin of the Agency for Intellectual Property of the Republic of Uzbekistan, No. 12 (128), 30.12.2011, pp. 46-47. *http://baza.ima.uz/#*

[3] Bahadirov G.A., Tsoy G.N., Nabiev A.M., Wringing of wet leather semi-finished product using moisture-removing cloth. International collection of scientific papers "Progressive technologies and systems of mechanical engineering". Issue 4 (71)', Donetsk, 2020, pp. 3-8. *http: //ptsm.donntu.org/arhiv%20nambe/pdf%20-71/index.htm*

[4] Amanov A.T., Bahadirov G.A., Amanov T.Y, Tsoy G.N., Nabiev A.M. Determination of strain properties of the leather semi-finished product and moisture-removing materials of compression rolls. Journal Materials, Volume 12, Issue 21, November (1) 2019. ISSN: 1996-1944. Basel, Switzerland. *https://doi.org/10.3390/ma12213620*

[5] Wright D.M. Deformation, yield, relaxation and recovery in partially processed leather. Doctoral thesis. University of Leicester. 1996. *http://nectar.northampton.ac.uk/2660/*

[6] Luo F., Zhong X., Gao M., Progress and mechanism of breaking glycoconjugates by glycosidases in skin for promoting unhairing and fiber opening-up in leather manufacture. A review. J. Leather Sci. Eng. 2, 12., 2020. *https://doi:10.1186/s42825-020-00025-0*

[7] Preethi S., Anumary A., Ashokkumar M., Probing horseradish peroxidase catalyzed degradation of azo dye from tannery wastewater. SpringerPlus 2, 2013, pp. 341. *https://doi.org/10.1186/2193-1801-2-341*

[8] Mehta M., Naffa R., Maidment C, Raman and atr-ftir spectroscopy towards classification of wet blue bovine leather using ratiometric and chemometric analysis. J. Leather Sci. Eng. 2, 3., 2020. *https://doi.org/10.1186/s42825-019-0017-5*

[9] Golovteeva A.A., Kutsidi D.A., Laboratory workshop on chemistry and technology of leather and fur. M.: Light and food industry: 1982, pp. 309, *https://www.twirpx.com/file/2792825/*

[10] Tikhomirov V. A., Planning and analysis of the experiment. M.: Light industry: 1974, pp. 283, *https://www.twirpx.com/file/236275/*

[11] Naima Benmakhlouf, Soufien Azouz, Afif Elcafsi, The determination of isosteric heats of sorption of leather: Experimental and mathematical investigations., Arabian Journal of Chemistry. Volume 13, Issue 2, February 2020, pp. 4286-4293,. *https://doi.org/10.1016/j.arabjc.2019.07.008*

[12] Jeff Wu C.F., Michael S. Hamada, Experiments: planning, analysis, and optimization. – 2nd edition., 2009, USA.

[13] Denis Constales, Gregory S. Yablonsky, Dagmar R. D'hooge, Joris W. Thybaut, Guy B. Marin, Chapter 9 - Experimental Data Analysis: Data Processing and Regression, Advanced Data Analysis and Modelling in Chemical Engineering, Elsevier, 2017,pp. 285-306, ISBN 9780444594853,. *https://doi.org/10.1016/B978-0-444-59485-3.00009-6.*

[14] Luiz Paulo Fávero, Patrícia Belfiore, Chapter 21 - Design and Analysis of Experiments, Data Science for Business and Decision Making, Academic Press, 2019, Pages 935-939, ISBN 9780128112168,. *https://doi.org/10.1016/B978-0-12-811216-8.00021-5.*

Acta of Turin Polytechnic University in Tashkent, 2022, 31, 39-45
Published Online March 2022 in Acta TTPU (http://www.acta.polito.uz/)

ONE-DIMENSION OF NOSTATSIONAL FILTRATION PROCESS OF GAS IN A TWO-LAYER POOR ENVIRONMENT MATHEMATICAL MODEL AND NUMBER OF METHODS OF SOLVING IT

Turdiyev T.T.*, **Xojibayev J.M., Tillayeva G.R..**
The Urgench branch of the Tashkent University of Information Technologies named after Muhammed al-Kharezmi
*Email: temurbek199002@gmail.com

Abstract– An analysis of the hydrodynamic development of the filtration process of liquids and gases in the porous medium, a mathematical model of the filtration process of gases in dynamically porous media, a finite difference method for solving the boundary value of gas motion in a porous medium and its algorithm considered.

Key words– linear law, quasilinear method, Sweep method

I Introduction

Based on data on the movement of liquids and gases in the real layer, some complex problems of underground hydraulics are studied and their solutions are found using mathematical methods. The movement of liquid and gas in the natural subsurface begins with the extraction of oil and gas. This movement is completely different from the movement of a pipe or an open well with its own characteristics.

At present, the design and operation of new oil and gas fields and the operation of wells cannot be imagined without the application of the laws of underground hydraulics. How to place the wells in a given layer; how many wells are in the stratum and in what order they should be included; what mode of operation should be maintained in them; how much water needs to be pumped into the layer to maintain pressure; it is necessary to direct and adjust the movement of liquid or gas in the formation, and many such questions are solved on the basis of the laws of underground hydraulics.

If we look at the history of underground hydraulics, the development of this science was founded in the middle of the XIX century by the French engineer G. Darcy. In 1856, he studied filtration phenomena experimentally and developed his own Darcy Law.

Slixter contributed to the development of underground hydraulics. He introduced the concepts of ideal and fictitious (artificial) soil, showing that the porosity of fictitious soil does not depend on the diameter of the particles of volumetric and surface voids, but on their location in the surface.

L.S. Leibenzon was the first to develop a differential equation of gas and gas motion in a porous medium based on theoretical and experimental research. He made a mathematical analysis of the methods of calculating oil and gas reserves in the strata, the problems of oil and gas extraction by water.

Further development of oil and gas underground hydromechanics acad. L.S. Leibenzon's students contributed. In the development of the theory of filtration in the oil and gas aquifer, Acad. S.A. Christianovich, professorial- B.B.Lapuk, I.A.Charny, V.N.Shelka - chev, K.S Basniyev. G.B. The Pikhachevs made a significant contribution.

II Main Part

Knowledge of their properties in porous or cracked environments is essential for the efficient operation of oil and gas fields. We consider the problem of non-stationary filtration of gas in two interconnected layers in a porous medium.

The following non-stationary filtration processes are assumed to be:

- Gas layers consist of inhomogeneous porous media;
- The lengths of the gas layers are the same distance;
- In the initial state, the layers are at the same pressure;
- The motion of a gas in both layers obeys the linear law of Darcy;

- The properties of the gas in both layers do not change over time.

Based on these requirements, it is necessary to determine the change in pressure function in both gas layers over time. At this time, the flow rate of gas wells varies, and they can be located anywhere in the gas layer (Fig.1).

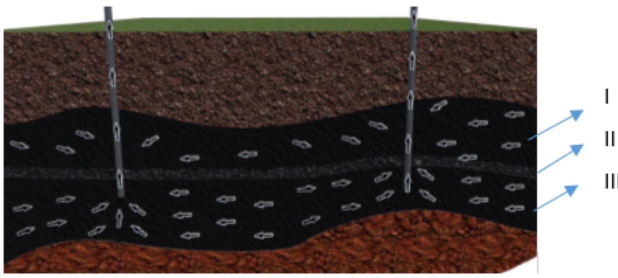

Fig. 1: Gas layers with poor permeability.
I - the first gas layer; II – poorly conductive layer III – the second gas extraction layer.

In the design and analysis of the operation of multilayer gas fields in the filtration processes of gases in a porous environment, it is necessary to take into account the presence of hydrodynamic connections between the layers. In this case, the use of highly efficient methods in the mathematical modeling of the gas filtration process in two-layer systems is required, because the corresponding system of equations is nonlinear and cannot be solved by analytical methods. If both layers are the same in collector properties, the problem can be expressed in a one-dimensional or two-dimensional boundary matter. In this case, the mathematical model of the one-dimensional mass can be thought as a system of equations of the nonlinear parabolic type.(1)

$$\begin{cases} \frac{\partial}{\partial x}\left[k_1(x)\frac{\partial P_1^2}{\partial x}\right] = 2\mu a_1 m_1 \frac{\partial P_1}{\partial t} - \frac{k_\Pi}{h_\Pi h_1}(P_2^2 - P_1^2), \\ \frac{\partial}{\partial x}\left[k_2(x)\frac{\partial P_2^2}{\partial x}\right] = 2\mu a_2 m_2 \frac{\partial P_2}{\partial t} + \frac{k_\Pi}{h_\Pi h_1}(P_2^2 - P_1^2) - Q, \end{cases}$$

$$0 < x < L \qquad (1.1)$$

Initial and boundary conditions

$$P_1(x) = P_{1H}(x) \qquad P_2(x) = P_{2H}(x) \qquad at \qquad t = 0 \qquad (1.2)$$

$$\begin{aligned} -k_1h_1\frac{\partial P_1}{\partial x} &= \alpha(P_A - P_1); \\ -k_2h_2\frac{\partial P_2}{\partial x} &= \alpha(P_A - P_2) \qquad x = 0 \end{aligned} \qquad (1.3)$$

$$\begin{aligned} -k_1h_1\frac{\partial P_1}{\partial x} &= \alpha(P_B - P_1); \\ -k_2h_2\frac{\partial P_2}{\partial x} &= \alpha(P_B - P_2) \qquad x = L \end{aligned} \qquad (1.4)$$

$$\int_S \frac{k_ih_i}{\mu}\frac{\partial P_i}{\partial n} ds = -q_i(t); \qquad i = 1,2 \qquad (1.5)$$

The following symbols are accepted in the system of equations and boundary conditions:

- P_1, P_2 - lower and upper layer pressures, respectively;
- P_H - initial layer pressure;
- k_1 and k_2 – layer permeability in the lower and upper layers, respectively;
- k_P – permeability coefficient of weak conductivity layer;
- h_1 va h_2 - the thickness of the bottom and top layer, respectively;
- h_P - weakly conductive layer thickness;
- μ – gas viscosity coefficient;
- $q(t)$ – bottom layer well flow;
- m_1, m_2 – porosity of the lower and upper layers, respectively;
- s_i – well contour;
- n_1 - number of wells.

To include dimensionless variables in the system of equations and in boundary conditions, we include the following.

$$x^* = \frac{x}{L}; \qquad k_1^* = \frac{k_1}{k_x}; \qquad k_2^* = \frac{k_2}{k_x}; \qquad k_P^*(x) = \frac{k_P}{k_x};$$

$$P_1^* = \frac{P_1}{P_x}; \qquad P_2^* = \frac{P_2}{P_x}; \qquad \tau = \frac{k_xP_xt}{\mu L^2}.$$

By performing these changes in the system and dropping the asterisk for convenience, we come to the following dimensionless problem:

$$\begin{cases} \frac{\partial}{\partial x}\left[k_1(x)\frac{\partial P_1^2}{\partial x}\right] = 2\alpha_1 m_1 \frac{\partial P_1}{\partial t} - \frac{k_p}{h_p}\frac{L^2}{h_1}(P_2^2 - P_1^2), \\ \frac{\partial}{\partial x}\left[k_2(x)\frac{\partial P_2^2}{\partial x}\right] = 2\alpha_2 m_2 \frac{\partial P_2}{\partial t} + \frac{k_p}{h_p}\frac{L^2}{h_2}(P_2^2 - P_1^2) - \delta q(t), \end{cases}$$

$$0 < x < 1 \tag{1.6}$$

Initial and boundary conditions

$$P_1(x) = P_{1H}(x) \qquad P_2(x) = P_{2H}(x) \qquad at \qquad t = 0 \tag{1.7}$$

$$-k_1 h_1 \frac{\partial P_1}{\partial x} = \alpha(P_A - P_1); \quad -k_2 h_2 \frac{\partial P_2}{\partial x} = \alpha(P_A - P_2) \qquad x = 0 \tag{1.8}$$

$$-k_1 h_1 \frac{\partial P_1}{\partial x} = \alpha(P_B - P_1); \quad -k_2 h_2 \frac{\partial P_2}{\partial x} = \alpha(P_B - P_2) \qquad x = 1 \tag{1.9}$$

$$\int_S \frac{k_i h_i}{\mu}\frac{\partial P_i}{\partial n} ds = -q_i(t); \qquad i = 1,2 \tag{1.10}$$

Limited difference method and its algorithm for solving the boundary value problem of gas motion in a two-layer porous medium

We use the non-disclosed finite difference method to solve the dimensional boundary value problem above (1.6) - (1.10) (7).

To solve the problem using this numerical method, we construct a grid of equal steps in the field

$$\{0 < x < 1, \quad 0 \le t \le 1\}$$

.

$$w_{h\tau} = \left\{ x_i = ih, \quad i = 0,1,...,n, \quad h = \frac{1}{n}, \quad t_j = j\tau, \quad j = 0,1,... \right\}$$

and by approximating the system of equations in the grid, we obtain the following finite difference scheme (1).

$$k_{1i-0.5}P_{1i-1}^2 - (k_{1i-0.5} + k_{1i+0.5})P_{1i}^2 + k_{1i+0.5}P_{1i+1}^2 - \\ -\frac{h^2}{\tau}2\alpha_1 m_1(P_{1i} - \hat{P_{1i}}) + \frac{h^2 k_{Pi}}{h_P}\frac{L^2}{h_1}(P_{2i}^2 - P_{1i}^2) = 0;$$

$$k_{2i-0.5}P_{2i-1}^2 - (k_{2i-0.5} + k_{2i+0.5})P_{2i}^2 + k_{2i+0.5}P_{2i+1}^2 - \\ -\frac{h^2}{\tau}2\alpha_2 m_2(P_{2i} - \hat{P_{2i}}) - \frac{h^2 k_{Pi}}{h_P i}\frac{L^2}{h_2}(P_{2i}^2 - P_{1i}^2) = 0;$$

The obtained differential equations are not linear with respect to the pressure function P, so the iteration method based on the quasilinear functions of nonlinear method is used. According to these methods, the nonlinear members of finite difference equations are presented as follows:

$$\varphi(P) = \varphi(\tilde{P}) + (P - \tilde{P})\frac{\partial \varphi(\tilde{P})}{\partial P}. \tag{1.11}$$

Here, P is the approximate value of the $\tilde{P}$ function determined during the iteration process

$$\tilde{P} = P_i^{(S)}, \quad and \quad P_i^{(0)} = \hat{P}_i.$$

The iteration process continues until the following conditions are met

$$max_{i,j}\left|P_{1i}^{(s)} - P_{1i}^{(s-1)}\right| \le \varepsilon, \quad max_{i,j}\left|P_{2i}^{(s)} - P_{2i}^{(s-1)}\right| \le \varepsilon. \tag{1.12}$$

Here:
ε – iteration accuracy, a small amount known in advance;
s - number of iterations.

If formula (1.11) is written for a nonlinear pressure function, we have the following formula

$$P^2 \approx 2\tilde{P}P - \tilde{P}^2.$$

Then, after applying the method of quasilinear functions of nonlinear terms, the coefficients of these quasilinear differential equations are as follows:

$$a_i = 2\tilde{P}_{1i-1}k_{1i-0.5}; \quad c_i = 2\tilde{P}_{1i+1}k_{1i+0.5};$$

$$b_i = a_i + c_i + \frac{h^2}{\tau} 2\alpha_1 m_1 + \frac{h^2 k_{\Pi i}}{h_\Pi} \frac{L^2}{h_1};$$

$$d_i = \frac{h^2 k_{\Pi i}}{h_\Pi} \frac{L^2}{h_1};$$

$$f_i = \frac{h^2}{\tau} 2\alpha_1 m_1 \hat{P}_{1i} + k_{1i-0.5} \tilde{P}^2_{1i-1} - -(k_{1i-0.5} + k_{1i+0.5}) \tilde{P}^2_{1i} + k_{1i+0.5} \tilde{P}^2_{1i+1};$$

$$a'_i = 2\tilde{P}_{2i-1} k_{2i-0.5}; \quad c'_i = 2\tilde{P}_{2i+1} k_{2i+0.5};$$

$$b'_i = a'_i + c'_i + \frac{h^2}{\tau} 2\alpha_2 m_2 + \frac{h^2 k_{\Pi i}}{h_\Pi} \frac{L^2}{h_2};$$

$$d'_i = \frac{h^2 k_{\Pi i}}{h_\Pi} \frac{L^2}{h_2};$$

$$f'_i = \frac{h^2}{\tau} 2\alpha_2 m_1 \hat{P}_{2i} + k_{2i-0.5} \tilde{P}^2_{2i-1} - -(k_{2i-0.5} + k_{2i+0.5}) \tilde{P}^2_{2i} + k_{2i+0.5} \tilde{P}^2_{2i+1};$$

We use the sweep method to solve this finite separation system. Then we have this system of finite differences above and the system of finite differences below the boundary conditions.

$$a_i P_{1i-1} - b_i P_{1i} + c_i P_{1i+1} + d_i P_{2i} = -f_i; \tag{1.13}$$

$$(3k_{10} h_1 - 2h\lambda\alpha) P_{10} - 4k_{11} h_1 P_{11} + k_{12} h_1 P_{12} = 2h\lambda\alpha P_A \tag{1.14}$$

$$(3k_{1n} h_1 - 2h\lambda\alpha) P_{1n} + 4k_{1n-1} h_1 P_{1n-1} - k_{1n-2} h_1 P_{1n-2} = -2h\lambda\alpha P_A \tag{1.15}$$

$$a'_i P_{2i-1} - b'_i P_{2i} + c'_i P_{2i+1} + d' P_{1i} = -f'_i; \tag{1.16}$$

$$(3k_{20} h_2 - 2h\lambda\alpha) P_{20} - 4k_{21} h_2 P_{21} + k_2 h_2 P_{22} = 2h\lambda\alpha P_A \tag{1.17}$$

$$(3k_{2n} h_2 - 2h\lambda\alpha) P_{2n} + 4k_{2n-1} h_2 P_{2n-1} - k_2 h_{2n-2} P_{2n-2} = -2h\lambda\alpha P_A \tag{1.18}$$

$$i, j = 1, 2, ..., N-1.$$

The solution of this finite distribution system (1.13) - (1.18) is determined from the following formulas

$$P_{1i} = A_i P_{1i+1} + B_i P_{2i+1} + C_i \tag{1.19}$$

$$P_{2i} = A'_i P_{2i+1} + B'_i P_{1i+1} + C'_i \tag{1.20}$$

$$i = 1, 2, ..., n-1.$$

Here:

$$A_i = \frac{c_i (b'_i - a'_i A'_{i-1})}{R_i}; \quad B_i = \frac{c'_i (a_i B_{i-1} + d_i)}{R_i}; \tag{1.21}$$

$$A'_i = \frac{c'_i (b_i - a_i A_{i-1})}{R_i}; \quad B'_i = \frac{c_i (a'_i B'_{i-1} + d'_i)}{R_i}; \tag{1.22}$$

$$C_i = \frac{(a_i B_{i-1} + d_i)(a'_i C'_{i-1} + f'_i) + (a_i C_{i-1} + f_i)(b'_i - a' A'_{i-1})}{R_i}; \tag{1.23}$$

$$C'_i = \frac{(a'_i B'_{i-1} + d'_i)(a_i C_{i-1} + f_i) + (a'_i C'_{i-1} + f'_i)(b_i - a_i A_{i-1})}{R_i}; \tag{1.24}$$

$$R_i = (b_i - a_i A_{i-1})(b'_i - a'_i A'_{i-1}) - (a_i B_{i-1} + d_i)(a'_i B'_{i-1} + d').$$

$$i = 1, 2, ..., n-1.$$

Here A_0; B_0; C_0; A'_0; B'_0; C'_0; s values are determined from the boundary conditions

$$A_0 = \frac{(b_1 - 4c_1)k_{11}h_1}{a_1 k_{12} h_1 - (3k_{10}h_1 - 2h\alpha)c_1}; \qquad (1.25)$$

$$B_0 = -\frac{d_1 k_{12} h_1}{a_1 k_{12} h_1 - (3k_{10}h_1 - 2h\alpha)c_1}; \qquad (1.26)$$

$$C_0 = \frac{f_1 k_{12} h_1 + 2h\alpha c_1}{a_1 k_{12} h_1 - (3k_{10}h_1 - 2h\alpha)c_1}; \qquad (1.27)$$

$$A'_0 = \frac{(b'_1 - 4c'_1)k_{21}h_2}{a'_1 k_2 h_{22} - (3k_{20}h_2 - 2h\alpha)c'_1}; \qquad (1.28)$$

$$B'_0 = -\frac{d'_1 k_{22} h_2}{a'_1 k_{22} h_2 - (3k_{20}h_2 - 2h\alpha)c'_1}; \qquad (1.29)$$

$$C'_0 = \frac{f'_1 k_{22} h_2 + 2h\alpha c'_1}{a'_1 k_{22} h_2 - (3k_{20}h_2 - 2h\alpha)c'_1}. \qquad (1.30)$$

using formulas (1.13 and (1.16) (for $i = n-1$), the right-hand boundary conditions (1.15) and (1.18) and the formulas (1.19), (1.20) (for $i = n-1$) on the ng side P_{1n} va P_{2n} we find.

After the reorganization, we obtain the following systems of equations, two of which are unknown P_{1n} and P_{2n}:

$$\left[(3a_{n-1} - c_{n-1}) - (4a_{n-1} - b_{n-1})A_{n-1} - d_{n-1}B'_{n-1}\right] P_{1n} + \\ + \left[(4a_{n-1} - b_{n-1})B_{n-1} - d_{n-1}A'_{n-1}\right] P_{2n} = \\ = \left[d_{n-1}C'_{n-1} + f_{n-1} + (4a_{n-1} - b_{n-1})\right];$$

$$\left[(3a'_{n-1} - c'_{n-1}) - (4a'_{n-1} - b'_{n-1})A'_{n-1} - d'_{n-1}B_{n-1}\right] P_{2n} + \\ + \left[(4a'_{n-1} - b'_{n-1})B'_{n-1} - d'_{n-1}A_{n-1}\right] P_{1n} = \\ = \left[d'_{n-1}C_{n-1} + f_{n-1} - (4a'_{n-1} - b'_{n-1})\right].$$

From these systems P_{1n} and P_{2n}, Depending on the solution we get:

$$P_{1n} = (S_2 \cdot S'_3 - S_3 \cdot S'_1)/(S_1 \cdot S'_1 - S_2 \cdot S'_2); \qquad (1.31)$$

$$P_{2n} = (S_3 \cdot S'_2 - S_1 \cdot S'_3)/(S_1 \cdot S'_1 - S_2 \cdot S'_2); \qquad (1.32)$$

Here:

$$S_1 = \left[(3a_{n-1} - c_{n-1}) - (4a_{n-1} - b_{n-1})A_{n-1} - d_{n-1}B'_{n-1}\right];$$

$$S_2 = \left[-(4a_{n-1} - b_{n-1})B_{n-1} - d_{n-1}A'_{n-1}\right];$$

$$S_3 = \left[f_{n-1} + d_{n-1}C'_{n-1} + (4a_{n-1} - b_{n-1})C'_{n-1}\right];$$

$$S'_1 = \left[(3a'_{n-1} - c'_{n-1}) - (4a'_{n-1} - b'_{n-1})A'_{n-1} - d'_{n-1}B_{n-1}\right];$$

$$S'_2 = \left[-(4a'_{n-1} - b'_{n-1})B'_{n-1} - d'_{n-1}A_{n-1}\right];$$

$$S'_3 = \left[f'_{n-1} + d'_{n-1}C_{n-1} + (4a'_{n-1} - b'_{n-1})C_{n-1}\right].$$

Conducting computer experiments and their analysis

The program was developed based on a mathematical model and a computational algorithm. The software consists of a block of input data, a block of calculation of the main indicators of gas field operation and a block of output of numerical results. The numerical results of the calculated indicators are presented to the user in visual form in tabular and graphical form. Calculation experiments were performed on different values of well debits and formation parameters.

These parameters and their values are given below:

- n = 101 - number of steps for a discrete field;
- h = 0.01 - step;
- p_{n1} = 200 atm. - pressure in the first layer;
- p_{n2} = 200 atm. - pressure in the second layer;
- Lesson k_1 = 0.01 - the coefficient of permeability of the first layer;
- Lesson k_2 = 0.01 - the coefficient of permeability of the second layer;

- Lesson $k_p = 0.0000001$ - sluggish layer permeability coefficients;
- $\mu = 0.02\ s_{pz}$ - gas viscosity coefficient;
- $m = 0.2$ - porosity coefficient;
- $x_l = 10000$ meters - the length of the layer;
- $q = 1000000\ m^3$/day - flow rate of wells;
- $n_t = 720$ days - calculation time;
- $h_1 = 10$ meters - the thickness of the first layer;
- $h_2 = 10$ meters - the thickness of the second layer;
- $h_p = 1$ meter - the thickness of the permeable layer.

Computational experiments were performed mainly on different values of stratum permeability, gas viscosity and well flow rate. Fig. 2 and 3 show the pressure drop in the wells and the pressure changes in the layers as a result of 720 days of operation of the field. There are two wells near the center with a flow rate $q = 1000000\ m^3$/sec. The results in these figures show that the pressure drop in the upper layer at the initial time is very small and the pressure drop stabilizes over time. This process is clearly seen in Fig. 2. The reason for the extraction of gas from the bottom layer is that here the pressure drop in the wells decreases rapidly at the beginning and then stabilizes.

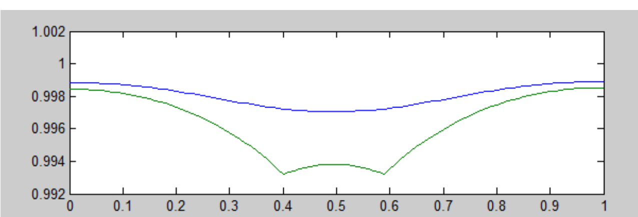

Fig. 2: Graph of pressure changes in the upper and lower layers ($k_p = 0.0000001$ lessons)

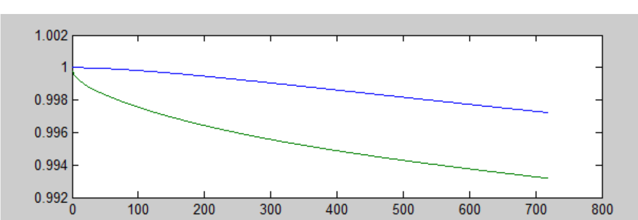

Fig. 3: Graph of pressure drop in the well and at the corresponding point in the upper layer ($k_p = 0.0000001$ lesson)

III CONCLUSION

The methods and techniques developed to calculate the key performance indicators of two-layer gas fields, as well as the software can be used in process analysis and design, as well as in the operation of multi-layer oil and gas fields.

Using the proposed numerical method, the solution of systems of equations can be easily generalized for a system of three or more equations. The results obtained are useful for analyzing the development of multilayer gas fields in the dynamic relationship between layers.

IV REFERENCES

[1] Grigoryan L.A., Timofeeva E.F. Mathematical modeling of the problem of oil field development // Natural and mathematical sciences in the modern world: Proceedings of the XVIII Intern. scientific-practical Conf. - Novosibirsk: SibAK, 2014. - No. 5 (17). - pp. 52-62.

[2] Davletbaev A.Ya., Filtration of fluid in a porous medium with wells with a vertical hydraulic fracturing fracture // Inzhenerno-fizicheskii zhurnal., Minsk, 2012. - T. 85, No. 5. - pp. 919-924.

[3] Nazirova E.Sh., Sodikov R.T., Construction of mathematical dependencies for some parameters of the reservoir environment // Actual problems of applied mathematics and information technologies - Al-Khorazmi: Proceedings of the conference. - T. 1., September 15-17, 2014, Samarkand, - pp. 132-133.

[4] Nazirova E.Sh., Modular analysis of the algorithm for solving problems of filtration of multiphase liquids in porous media // Uzbekistan magazine "Problems of Informatics and Energy". 2014, - No. 5., - pp. 48-52.

[5] Nazirova E.Sh., Sodikov R.T., Bakhriddinov A.K., Creation of the Matlab system for visualizing the solution of problems of two-dimensional parabolic equations // The value of information and communication technologies in the innovative development of the real sector of the economy: Abstracts. report Republican scientific and technical conference. Part 1. - Tashkent, 2017, - pp. 332-334.

[6] Nazirova E.Sh., Numerical modeling of oil filtration processes in multi-layer porous media with dynamic connection between layers // Descendants of Muhammad Al-Khorezmi., - Tashkent, 2018., - No. 4 (6)., - pp. 10-14.

[7] Nazirova E.Sh., Mathematical model of oil filtration process in multi-layer porous media // Actual problems

of mathematics and mechanics - CAWMA-2018: Abstracts. report Republican scientific and practical conference with the participation of foreign women scientists. October 25-26, 2018, - Khiva, - pp. 50-51.

Acta of Turin Polytechnic University in Tashkent, 2022, 31, 46-50
Published Online March 2022 in Acta TTPU (http://www.acta.polito.uz/)

TELEVISION SYSTEMS FOR MEASURING THE COORDINATES OF INDUSTRIAL AND MOBILE ROBOTS

Rakhmanova E.E.[1], Gulyamova N.B.[2]
Tashkent state technical university named after Islom Karimov
Address: 2, University str., 100095, Tashkent, Uzbekistan
[1]Email: raxmanovae07@gmail.com

Abstract– Nowadays, the use of innovative intelligent technologies in the control of industrial robots is becoming increasingly popular. This article discusses the use of television systems in measuring and controlling the coordinates of industrial robots. It is possible to control the object of movement and speed parameters of the executive element of the industrial robot through television systems. With the information detected by the television measurement system, broader possibilities of robot control are provided by flexible modification of control programs in real time. Using monocular television camera systems to measure the coordinates of industrial robots, it is possible to study space and underwater systems, detect errors that occur during manipulation. The structural and geometrical dimensions of the monocular television measuring camera system, the functional scheme of the correlation optical measurement system to account for velocity in moving positions, the functional scheme of the differential correlation optical measurement system and their use, and mathematical models of calculating detected errors are given.

Key words– Industrial robot, coordinate measurement of industrial robots, television measuring system, monocular television measuring camera system, industrial robot control, mobile robots, correlation optical measurement.

I Introduction

In many industrial robots, it is necessary to determine the position of a controlled object or its individual points in three-dimensional space. Either the simplest technical vision system TVS designed to solve such problems are built according to the classical stereoscopic scheme, or they use a two-dimensional flat image analyzer, for example, a coordinate or matrix photodetector in combination with a rangefinder [1,2]. Let's consider some ways of using the survey television systems of the robot to determine the spatial coordinates of objects. Such systems, in particular, have found application in supervisory control systems for robots.

II Methodology

A monocular television system can be used to determine the polar angles of objects (Fig. 1). In the coordinate system associated with the camera, the polar angles of point N on the object surface are determined by the formulas:

$$\alpha_{Nk} = \arctan \frac{x_{N\exists}}{k(F+\delta_{CM})}; \quad \beta_{Nk} = \arctan \frac{k(F+\delta_{CM})}{z_{N\exists}\cos\alpha_{Nk}}; \quad (1)$$

where k – is the image magnification factor equal to the ratio of the image size on the screen to the size of the image on the photo target of the transmitting tube with the coordinate system $Z_{mish}\ O_{mish}\ X_{mish}$; $x_{N\partial}, z_{N\partial}$- coordinates of the image of point N on the screen (relative to the center of the screen); F - focal length of the lens; δ_{sm} - linear displacement of the lens [1,3].

To measure the third coordinate - range - the method of automatic optical focusing (AOF) can be used. The distance to a given point on the screen is determined by the lens shift δ_{sm}, which ensures maximum image detail in a small neighborhood of this point on the photo target of the transmitting television tube [3, 4]. The measurement error of the angular coordinates of the considered system is determined by the nonlinearities of the sweeps of the transmitting camera and the television receiver. The error in determining the range by the AOF method for the same setup also reaches 10%. The described television system for measuring coordinates is used in target designation systems for space and underwater robots.

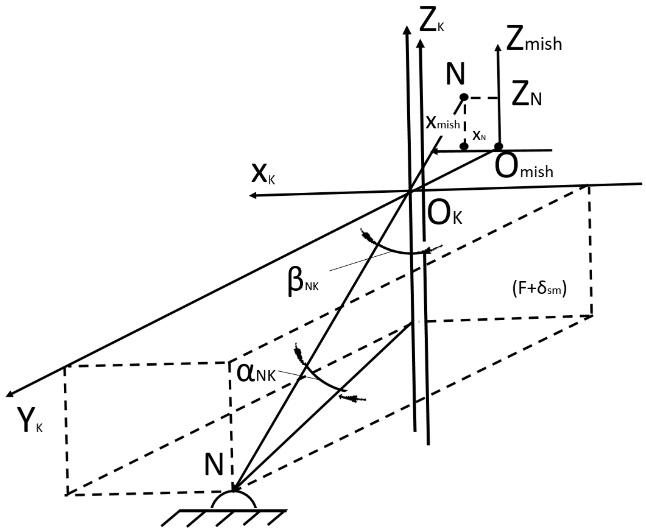

Fig. 1: Scheme of measuring the coordinates of the target using a monocular television camera.

III Monocular television coordinate measurement system

The error in measuring the coordinates of objects can be reduced if the objects are indicated not in the space of images, but in the space of objects (Fig. 2, a) using a directional light source. Television systems for measuring coordinates with one transmitting tube and a source of directional light are similar in principle to the active optical rangefinder described above [5]. The TVS camera (Fig. 2, a) is located in the receiving branch, and the directional light source with the guidance drive is placed in the transmitting branch of the rangefinder. The distance from the emitter to the target (Fig. 3, b) is determined by the following expression:

$$l_i = \frac{d \sin \beta_{ts-k}}{\sin(\beta_{ts-i} - \beta_{ts-k})} \tag{2}$$

where the angle β_{ts-k} is determined by the formula (1), the angle β_{ts-i} is the angle of rotation of the emitter, d is the base of the rangefinder. Here, the angles l_i, a and β are taken into account to determine the Cartesian coordinates of the point being measured:

$$x_1 = l_i \cos\beta \sin a; \quad x_2 = l_i \cos\beta \cos a; \quad x_3 = l_i \sin\beta. \tag{3}$$

The Cartesian coordinates of the target in the camera coordinate system can be calculated using (3). The relative measurement error of the angular coordinates in the coordinate system associated with the light source is determined by the error of the devices for measuring the rotation angles of

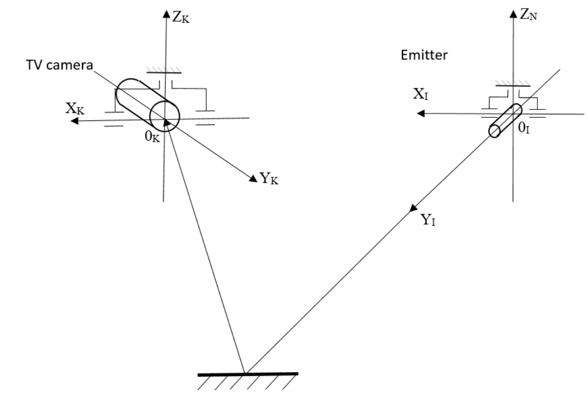

Fig. 2: Schemes of a monocular television system for measuring coordinates with a source of directional light: *a*) - structural;

the light source pointing mechanism. For example, when using precision potentiometers, this error does not exceed 0.3% [6,7].

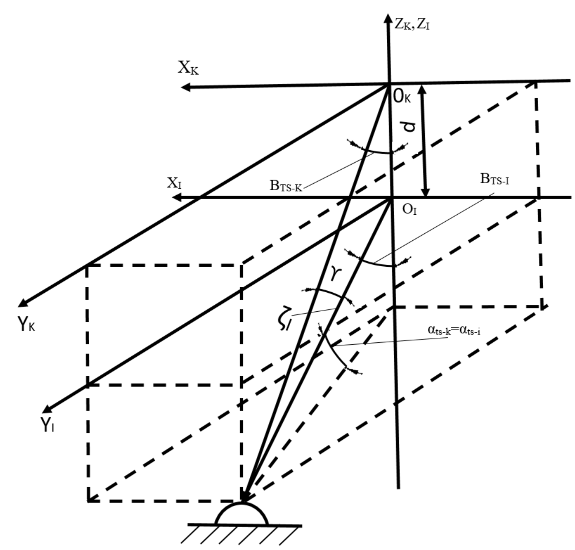

Fig. 3: Schemes of a monocular television system for measuring coordinates with a source of directional light: *b*) - geometric.

The error in measuring the range with a basic geometric rangefinder depends on the error in measuring the target viewing angles and the parallax angle, which in our case is equal to:

$$\gamma = \beta_{ts-i} - \beta_{ts-k}$$

Range measurement error at $l_k \geqslant d$

$$\Delta l_k = \frac{d}{\gamma}(\cos \beta_{ts-i} \Delta \beta_{ts-i}) + \sin \beta_{ts-i} \delta \gamma \tag{4}$$

The determining factor in this amount is the measurement error of the television receiver, so the error in measuring the range to the target does not exceed 10%.

IV ANALYSIS AND RESULTS

The papers describe devices for determining the spatial coordinates of objects with two transmitting cameras. It points out the difficulties of the pointing purpose associated with the identification of the characteristic points of an object when working with separate images, as well as with the complexity of introducing an electronic label into a stereoscopic image and managing it. This problem is solved quite simply if the objects are pointed with a directional light source (Fig. 4). Target coordinates can be calculated using formulas similar to those given for the single camera and emitter method.

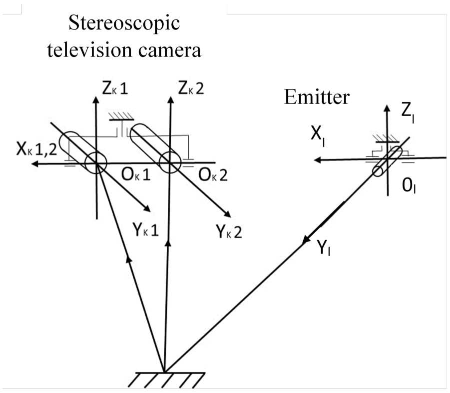

Fig. 4: Scheme of a stereoscopic television system for measuring coordinates with a source of directional light.

Measuring the range to the target by the methods described above gives low accuracy. This drawback can be overcome if, instead of a directional light source, special range-finding devices, such as laser or ultrasonic, are used. The latter should also be equipped with directional light sources that provide visual registration on the TVS screen of the moment the rangefinder is pointing at the object. The rangefinder is guided using an optical-mechanical or mechanical scanner (scanning device), the rotation angles of which determine the polar angles of the target. Distance measurement error when using ultrasonic rangefinders is $5 \cdot 10^{-3}$, and for laser rangefinders -10^{-3}. At the same time, there is no need for calculations inherent in the geometric method. Another feature of the stereoscopic television system for measuring coordinates with a directional light source is the measurement of the correlation of the robot's speed [8, 9].

The correlation method of measuring this speed is based on the automatic calculation of the correlation function of the reflected signals received from two points on the surface relative to which the movement occurs, and on determining the time shift between these signals. The positive qualities of correlation velocity measurements are their non-contact and high measurement accuracy [1,2,10].

Considered in Fig. 5 is a functional diagram of the correlation optical meter of the speed of the robot. Two sources of light strokes $L1$, $L2$, focused on the surface, are located one after the other at a distance l along the longitudinal axis of the robot. During its movement, due to structural heterogeneity and surface roughness, the brightness of the strokes changes. The stroke image is perceived by the receiving optical system and fed to photodetectors $FP1$, $FP2$. Since the second stroke is displaced relative to the first in the direction of movement by a distance l, then the signal $f_1(t)$, characterizing the brightness of the first stroke, will be repeated on the second stroke with some delay τ_T, i.e. the second signal $f_2(t)$ will be close in shape to the first signal through τ_T: $f_2(t) \approx f_1(t - \tau_T)$.

Cross-correlation function of these two signals:

$$R(\tau) = M\left[(t-\tau)f_2(t)\right] = \lim_{T\to\infty}\frac{1}{T}\int_0^T f_1(t-\tau)f_2(t)dt =$$

$$= \overline{f_1(t-\tau)f_2(t)} = \overline{f_1(t-\tau)f_1(t-\tau_T)} = A(t-\tau_T) \quad (5)$$

The function $R(\tau)$ has a maximum at $\tau = \tau_T$. where τ - is the introduced adjustable delay. It can be implemented using the multiplication block $f_1(t-\tau)$ and $f_2(\tau)$ followed by smoothing (integrating filter IF). The speed of movement of the robot $\upsilon = l/\tau_T$.

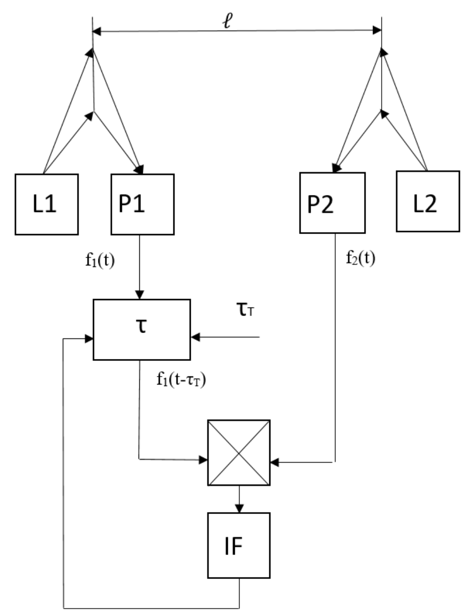

Fig. 5: Functional diagram of a correlative optical speed meter.

One of the most effective methods for constructing an automatic correlator is the method of double relay correlation functions based on the replacement of continuous functions $f_1(t)$, $f_2(t)$ by relay functions (signum functions) [1,11,12]. This method makes it possible to find, using rather simple hardware, the position of the maximum of the correlation function of a random continuous signal on the time delay axis. The double relay autocorrelation function is determined by the formula:

$$A(\tau) = \lim_{T\to\infty} \frac{1}{T} \int_0^T sign[f(t)] \times sign[f(t+\tau)]\, dt \qquad (6)$$

In this case, the multiplier device in the correlator circuit is reduced to a simple coincidence circuit.

Considered in Fig. 6 shows a functional diagram of a differential correlation speed meter. Signals $f_1(t)$, $f_2(t)$ come from the amplifiers U1, U2 to the shapers of the signum signals SSSh1, SSSh2. From the output F1, the sign signal $f_1^{'}$ is fed to the converter of the sign signal into pulses corresponding to the zero values of the sign signals. From the output of the converter C, the signal $f_1^{''}$ is fed to the coarse delay circuit $\tau^{'}$, the delayed signal $\tau^{'}$ is fed to the fine delay circuit τ.

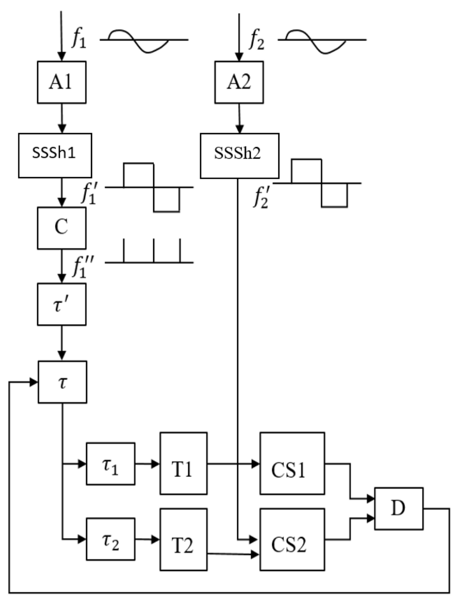

Fig. 6: Functional diagram of a differential correlation speed meter.

The delayed signal is divided into two channels. One channel carries out a delay for time τ_1, and the second - for τ_2. Delays τ_1, τ_2 are necessary for the implementation of the differential circuit of the automatic fine delay controller. The signals delayed by τ_1, τ_2 are fed to the generating triggers T1, T2, and then to two matching circuits CS1, CS2, which control the electronic key. In the emitter of the electronic key there is an integrating capacitor, the charge on which is determined by the time of the on state of the electronic key [3,13,14]. The voltage accumulated on this capacitance controls the precise delay circuit τ. At the same time, this tension, proportional to the speed of the robot, enters the navigation system of the robot.

V Conclusion

All the researches and analyzes considered show that the use of television systems in increasing the functionality of industrial robots will help to bring the management to the level of intelligence. The article fully explains the use of television systems in measuring and controlling the coordinates of industrial robots on the basis of mathematical expressions that can control the object of movement and speed parameters of the executive element. The structural and geometric dimensions of the television measuring camera system were analyzed in depth. The functional scheme of the correlation optical measurement system, the functional scheme of the differential correlation optical measurement system and the methods of their use, taking into account the speed of movement, were analyzed in depth. From the research reviewed, it can be said that the use of television systems in measuring and controlling the coordinates of industrial robots allows for higher efficiency and improved quality performance.

VI References

[1] Hartley R., Zisserman A., Multiple View Geometry in Computer Vision. 2nd ed. Cambridge: Cambridge University Press, 2003., pp. 655.

[2] Bouguet J.Y., Visual methods for three-dimensional modeling: PhD Thesis. Pasadena: California Institute of Technology, 1999., pp. 214.

[3] Trobina M., Error Model of a Coded-Light Range Sensor: Technical Report: BIWI-TR-164 / ETH-Zentrum. Zurich, 1995., pp. 36.

[4] Putjatin E.P., Image Processing in Robotics // Mechanical Engineering - Moscow, 1990. - pp. 320.

[5] Ablameiko S.V., Lebedev V.I., Lagunovsky D.M., Automatic Image Analysis and Control // Minsk, 1993. pp. 103.

[6] Popov E.P., Control and Software of Complex Robotics Systems// Izvestiya RAN. Theory and Control Systems, №1, 1995.

[7] Zhabsky E.V., Makarov A.Yu., Television system for measuring the coordinates of objects. // Patent № SU 1107341.

[8] Ovchinnikov A., Makaretsky E., Liem Khieu Nguyen, Television measuring systems for controlling traffic speeds // Components and technologies No 4, 2007, pp. 124-129.

[9] Rakhimov T.O., Algorithm for controlling multi-coordinate mechatron modules of an industrial robot / Journal of Modern Technology and Engineering Vol.5, No.2, 2020, pp.247-253.

[10] Nazarov Kh.N., Rakhimov T.O. The concept of force-moment sensing of multi-position mechatronic modules of intelligent robots / Technical science and innovation. Tashkent, 2021. Vol 2, №10. pp. 206-213 doi.org/10.51346/tstu-01.21.2-77-0127

[11] Babich A.M., Methods and algorithms for determining the spatial characteristics of stationary objects in the navigation of a mobile robot with a monocular vision system // Problems of Radioelectronics. Series "Information display and control systems of special equipment", 2012, Edition 1, pp. 156-162.

[12] Nazarov Kh.N., Rakhimov T.O., The concept of the mathematical description of the multi-coordinate mechatronic module of the robot. Acta of Turin Polytechnic University in Tashkent, International scientific and technical journal, 2020, pp. 15-20.

[13] Babich A.M., The use of monocular vision system in estimating the distance to obstacles // Radio Electronics Issues, Series "Electronic Calculating Technique", 2008, Edition 5, pp. 107-111

[14] Tishenko A.S., Mikhailov V.V., Mobile robot navigation based on on-board vision system // Mechatronics, Automation, Control. 2009, №12. p. 44-50

Acta of Turin Polytechnic University in Tashkent, 2022, 31, 51-54
Published Online March 2022 in Acta TTPU (http://www.acta.polito.uz/)

CALCULATION OF THE AMOUNT OF EMISSIONS OF HARMFUL SUBSTANCES BY CARS AT URBAN INTERSECTIONS

Bazarov B.I.*, Ernazarov A.A..**
*Tashkent State Transport University, **Andijan machine - building Institute
*Email: baxtbb@mail.ru
**Email: aziz-ernazarov@mail.ru

Abstract– A study of the traffic flow of one of the busiest central streets of the city of Jizzakh – I. Karimov Avenue. A complete description of the intersections of this transport highway is given. To perform the calculations, observations and counting of the number of vehicles crossing intersections were carried out. The calculation of the amount of exhaust gas emissions into the atmosphere was made.

Key words– Road transport, motorway, vehicle emissions, intersection, structure of the flow of vehicles.

I Introduction

Automobile transport has become the most serious source of atmospheric air pollution in our time. This is especially noticeable in large cities.

The main consequence of the increase in the number of vehicles is the increase in anthropogenic impact on the environment and, above all, on the atmosphere of built-up areas. Car emissions, first of all, are dangerous because they enter directly into the surface layer of the atmosphere, where the wind speed is negligible and therefore gases are poorly dispersed [1,2,4,6].

The purpose of this work is to identify the maximum possible concentrations of pollutants emitted by vehicles on I.Karimov Avenue in the city of Jizzakh. During the operation of transport, a huge amount of dust and toxic substances contained in the exhaust gases of power plants enter the atmosphere, high noise levels are created, air, soil, water bodies are polluted as a result of the discharge and spillage of fuels and lubricants, many other substances harmful to the natural environment and humans are formed. The level of gas contamination of highways and adjacent territories depends on the intensity of car traffic, the width and relief of the street, wind speed, the share of freight transport and buses in the total flow, and other factors. It is difficult to disperse car emissions on cramped streets. As a result, almost all residents of the city experience the harmful effects of polluted air.

In the period July – August 2021, a study of the traffic flow along the entire length of I. Karimov Avenue (Jizzakh) was conducted. This urban transport highway was chosen as the busiest, connecting the main transport overpasses of the city of Jizzakh, both intra-city routes of motor transport and intercity routes pass through it.

The total length of I.Krimov Avenue is 7197 m. The width of the roadway is 23 m.. The number of traffic lanes in each direction is 3. There are six regulated intersections: from Mustakillik Street, Baynaminal Street, Khamrakulova Street, Shifokorlar Street, Kalia Street, Tashkent Street.

The need to divide I.Karimov Avenue into separate section is caused both by the presence intersections of various types and by the different nature of traffic flow throughout the avenue.

The following division of I. Karimov Avenue into section was carried out (the approximate length of each section was determined using a navigator), the frequency of traffic light was determined for regulated intersections, taking into account the effect of prohibiting ("red" and 2 "yellow") and permitting ("green") traffic light signals. During the research work, the "Methodology for determining vehicle emissions for conducting summary calculations of urban air pollution" was used to estimate the values of emissions of pollutants into the atmosphere by motor vehicles on urban highways[3].

II Calculation of emissions of moving vehicles

The emission of the i-th pollutant (g/s) by a moving motor vehicle flow on a motorway (or its section) with a fixed length L (km) is determined by the formula:

$$M_{Li} = \frac{L}{3600} * \sum_{1}^{k} M_{k.i}^{m} * G_K * r_{Vk,i} \quad (1)$$

where:

$M_{k.i}^{m}$ (g/km) is the mileage emission of the i-th harmful substance by k-th group cars for urban operating conditions;

k - number of groups of cars;

G_K (1/hour) - the actual highest traffic intensity, i.e. the number of cars of each of the k groups passing through a fixed section of the selected section of the motorway per unit of time in both directions along all lanes;

$r_{Vk,i}$ - correction factor taking into account the average speed of traffic flow on the selected highway (or its section);

1/3600 - conversion factor "hour" to "sec";

L (km) - the length of the motorway (or its section) from which the length of the queue of cars in front of the forbidding traffic light signal is excluded and the length of the corresponding intersection zone (for intersections where additional surveys were conducted)[4].

Calculation of vehicle emissions in the area of a regulated intersection.

When calculating the levels of air pollution in the intersection zones, it is necessary to proceed from the highest values of the content of harmful substances in the exhaust gases characteristic of the modes of movement of cars in the area of the intersection of highways (braking, idling, acceleration). The release of the i-th pollutant (g/min) in the intersection zone at a traffic light prohibiting signal is determined by the formula:

$$M_{Ci} = \frac{P}{40} \sum_{n-1}^{N_{cycle}} \sum_{k-1}^{N_{groups}} (M_{Ci,k} * G_{k.n}) \quad (2)$$

where:

P (min) is the duration of the prohibiting signal of the traffic light (including yellow);

N_{cycle} - the number of cycles of the forbidding traffic light signal for a 20-minute period of time;

N_{groups} - number of groups of cars;

M_{Ci} (g/min) is the specific emission of the i-th pollutant by cars of the k-th group that are in the "queue" at the forbidding traffic light signal;

$G_{k.n}$ is the number of cars of group k that are in the "queue" in the intersection area at the end of the nth cycle of the traffic light prohibiting signal.

Thus, for a motorway (or its section) in the presence of a regulated intersection, the total emission M will be equal to:

$$M = \sum_{1}^{n} (M_{C1} + M_{C2}) + M_{L1} + M_{L2} + \sum_{1}^{m} (M_{C3} + M_{C4}) + M_{L3} + M_{L4} \quad (3)$$

where:

M_{C1}, M_{C2}, M_{C3}, M_{C4} is the emission into the atmosphere by cars located in the intersection zone with a forbidding traffic light signal;

M_{L1}, M_{L2}, M_{L3}, M_{L4} - emission into the atmosphere by cars moving along this highway during the time period under consideration;

n, m - the number of stops of the traffic flow before the intersection, respectively, on one and the other streets forming it for a 20-minute period of time;

indexes 1 and 2 correspond to each of the 2 directions of traffic on a highway with a higher traffic intensity, and 3 and 4 correspond respectively for a highway with a lower traffic intensity[3].

As initial data for calculating vehicle emissions into the atmosphere, the results of field surveys of the structure and intensity of traffic flows with a subdivision for the main categories of vehicles were used[6].

Emission calculations were performed for the following harmful substances entering the atmosphere with the exhaust gases of cars:

- carbon monoxide (CO);
- nitrogen oxides NO_x (in terms of nitrogen dioxide);
- sulfur dioxide (SO_2);

To determine the characteristics of traffic flows on the selected sections of I. Karimov Avenue, the accounting of passing vehicles in both directions with a subdivision by groups was carried out, Table 1.

This table shows the number of vehicles passing through the corresponding section of I. Karimov Avenue for 1 hour of observation time on this section. The observation time is selected - the summer period, the observation hours are 11-00 to 14-00, the days of the week are Saturday and Sunday, since during this period there is a maximum load of motor traffic on the selected overpass of the city.

A preliminary analysis of Table 1 allows us to identify the most loaded sections of the highway.

In our case, this is the intersection with Mustakillik Street and the intersection with Tashkent Street. There is the greatest movement of vehicles here – up to 1,500 cars per 1 hour (during peak hours). A significant load of the intersection with Tashkent Street is due to the fact that this intersection is a link between intra-city transport networks and intercity.

The analysis of Table 1 by groups of vehicles allows you to specify the type of vehicles represented on the streets of the city in greater numbers - passenger vehicles - about 88%

TABLE 1: ACCOUNTING OF MOTOR VEHICLES

Vehicle group	I. Karimov Avenue				
	Intersection with Mustakillik Street	Intersection with Baqnaminal Street	Crossroads with Shifokors' Street	Intersection with Kaliya Street	Intersection with Tashkent Street
P - passenger car	1282	658	782	721	1498
T<3 t - trucks	52	87	53	76	86
T>3t trucks	6	1	1	1	16
B - the buses	48	33	29	32	83
DT – disel trucks	13	0	0	0	26
Total	**1401**	**779**	**865**	**830**	**1709**

of the total number of passing vehicles on the studied street, 4% - buses of the "Isuzu" type.

In the study of regulated intersections, the length of the queue of standing vehicles for a forbidding traffic light signal is taken into account, the data obtained is supposed to be used to calculate the dispersion of emissions in the direction of residential areas.

The calculation of emissions of pollutants by vehicles at each allocated site was carried out with the distribution by groups of vehicles for both moving and standing vehicles at regulated intersections according to the above methodology, Tables 2-4, Fig. 1-3.

Name of the intersection	Mass emission, g/s	g/s per 1 m
Mustakillik Street	5,281	0,021
Street B a nominal	1,400	0,006
Shifokors' Street	0,414	0,007
Kaliya Street	1,493	0,008
Tashkent Street	4,596	0,021
Total	**13,184**	**0,063**

TABLE 2: CALCULATION OF CO EMISSIONS (TOTALS)

A preliminary analysis of CO emissions allows you to specify the areas (for this substance) with the highest values – the intersection with Mustakillik Street and Tashkent Street.

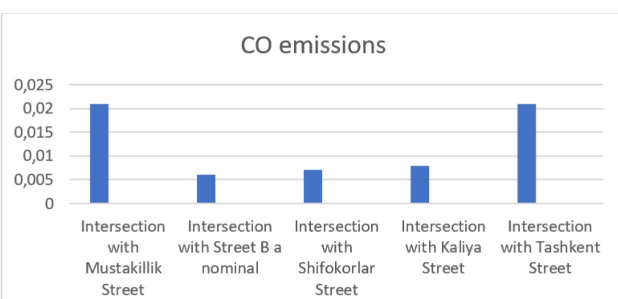

Fig. 1: Emission of CO g/s per 1 m. of linear sections

Name of the intersection	Mass emission, g/s	g/s per 1 m
Mustakillik Street	0,204	0,000917
Street B a nominal	0,089	0,000413
Shifokors' Street	0,055	0,000379
Kaliya Street	0,078	0,000419
Tashkent Street	0,230	0,001921
Total	**0,656**	**0,004049**

TABLE 3: CALCULATION OF NO_x EMISSIONS (TOTALS)

A preliminary analysis of NO_x emissions allows you to specify the areas (for this substance) with the highest values – the intersection of Mustakillik streets and Tashkent streets.

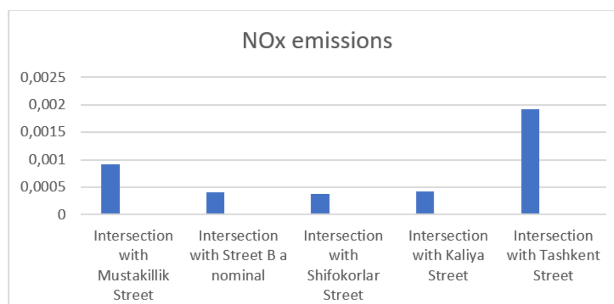

Fig. 2: NO_x emission g/s per 1 m. of linear sections

Further analysis of the tables will make it possible to determine such positions as the most polluted section of I. Karimov Avenue, "the type of vehicles that have the greatest negative impact on the OS", "the concentration of harmful substances mg/m3 from vehicles", the dependence of the emission of harmful substances on the mode of movement of vehicles and the type of vehicles, etc.[5].

The city of Jizzakh is characterized by compact urban development, the main highways run through all residential areas and vehicle emissions have a direct negative impact on the health of the city's population. Therefore, the issue of the impact of vehicle emissions on the health of the population for our city is relevant, requires its study and making important decisions.

Name of the intersection	Mass emission, g/s	g/s per 1 m
Mustakillik Street	0,00677967	5,74087E-05
Street B a nominal	0,004817484	2,23032E-05
Shifokors' Street	0,00143092	2,55522E-05
Kaliya Street	0,004913175	2,64149E-05
Tashkent Street	0,006289401	5,87794E-05
Total	**0,01923065**	**0,000190458**

TABLE 4: CALCULATION OF CO_2 EMISSIONS (FINAL VALUES)

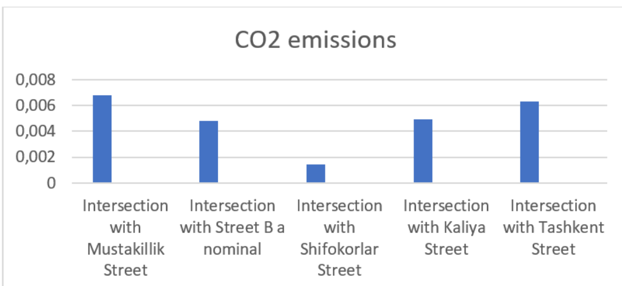

Fig. 3: CO_2 emission g/s per 1 m. of linear sections

As a result of the conducted field surveys of urban highways, streets and intersections with increased traffic intensity were identified. A study of the traffic flow of one of the busiest central streets of the city – I. Karimov Avenue.

III CONCLUSION

The analysis of the collected and calculated data made it possible to identify the busiest sections of the considered urban highway, classify the traffic flow, identify groups of vehicles that make the greatest contribution to the pollution of the city's atmosphere (taking into account the traffic flow mode). The practical work carried out will make it possible to use the data obtained in the future to compile summary reports on emissions, specific calculations on atmospheric air pollution and subsequent assessment of the impact of polluted air on the population living along urban highways, as well as to give some recommendations on the organization and regulation of vehicle traffic within residential areas of the city: the creation of additional road interchanges, redirection of freight transit vehicles to bypass residential areas, etc.

IV REFERENCES

[1] Grushnikov V. A., Aspects of alternative ecology of motor transport // Transport: science, technology, management. Scientific Information collection, 2021, No. 9, pp. 39-43., *doi: 10.36535/0236-1914-2021-09-7.*

[2] Litman T., Smart Transportation Emission Reduction Strategies. Identifying Truly Optimal Ways to Conserve Energy and Reduce Emissions., Victoria Transport Policy Institute, 2015.

[3] Kazhaev A., Almetova Z., Shepelev V., Shubenkova K., Modelling urban route transport network parameters with traffic, demand and infrastructural limitations being considered., IOP Conference Series: Earth and Environmental Science 177, 2018, *doi: 10.1088/1755-1315/177/1/0120.22*

[4] Kerimov M., Safiullin R., Marusin A., Evaluation of functional efficiency of automated traffic enforcement systems Transportation Research Procedia, 20 (2017), pp. 288-294, *doi: 10.1016/j.trpro.2017.01.025.*

[5] Marusin A., Danilov I. A Method for assessing the influence of automated traffic enforcement system parameters on traffic safety Transportation Research Procedia, 36 (2018), pp. 500-506, *doi: 10.1016/j.trpro.2018.12.136.*

[6] Bazarov B. I., Kalauov S. A., Vasidov A. X. Alternative motor fuel/ Monograph. Tashkent: SHAMS ASA, 2014.

Acta of Turin Polytechnic University in Tashkent, 2022, 31, 55-61
Published Online March 2022 in Acta TTPU (http://www.acta.polito.uz/)

DEVELOPMENT OF THE NETWORK OF URBAN ROADS AND STREETS (ON THE EXAMPLE OF THE CITY OF URGENCH)

Fazilat Saydametova[1], Amir Beketov[2],Shakhnoza Khalimova[3] and Abduvokhid Yunusov[4]
Tashkent State Transport University
Email: [1]fazilat@tstu.uz,[2]beketovamir@umail.uz,
[3]khalimovashakhnoza@umail.uz, [4]abduvokhid.yunusov@gmail.com

Abstract– The article analyzes the state of the road network in Urgench. The importance of the organization of highways in improving the future road network of the city will be considered as a key issue. It covers the results of studies on the organization of the process of safe traffic and improving the capacity of the road, as well as suggestions and recommendations for solving existing problems. The proposed measures will significantly alleviate congestion on the city street network without disrupting transport links within the city.

Key words– urban road network, infrastructure, urban public transport, capacity of road, congestion, results, analysis, traffic flow.

I INTRODUCTION

An increase in traffic intensity, traffic flows and, as a result, congestion, excessive pollution and increased noise levels due to long stays at intersections, public transport delays due to disruption of public transport schedules, as well as an increase in traffic accidents has become a actual problem in the city of Urgench, along with other large cities. Therefore, the search for a modern solution to the problems of the city's transport complex, the development of transport infrastructure and the development of the road network remains relevant.

It is known that a rapid increase in traffic intensity on the road network of the city of Urgench is accompanied by an increase in traffic intensity due to a decrease in the capacity of streets and the speed of vehicles (especially cars). The main reason for these problems is due to the rapid increase in the number of vehicles on urban streets. Competent organization of the urban street and road network will largely achieve the reliability of the entire urban transport system, the quality of service and the adoption of the necessary engineering and technical solutions, including the reduction of traffic accidents.

In accordance with the Decree of the First President of the Republic of Uzbekistan dated December 6, 2012 No. DP-1874 "On measures to implement the master plan for the city of Urgench, to fundamentally improve the improvement and water supply of the population of the Khorezm region", Design Institute "Uzshaharsozlik LITI" developed a program for the development of the road network until 2030 and is gradually implementing it [1].

However, it should be noted that in addition to the achievements in the industry, there are many problems that have yet to be solved. The fact that the indicators set by the current regulations in the field of urban transport exceed the normative indicators requires scientific research and the development of necessary measures in this area.

II MATERIALS AND METHODS

Scientists from a number of CIS countries and the world in their works, monographs and scientific articles gave a lot of information on the development of the urban street and road network, made important scientific and practical conclusions. But the vast majority of researchers have set themselves the task of finding options for optimizing urban transport and the road network in large cities [2-6]. Currently, traffic congestion and the associated increase in road traffic accidents are also increasing in cities with less than 100,000 inhabitants.

It is no secret that the development of transport infrastructure plays an important role in the development of economic sectors. In this regard, in accordance with the "Strategy of Actions", initiated and implemented by the President of the Republic of Uzbekistan Sh. Mirziyoyev, a specific action plan has been defined and is gradually being implemented in five priority areas of development of the Republic of Uzbekistan. Including, in paragraph 4.3. noted that "...development and modernization of road transport, engineering, communication and social infrastructure to improve the living conditions of the population..." [7].

III RESULTS AND DISCUSSION

In particular, the number of private vehicles in the city of Urgench in 2009 increased by 789 vehicles compared to 2008, and in 2010 this figure was 836 vehicles. As of November 2010, the total number of private vehicles in Urgench reached 13,242 units. In other words, in 2009 the number of vehicles registered in the city increased by 6.9% compared to 2008, and by 2010 this value had changed by 13.9%. As of January 1, 2020, more than 137,000 vehicles were registered in the Khorezm region, of which the number of vehicles registered in Urgench in 2017 was more than 20,429,000 vehicles. This means that the number of private vehicles in the city of Urgench has increased by 75.8% over the past 8 years. The graph of the steadily growing number of vehicles and population growth in the city (by years) is shown below (Fig. 1, 2).

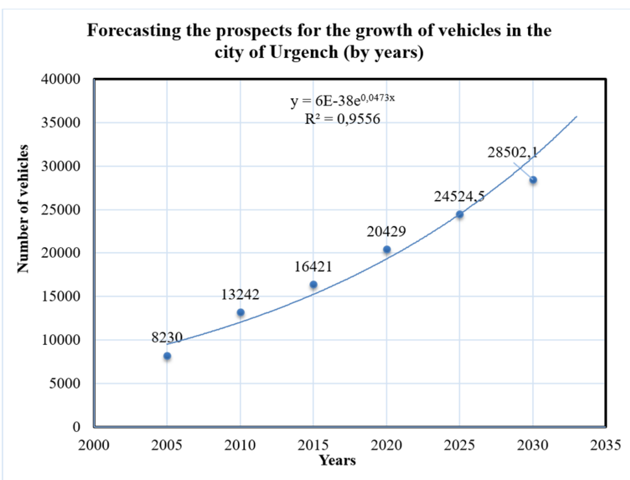

Fig. 1: Forecasting the growth of vehicles in the city of Urgench (by years). Source: compiled by the author based on research results.

It should also be noted that the city has not only vehicles registered in the area, but also traffic entering the city. According to the Urgench MDIA, 1,092 vehicles enter and leave the city daily. There are currently 10,125 vehicles in Urgench, including 8,775 personal and 1,350 company vehicles.

Based on modern urban planning concepts, measures are planned to improve the transport system of the city of Urgench, increase the capacity of the street and road network, as well as create a modernized, more convenient scheme of

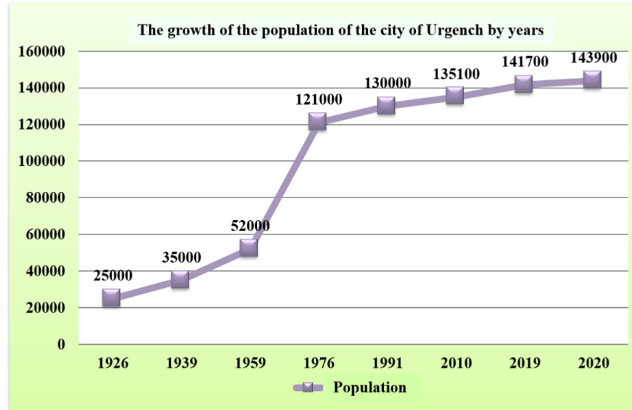

Fig. 2: Diagram of population growth in the city of Urgench (as of January 1, 2020)[1]. Source: compiled by the author based on research results.

[1]Data of the Khorezm Regional Department of Statistics

the transport system to create a modern image of the city, can be divided into organizational and road construction. Studying the methods for solving transport problems applied to the street networks of developed cities, as the most optimal solutions, presenting the following solutions in the development of the street network in Urgench (Fig. 3):

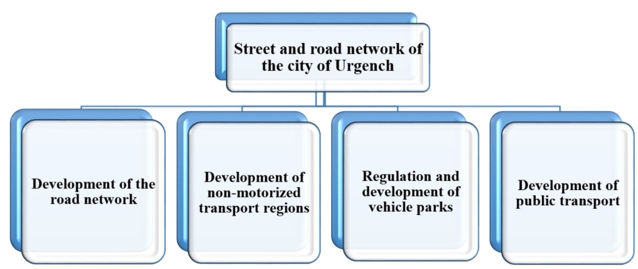

Fig. 3: The proposed solution to existing problems in the road network of the city of Urgench.

- On the development of the road network of the city of Urgench:

*Development of public transport.*Today, the fact that public transport in the city is only motor transport, including personal vehicles, due to the expansion of the urban area due to population growth, the construction of new streets and roads, makes urban public transport inefficient, modes of transport also require changes by examining the effectiveness of existing routes.

Also creating a separate lane for public transport. In this case, the outer lane is reserved for public transport. This, in turn, prohibits private vehicles from driving in that lane, or may also allow it to run during certain hours. During rush hour, this lane serves only public transport. Also, when transferring public transport to immovable minor roads, the lane can be redirected through traffic signs.

Fig. 4: Arrangement lane reserved for public transport

Organization of vehicle parks. It should be noted that the problem of vehicle parking has become relevant for the streets of Urgench in recent years. In particular, in the city of Urgench there is a large shopping center "Urgench Farmer's Market", "Urgench Clothing Market", "Central Department Store" (CDS), densely populated places (parks, squares, entertainment centers, squares, etc.). The main reason for the problem of congestion on the streets of Al-Khorezmi, A. Bahodirkhan, Gurlan, Dusov, Khudaibergenov, P. Mahmud is that the throughput of the parking system does not meet the requirements or there is insufficient capacity (35-50 places). Therefore, in order to effectively serve the population of city streets and roads, it is necessary to create modern multi-storey vehicle parks and a complete ban on parking on the main streets that form the basis of the city's street network, and temporary parking on local streets. It is also possible to study the specific geology of the city of Urgench and the rational use of underground urbanization, the introduction of the construction of underground parking lots (Fig. 5)

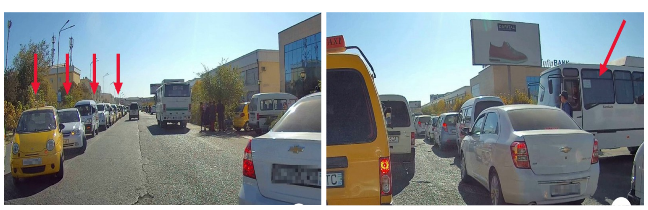

Fig. 5: Traffic jams in front of the Central Farmer's Market in the city of Urgench

Vehicles left in the outer lane have a negative impact on traffic flow, especially during rush hours, causing traffic congestion and reducing road capacity. In many cases, due to the lack of permanent parking lots for vehicles in the city of Urgench, drivers mainly stop on the carriageway of the main streets adjacent to the markets, thereby creating an emergency situation in these sections. Therefore, the design and construction of modern parking lots is one of the main tasks facing the urban planning activities of the city of Urgench. To solve the problem, the following was identified:

- Expansion of paid parking lots in the central districts of the city;
- Construction of short-term parking lots that do not interfere with traffic, including interchanges;
- Construction of parking lots for permanent storage of vehicles.

System "Permanent traffic". It is known that the non-intersection of pedestrian and vehicle traffic on the roads serves to increase the throughput of the road. At intersections where pedestrians are not moving, it is necessary to regulate the "red light", i.e. optimize their work (for example, reduce the burning time). The solution to the system of "permanent traffic" is the introduction of underground and surface routes of movement.

The intersection of pedestrian and vehicle traffic on the streets and roads of the city of Urgench at the same level leads to a decrease in the throughput of the road. To improve traffic at urban intersections, it is necessary to introduce a system of "permanent traffic" and regulate the "red light" of traffic lights at pedestrian crossings, i.e. optimize their work (for example, reduce the burning time) [8]. In connection with this study, it was revealed that there are 46 traffic lights on 86 streets of Urgench, of which 15 traffic lights do not meet the established requirements. For this reason, the use of a circle instead of a traffic light, that is, the introduction of a traffic rule in a self-regulating frame due to the fact that the traffic light can be turned off, is effective when using solar panels for lighting. (With the cost of one traffic light at least 16 million, the number of violations, such as crossing the red light, as well as vehicle accidents, the consumption of cash and electricity will be reduced).

Moto- and velo- transport. From the experience of developed countries, it is known that the development of cycling in cities will solve a number of problems associated with urban transport. A bicycle is an environmentally friendly and convenient form of transport. The organization of bike paths requires no more money than roads: it works without fuel, does not harm the environment with harmful gases and traffic noise, and also has a positive effect on the health of urban residents [9].

The city of Urgench has great potential to develop safe cycling on city roads and streets, as the city has dense housing, smooth roads and a mild climate zone that is conducive to cycling. A dense network of various road surfaces, including settlements, will help the development of cycling infrastructure. In this sense, it is necessary to take targeted measures for the use of this mode of transport.

Development of the street and road network. In order to develop the road network of the city of Urgench, the following have been determined:

- Construction of a ring road to ensure uninterrupted traffic in the city, i.e. in the general plan of the city of Urgench, create a complete ring of the city, which will be transit through the city streets with the routes of Khanka, Chalysh, Gurlan, Shavat, Khiva, Yangiarik and Yangibazar;
- Reconstruction of the street and road network in order to ensure the priority of public transport;
- Arrangement of sidewalks that do not impede traffic;
- Application of local measures to improve traffic capacity and traffic safety;
- Construction of transport hubs.

Development of non-motorized transport regions. Of course, it is gratifying that bicycle paths have been built on new roads in our country in recent years. This is due to the fact that bike lanes not only eliminate the congestion of the street network, but also serve to improve the urban environment. Therefore, in the city of Urgench -

- Organization and development of bicycle paths in the city center;
- Formation of a pedestrian zone around historical buildings and densely populated areas of the city;
- It is necessary to limit and control the use of transport in the recreational areas of the city.

Analyzing the situation and problems in the street-road network of the city of Urgench, using the existing transport scheme of the city of Urgench, sections were identified where it is possible to design high-speed roads and roads leading to high-speed roads.

The main traffic flows entering the city of Urgench pass along the following routes:

1. 4R-156 - the automobile road of national importance "Urgench- Khanka -Khazarasp-Republic of Turkmenistan" approach to the city from the south-west, from the east along the ring road crossing the city in latitude.

2. 4K-931 - district traffic crosses the village of Chotkopir, and then the Shovot district. The road is of the II technical category and consists of an asphalt concrete pavement. Currently, the intensity of traffic from Khozarasp to Urgench is 15,089 vehicles per day.

3. 4P-157 - The Urgench-Yangiaryk automobile road of national importance of category I enters the city from the south, crosses the ring road in the meridional direction and exits along the overpass to Khanka Street. The intensity of traffic on this route is 8955 vehicles per day.

4. 4R-158 is the national automobile road of the II category "Urgench-Khiva", entering the city from the north-west, in the direction of the meridian. The traffic intensity is 18,504 vehicles per day.

5. Two automobile roads of republican significance, connecting from the north-west of the city, i.e. 4P-159 - "Urgench-Shavat" and 4P-160 - "Urgench- Gurlan". The intensity of traffic on these roads is 100,578 and 14,806 vehicles per day, respectively.

6. 4P-162 - automobile road along which all traffic along the routes Shovot, Gurlan, Khiva, Yangiarik, Chalysh and Khazarasp pass. Today it is the busiest, I and II technical category, asphalt concrete urban road. Its traffic intensity exceeds 16,100 vehicles per day, including 1,325 trucks.

7. 4P-162A automobile road - a meridional route passing through Al-Khorezmi street, connecting the city with Urgench airport and railway station. This is the central street of the city leading to the railway station. The number of vehicles registered in this direction per day amounted to 7295 units.

Currently, the number of registered vehicles in Urgench is more than 20,429, and the number of vehicles entering the city is more than 1,092, which carries about 10,125 passengers through the streets of the city daily (2,286 vehicles: 246 buses, 595 taxis and 1,445 fixed-route taxis), including 8775 private and 1350 official vehicles. Recent studies show an increase in the congestion of the street and road network in the city of Urgench, a decrease in the capacity of the street and road network. Of course, a number of measures have been taken to implement the Decree of the First President of the Republic of Uzbekistan dated December 6, 2012 No. PP-1874 “On measures to implement the master plan for the city of Urgench, to radically improve the improvement and water supply of the population of the Khorezm region” [10]. In particular, during the years of independence, the roads that make up the street network of the city of Urgench have been improved. Many roads, overpasses and bridges, transport interchanges have been built. However, based on today’s observations of the city’s street network, it can be said that this street network is weak enough to solve problems. That is, despite the fact that many automobile roads of the city have sufficient street sizes in accordance with current regulations, the width of the carriageway does not always correspond to the existing traffic intensity. The city has not yet formed a complete outer road ring that can cope with the flow of transit traffic, all external automobile roads flow into city streets. As a result of this distribution of traffic flows and the fact that many city automobile roads are 2-3 lanes wide, long traffic jams are observed at intersections and streets even during the peak period.

It should be noted that the main cause of the problem in the road network of the city of Urgench is the flow of trucks, vehicles and route vehicles from the main roads entering the city not only for any purpose in the city, but in many cases to close the road and save time unintentionally merges into the internal traffic flow of the city due to the lack of ring roads, overpasses, high-speed roads that cross the city.

Therefore, in the general plan of the city of Urgench, it is advisable to create a complete ring of the city, which will pass through the streets of the city in the direction of Khanka, Chalysh, Gurlan, Shavat, Khiva, Yangiaryk and Yangibazar.

In turn, the creation of a motor road to the "Big High-Speed Ring Road" in the city of Urgench in the future will increase the capacity of the city road and transport network, reduce the congestion of city roads, and increase freight and passenger traffic. Below is a perspective diagram of the city's automobile roads (Fig. 6).

Fig. 6: Scheme of " Ringroad" of the city of Urgench.
Note: where green lines are the proposed ring road and high-speed roads leading to the city of Urgench, yellow lines are part of the high-speed road leading to the city center, and red lines are roads leading to the high-speed road.

Considering that the intensity of traffic on the Ringroad around the city in the future will be about 20.0 thousand per day, the project proposes to build 14 intersections and 4 overpasses to ensure traffic and pedestrian safety.

And roads can be designed as 4, 6 or 8 lanes, depending on the speed of traffic. According to SHNK 2.05.02-07 "Automobile roads" of the Republic of Uzbekistan, roads should provide a speed of 120-100 km/h [11]. The connection of the rolling stock must be carried out through intersections at different levels and junctions at the same level (without crossing the flows of the direct direction), located at a distance of at least 3 km from each other.

According to the main objective of the study, in the master plan of the city of Urgench, evaluating the economic efficiency of creating a complete ring of the city of Urgench, which will pass through the streets of the city with the routes Khanka, Chalysh, Gurlan, Shavat, Khiva, Yangiarik and Yangibazar.

1. The loss of time of various vehicles (cars, trucks and buses) "Before and After" from the event is determined. To do this, first of all, the travel time of various vehicles (buses, trucks and cars) is determined as follows [12]:

$$t = \frac{S}{V}$$

S- measurement distance, m;
V- speed of various vehicles - m/s;
t- transit time, s.
Cars:

$$t_1 = \frac{9.3}{22.15} = 0.42s \quad t_2 = \frac{9.5}{79} = 0.12h$$

Trucks:

$$t_1 = \frac{9.3}{18.6} = 0.5s \quad t_2 = \frac{9.5}{47.5} = 0.2h$$

Buses:

$$t_1 = \frac{9.3}{20.2} = 0.46s \quad t_2 = \frac{9.5}{79} = 0.12h$$

2. The time of vehicles is determined during a certain movement:

$$\Delta t = t^{after} - t^{before} \quad s;$$

t^{after} - in this case, the passage time after the event has occurred, s; t^{before} - time of passage before the event, s.
Cars:

$$\Delta t = t^{after} - t^{before}; \quad \Delta t = 0.3s;$$

Trucks:

$$\Delta t = 0.3s;$$

Buses:

$$\Delta t = 0.3s;$$

3. Determining the annual loss according to the specific loss time using the following formula [12]:

$$T_l = (N \cdot \frac{\Delta t}{3600})t_c \cdot 305 \quad h;$$

T_l - time of loss of various vehicles during the year, hours;
N - traffic intensity, units /day;
Δt - time lost by various vehicles, s;

t_s - daily working hours, 10 hours, 305 working days a year.

$$T_l = (21550 \cdot \frac{0.3}{3600}) \cdot 3050 = 5477.3 \quad h;$$

$$T_l = (2000 \cdot \frac{0.3}{3600}) \cdot 3050 = 508.4 \quad h;$$

$$T_l = (1520 \cdot \frac{0.3}{3600}) \cdot 3050 = 386.3 \quad h;$$

Thus, the amount of lost time for the year was 5477.3 hours for cars, 508.4 hours for trucks and 386.3 hours for buses. Naturally, there will be material damage due to lost time. Therefore, based on the data presented in Fig. 7, calculating the average cost by type of vehicle for 1 hour [12]:

Vehicle types		
Buses	**Trucks**	**Cars**
Mercedes-Benz 50-98 thousand sum	Isuzu 60-70 thousand sum	Cobalt, Lacetti 17-35 thousand sum
Isuzu 35-70 thousand sum	GAZ-53, ZIL-130 85-100 thousand sum	Spark 12-25 thousand sums
Minibuses 15-60 thousand sum	KAMAZ 1 20-130 thousand sum	----

Fig. 7: Calculating the average cost by type of vehicle for 1 hour

4. Determine the cost of lost time (in money) of various vehicles using the following formula:

$$C = Y_l \cdot C_c \quad sum;$$

Average cost of C_s - vehicles for 1 hour work, thousand sum. The sum of these costs is presented in Fig. 7.

Cars: S = 5477.3 · 35 000 = 191 705 500 sum;

Trucks: C = 508.4 · 12 500 0 = 63 550 000 sum;

Buses: C = 386.3 · 98 000 = 37 857 400 sum;

General costs: $\sum$ = 293 112 900 sum;

5. The total cost of the trip is determined as follows:

$$C_{tot} = C_{cons.} + C_{tr.c} + C_{trav.ex}$$

Here:

$C_{cons.}$v- cost of road construction;

$C_{tr.c}$- transportation costs (due to lost time);

$C_{trav.ex}$ - travelling expenses;

Calculate the total cost of travel along Al-Khwarizmi Street:

$$C_{tot} = C_{cons.} + C_{tr.c} + C_{trav.ex} = 0 + 32679212 + 50000000$$

$$C_{tot} = 82679212 \quad sum;$$

10 years later: with capital repairs

$$C_{tot} = 826792120 + 700000000 = 1 + 526792120 \quad sum;$$

Calculating the total travel costs for 1 km of the proposed Big High-Speed Ring Road of the city of Urgench:

$$C_{tot} = C_{cons.} + C_{tr.c} + C_{trav.ex}$$

C_{tot}=1 bln.sum + 0 + 10 000 000 = 1 bln. 10 mln.sum
After 10 years:
C_{tot}= 100 mln. sum + 1 bln = 1 blm. 100 mln. sum

1,526,792,120 sum, for 1 km of the projected Big High-Speed Ring Road and 1 bln 100 mln. Economic efficiency per km amounts to 426,792,120 sum with a payback period of capital investments of 10 years.

IV Conclusions

The existing problems in the street and road network of the city of Urgench, the causes of which are being studied on the basis of specific evidence, and the proposed optimal ways to solve them - organizational measures to improve the road network of the city, the priorities for solving problems in the transport system and according to the calculation schemes are as follows general conclusions:

- The current issue in the street-road network of the city of Urgench, in particular, the low capacity of the street-road network at the appointed time, the need for unregulated intersections of different levels, city highways;

- Identified the need to study the state street and road network of the city of Urgench and development of proposals for their improvement.

- Insufficient attention to the use of public transport in the city's road network was revealed and the necessary recommendations were developed;

- In order to further improve the density of the street-road network of the city of Urgench, it is necessary to take measures to regulate traffic on existing roads in some districts.

- In the master plan of the city of Urgench, proposals and recommendations have been developed for creating a complete ringroad of the city, which will reduce the transit of city streets, and its economic efficiency has been determined.

V REFERENCES

[1] Resolution of the President of the Republic of - Uzbekistan dated December 6, 2012 No PR-1874 "On measures to radically improve the improvement and water supply of the population of Khorezm region, the implementation of the master plan of Urgench".

[2] Masucci A.P., Stanilov K., Batty M., Limited Urban Growth: London's Street Network Dynamics since the 18th Century., PLoS ONE 8(8): e69469., 2013., *https://doi.org/10.1371/journal.pone.0069469*

[3] Anastasiadou K., Vougias S., "Smart" or "sustainably smart" urban road networks? The most important commercial street in Thessaloniki as a case study, Transport Policy, Volume 82, 2019, pp. 18-25, ISSN 0967-070X, *https://doi.org/10.1016/j.tranpol.2019.07.009.*

[4] Dominique Lord, Bhagwant N. Persaud, Estimating the safety performance of urban road transportation networks, Accident Analysis and Prevention, Volume 36, Issue 4, 2004, pp. 609-620, ISSN 0001-4575, *https://doi.org/10.1016/S0001-4575(03)00069-1.*

[5] Chan, S.H.Y., Donner R.V., Lämmer S., Urban road networks — spatial networks with universal geometric features?, Eur. Phys. J. B 84, pp. 563–577, 2011. *https://doi.org/10.1140/epjb/e2011-10889-3*

[6] Strano E., Nicosia V., Latora V., Elementary processes governing the evolution of road networks. Sci Rep 2, pp.296, 2012. *https://doi.org/10.1038/srep00296*

[7] Decree of the President of the Republic of Uzbekistan, № F-5024 of 15.08.2017, Measures for the future implementation of the action strategy on five principles of development of the Republic of Uzbekistan in 2017 – 2021.

[8] Information about the city on the official website of the Urgench city Administration. *https://urganchshahar.uz/*

[9] Azizov K.Kh., Darabov M., Sayfutdinova R.A., "Ensuring traffic safety on city streets". Tashkent: TADI, 2009. pp. 132.

[10] Decree of the President of the Republic of Uzbekistan Sh.M.Mirziyoev dated February 14, 2017 No PF-4954 "On measures to further improve the management system of road facilities." Tashkent, Collection of Legislation of the Republic of Uzbekistan, 2017, No. 7, Article 84.

[11] State Committee of the Republic of Uzbekistan for Architecture and Construction, Town Planning Norms and Rules (SHNQ) 2.05.02-07 "Motor roads". Tashkent, 2007. *https://mc.uz/gradostroitelnye-normy/*

[12] Azizov Q.H., Darabov M., "Guidelines for calculating the cost-effectiveness of the organization of safe movement." Tashkent - 2020.

[13] State institution "The National center of legal information "Adolat" under the Ministry of justice of the Republic of Uzbekistan *https://lex.uz/en/*

[14] The Voice of Tashkent is the city's online newspaper. *http://vot.uz/article/2016/02/18/ih-ne-obehat*

Acta of Turin Polytechnic University in Tashkent, 2022, 31, 62-69
Published Online March 2022 in Acta TTPU (http://www.acta.polito.uz/)

WAYS TO IMPROVE THE MARKETING STRATEGY OF AUTOMOBILE ENTERPRISES

Sharipov K.A.[1], Zayniddinova U.J.[2]
[1]Tashkent state University of Economics, Rector
[2]Tashkent Institute Of Finance, Assistant professor

Abstract– The article describes the organizational framework for improving marketing strategies in the automotive industry. The five main organizational parts of the marketing efficiency of the automotive industry or its division are explained. Emphasis is placed on using mathematical models to study market conditions in the automotive industry.

Key words– Enterprise, auto industry, competition, potential, opportunity, profit, need, result, population, strategy, product, business, organizational basis, partner, joint activity.

I Introduction

Benchmarking systems used in the country's automotive industry take into account the automotive industry's characteristics and reflect the automotive industry's benchmarking strategy. It is difficult to find a complete answer to an existing problem in formulating a benchmarking strategy. It depends on several factors, including the relationship between the economic and financial condition of enterprises, the emerging market situation, the type of product, competition, and the process of improving the product by changes in market requirements of the enterprise.

Complex forms of implementing a benchmarking strategy are used in processes where, for various reasons, enterprises are unable to adapt to existing market conditions or lose their market position.

There are many strategies in the benchmarking system, and achieving benchmarking goals in the automotive industry allows you to choose the market and product type that meets the general requirements. The organizational basis of this strategy is:

- improving the organizational structure;
- business development (entry into new markets, introduction of new products into old markets, formation of new market segments based on market innovations);
- reduction of the production of harmful goods (exit from some markets and concentration of forces for promising markets);
- formation of joint activities with a foreign partner.

The organizational framework of the benchmarking strategy of the automotive industry will be improved in the long or short term, depending on market conditions. In the automotive industry, using mathematical models of market conditions or studying the strategy in terms of game theory, they are selected as "mini-max" (maximum expediency regardless of risk), "max-min" (minimum bet regardless of practicality), or a combination of the two.

The following factors are essential in this process:

- segmentation of the markets in which the automotive industry operates (or expects to operate) so that the same attitude usually distinguishes the segments in different markets for advertising, product promotion, and other benchmarking activities;
- the system of selection of the optimal segment should be based on the provision of the complete leadership of the automotive industry (sufficient capacity, favorable prospects, a minimum or even zero level of competition, the level of unmet needs);
- method of entering the market with a new product, the full compliance of the product with the capacity with consumer characteristics, the reputation of the enterprise in the consumer market, as well as the scale of demand for the product;
- consideration of unfavorable market conditions in ensuring the continuity of the new product on the market.

The effectiveness of benchmarking of the automotive industry or its division depends on the following five main organizational components of the line of business:

- customer focus;

- benchmarking integration;
- degree of data processing and assimilation;
- strategic orientation;
- fast efficiency.

Japanese automotive enterprises have a strong position in improving the benchmarking strategy of the automotive industry, and the benchmarking platform of the automotive industry of this country plays a unique role in new markets. The country's automotive industry is using a strategy of gaining a foothold in the needs of non-domestic countries and then using the experience gained to test themselves in other markets ("laser beams"). For example, Japan has only been operating in Finland, Norway, Denmark, and Ireland for several years to enter the markets of only Western European countries with its cars. After the companies gained a high reputation in these countries, they joined more complex needs in Belgium, the Netherlands, Switzerland, Sweden, and Austria.

The very long-term consistency inherent in the activities of the Japanese auto industry is noteworthy, as it is essential to own the most popular, cheapest cars accordingly, to meet the needs of smaller buyers.

II Analysis of the relevant literature

To increase the benchmarking system's efficiency, foreign scholars conducted extensive research, such as Bankin A., Bekvit G., Berdyshev S.N., Bojuk S., Gorshteyn M., Karasev A., Fathuddinov R., Harding G., Shkardun V., and others.

Local economists, such as Ergashkhodjaeva Sh., Sharifkhodjaev U.U., Ikramov M.A, Abdukhalilova L.T., Nabieva N.M., Salimov S.A., T.A. Akramov, G.B. Muminova and others made a research on the formation and systematic mapping of benchmarking strategy of industrial enterprises in Uzbekistan.

The primary purpose of the above research is to increase the efficiency of enterprises through the formation of benchmarking strategy for industrial enterprises, the systematic study of the dependence of benchmarking process on competitive enterprise advantage, consumer and competitor orientation. However, given the role of international competition and national production in the activities of industrial enterprises, in particular, the automotive industry, the process of improving the benchmarking strategy of enterprises has not been studied as an object of independent research.

Resolution of the President of the Republic of Uzbekistan dated July 18, 2019y PQ-4397 "On additional measures for the accelerated development of the Republic of Uzbekistan" and its practical implementation ensured the accelerated development of the automotive industry. In addition, it increased its investment attractiveness, positively impacting the automotive industry's market activity by introducing mechanisms and management methods

III Research methodology

Comparative analysis, logical and abstract reasoning, monographic observation, and other methods were widely used in the research process.

IV Analysis and results

In the modern benchmarking system, the benchmarking strategy of automotive companies with great success is based on scientific and technical innovations and consistency in the process of overcoming competitors.

However, the full standardization and unification of the automotive industry structure do not meet the constant goal of the benchmarking strategy. Therefore, the system of standard indicators used to develop the plan includes the following:

- the expected market share;
- the volume of its production, taking into account the differentiation of passenger cars, market share, and the description and forecast of the target market;
- projected profit and its growth rate;
- the structure of financial costs (development of passenger cars, logistics, sales and promotion, advertising, services);
- calculation of production costs for one car;
- determination of profit (gross, net, gain from the sale of each product);
- evaluation of the effectiveness of car sales;
- evaluation of production profitability and other indicators.

The benchmarking complex can be studied as an integral part of a product or manufacturing department benchmarking program and a separate type of benchmarking program that aims to develop a decision based on the company's market policy direction. The model structure of a similar program consists of the following sections:

- forecasting the development of the target market (segment);
- the general strategy of the firm about the target market;
- commodity policy;

- communication policy;
- sales policy;
- pricing policy;
- sources of financing and budget for the implementation of the benchmarking complex;
- monitor the implementation of the program.

In developing the benchmarking strategy of GM Uzbekistan CJSC, it is advisable to take into account the following recommendations:

1. Strategy, in the section "Forecasting market development" the following recommendations are given, namely:
   - the volume of domestic production of similar goods;
   - market share calculation;
   - sales volume;
   - sales infrastructure structure;
   - the level and dynamics of solvent demand;
   - the expected price level;
   - requirements for the quality and technical level of the car;
   - purchase motives and behavioral characteristics;
   - level of service demand;
   - average volume of one purchase.
2. The section "Enterprise market strategy" assesses the possibility of sales in the selected market by identifying the main competitive advantages of the transport enterprise. The following descriptions are essential for this:
   - expected profitability of activity in the selected target market;
   - the planned volume of car sales of the enterprise;
   - dynamics of market share of the enterprise;
   - expected profitability of activity in the selected target market;
   - the planned volume of car sales of the enterprise;
   - dynamics of market share of the enterprise;
   - demand dynamics and potential demand measurement.

The company's competitive advantages are described in terms of product, price level, range of services provided, the efficiency of the sales channel, compliance of communication policy with current conditions, and popularity of its brand among potential buyers.

This section of the strategy must assess the availability of resources (financial, production, benchmarking, human) in the selected market. The following information is taken into account in the development of product policy:

- level of novelty of the product;
- assortment of products;
- the number of similar goods or substitute goods in the market segment;
- the degree to which the market segment meets the needs of specific customers;
- car quality;
- technological complexity;
- level of requirements for pre-sale and after-sales service;
- expediency of standardization or brand flexibility;
- patent protection and patent purity for a new car
- the compatibility of the existing organizational structure of the company with the new production;
- the cost of creating a new car;
- mandatory car certification in the target market;
- profitability of production and sale of new cars in the target market;
- the repayment period of the investment;
- the timing of the development of a new range and its optimization;
- costs for one car, etc..

The following should be taken into account when developing a sales policy:

- application of the market segment to the sales network;
- organizational structure of sales of the enterprise and the number of qualified sales staff;;
- assessment of the company's experience in the market segment;
- assessment of the appropriateness of using the services of intermediaries;

- opportunities to increase sales with the help of intermediaries;
- a policy of intermediaries towards the enterprise;
- availability of financial resources for the creation of a sales system;
- comparative assessment of the profitability of the individual sales system and alternative offers;
- delivery of cars to the market;
- number of potential customers;
- the nature of the order distribution;
- geographical concentration of sales;
- habits and preferences of end consumers;
- divisibility of the car;
- variability and instability of the car;
- the struggle of the company's management;
- control of the sales channel, etc.

It is useful to consider the following parameters when developing a pricing policy:

- selection of a method of price organization by the capabilities and objectives of the enterprise, taking into account the practice of competitors;
- price level for one car;
- price dynamics corresponding to the stage of the car's life cycle;
- price ratio in the range (nomenclature) on the level of novelty, quality differences, and technical level of the car;
- price level relationship with analog competing in the target market;
- degree of elasticity of demand;
- level of functional and pure competition;
- selection of a price strategy for the release of a new car on the target market;
- service policy, the degree of popularity of the brand, the length of the sales channel and the type of sales intermediaries, terms of delivery, discount system, etc.

3. In the section "Communication policy" it is recommended to allocate the budget to the individual organizers of the policy of moving the car to the market and justify their choice, to address the issue of means of communication.

   To decide on an advertising company, the following needs to be analyzed:

- features of advertising policy;
- advertising arguments;
- plan of the advertising company;
- targeted and practical advertising tools in the market segment;
- the number of advertising costs;
- methods of assessing the effectiveness of advertising;
- conformity of advertising to the nature of the product;
- the relationship of advertising activities with the period of life of the product;
- assessment of the main types of fairs and exhibitions and the possible effects of their participation;
- selection of incentives for end-users and sales intermediaries;
- methods of allocating funds for sales promotion, fixed interest, determining the percentage of profit, the volume of sales in the future or the past, etc.

In the process of implementing the benchmarking strategy, it is necessary to consider the following by determining the budget:

- the total amount of costs for the implementation of all benchmarking measures provided for in the strategy;
- marketing research costs;
- costs of benchmarking research;
- costs of forecasting market development;
- expenses for studying the individual production and sales capabilities of the enterprise;
- the cost of creating a benchmarking program;
- expenses for salaries of employees of the benchmarking department of the enterprise;
- the cost of paying for the services of special benchmarking and advertising organizations;
- costs of paying for the services of trade intermediaries;
- expenses for preliminary and final evaluation of the effectiveness of the benchmarking program;
- Costs and monitoring to control over the implementation of the benchmarking program.

Supposed that the primary goal of GM Uzbekistan CJSC is to make a profit, it is necessary to increase sales of profitable goods and increase their share. These, in turn, lead to several tasks. These tasks are benchmarking studies and require the development of a benchmarking strategy.

The development of benchmarking strategies requires addressing key issues in identifying the potential of automotive enterprises and defining appropriate strategies, determining the extent to which selected and structured factors have been formed in the automotive industry of Uzbekistan to determine the company's future goals.

According to the proposed model of determining the capacity to develop benchmarking strategies in the automotive industry, all the selected factors are interrelated and can be expressed in terms of multivariate function:

$$INN(F) = f(F_n) \rightarrow max, \tag{1}$$

whereas: INN - the potential to develop a marketing strategy;F_n – a group of n factors that form the basis for developing a marketing strategy.

According to the results of the standard model (F1), the lack of an effective benchmarking environment for enterprises in the automotive industry does not allow to determine the main directions for the development of benchmarking strategies in enterprises. Consumption-oriented, competitive environment in the automotive market of Uzbekistan limits the ability of enterprises to develop and implement benchmarking strategies, ie, the coefficient $W_{(F1)}$=-0,03.

All the necessary measures aimed at creating a competitive environment in the automotive market of Uzbekistan limit the activities of enterprises in developing effective benchmarking strategies.

The use of benchmarking (F2) in the automotive industry positively impacts the development of production and market opportunities in them. That is, the availability of benchmarking databases used in the practice of enterprises, the longevity of target plans, and the fact that enterprises are adequately equipped with modern information and communication technologies to increase the capacity to develop benchmarking strategies, and its value is $W_{(F2)}$ = 0,02.

Factors strongly influencing the development and implementation of benchmarking strategies in the context of Uzbekistan are participation in the value chain in the automotive industry ($W_{(F2)}$= 0,97). According to the results, the scope of internal and external benchmarking of enterprises, and the scope of use of benchmarking services can be identified as the most important factors in increasing the capacity to develop benchmarking strategies in enterprises.

Based on the study of the capacity of the automotive market, its growth dynamics are assessed, which is the basis for the formation of production capacity and the structure of the distribution network for the sale of goods. Keeping in mind that applying the results of market activity should guarantee the planned profit, covering the costs associated with operating in the market.

The study of the attractiveness structure of the automotive segment includes the analysis of the level of competition, the competitiveness of existing products, customer attitudes, the sustainability of the segment's demand for offered and existing goods, and the need and opportunity to market an entirely new product. In addition, revenue is a critical factor in stratifying customer attitudes.

In the domestic car market of Uzbekistan, it is expedient to segment consumers by income into three groups.

In practice, the first group, the highest-income buyers, make up 10% of the total buyers. They buy the highest quality goods, these premium cars in the automotive industry, and their group's purchasing power and self-esteem allow it. Such groups exist in every country, and the amount of their income depends on the country's total wealth.

In Uzbekistan, this group of consumers has an annual family income of 50 million soums. They buy Captiva and Malibu cars.

Goods	**Markets**	
	Current	**New**
Current	Deep market penetration strategy: - acceleration of sales; - search for new customers; - breaking competitors; - expansion of car consumption	Market development strategy: - new markets; - new sales areas; - international markets; - creation of new areas of car use.
New	Car development: - production of a new car; - development of transactions; - license; - skilled sales.	Diversification: - horizontal; - vertical; - concentric.

TABLE 1: CAR MARKET MATRIX

The second group includes the average income earners in each country, and their number is very high, although, in this group, there is a more specific stratification; in general, they are the primary buyers of gross goods, which sets the available standard of the market in this country. For example, in Uzbekistan, the annual family income of this group of consumers is 40-50 million. They buy Lacetti, Cobalt, and Spark models.

The third group consists of buyers who receive a minor income per person. They often use various forms of social security, spending about 80% of their income on basic needs.

In times of crisis, the production of products based on the needs of consumers increases the competitiveness of the enterprise in the market. It allows it to carry out its activities effectively. Research shows that when there are problems with financial resources for technological innovation, innovative benchmarking is a critical driver in an enterprise's competitive struggle. The activity of an enterprise in a market environment is determined by its customers. If customers value the enterprise's products and services more than the cost of creating them, the business will thrive. Otherwise, it will need outside help, or such an enterprise will face a crisis.

According to the analysis of the activities of enterprises, the use of innovations in benchmarking allows to meet consumer demand and conquer new markets fully.

Scientific research has shown that innovation can be divided into two groups according to its importance:

1. **Innovation by form:** product innovation (the material result of innovative activity), innovative services (intangible effect), process and technological innovation (technology change), personnel innovation, and new or improved production systems.

2. **Innovation according to the level of novelty:** incremental (lower, increasing), modular, architectural, and radical (upper).

   Consequently, innovation involves changes in products, services, and processes that characterize creation and make it effective. Studies show that technology development must go hand in hand with innovation management and benchmarking. These include:

   (a) Forms of technological innovation and the acquisition of new markets;

   (b) Develop new ways to stimulate consumer activity;

   (c) Combined innovative benchmarking.

When studied from a macroeconomic perspective, several problems can be solved with the help of innovations. Until recent years, firms have been increasing their revenues through extensive development, in other words, increasing the number of goods produced. While the cessation of population growth in developed countries requires the widespread and effective use of innovations in the economies of these countries, another factor is the rise in prices for raw materials, which is an important impetus for accelerating the innovation process.

The innovative product, in turn, is characterized by physical and informational factors. An innovative brand that the modern consumer studies as a set of specific physical features are not attractive to consumers, so the demand for them is not high.

The consumer must first accept the general concept of the product, which expresses his desire for several features of the

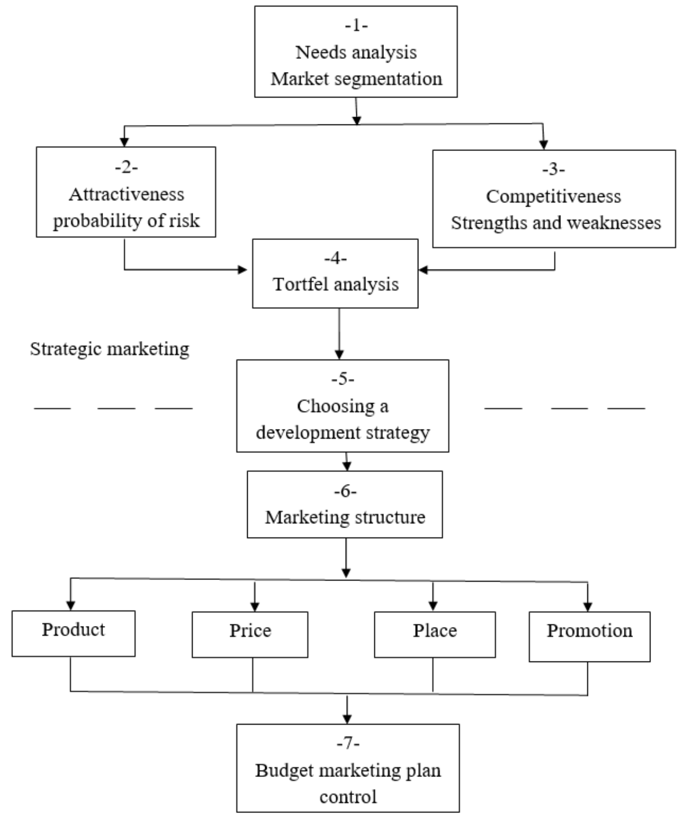

Fig. 1: Innovative benchmarking complex

product, such as physical, informational, and delivery terms. Then, to satisfy consumer expectations, an expanded product concept will be developed to provide additional benefits.

Research shows that innovative benchmarking is the basis of market research and the search for a competitive strategy for the enterprise. Therefore, the approach to innovation management through benchmarking is studied comprehensively. It is considered mainly from the point of view of both producer and consumer.

Innovative benchmarking, in turn, consists of seven main stages, including the development of an innovation strategy, market analysis, and operational benchmarking.

One of the primary forms of innovative benchmarking is strategic and operational benchmarking.

One of the main directions of strategic innovation benchmarking is to develop a strategy for introducing innovations to the market:

- development of programs and plans for innovative benchmarking activities;

- development of benchmarking innovations and monitoring of their application;

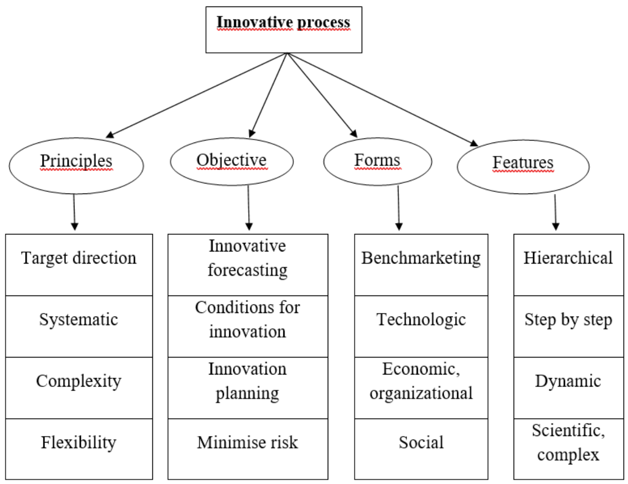

Fig. 2: Structural features of the innovative marketing process

- implementation of a single innovative policy from product development to customer service;
- coordination of innovative activities at the enterprise and abroad;
- ensuring continuous improvement of the practice of developing benchmarking innovations with the help of qualified personnel;
- formation of target groups for a comprehensive solution to the problems of innovative benchmarking.

The main tasks of the enterprise's innovation activity are to formulate an essential innovation benchmarking strategy with top management, define its location in the market segment, appoint executors, and set a deadline for the implementation of a specific practical directive for each participant in the market relations. Therefore, strategic benchmarking research includes critical structural features of innovative benchmarking processes that are part of an enterprise's innovation policy.

According to research, the strategy and tactics of innovation entry into the market are essential for benchmarking activities. It includes a competitive innovation strategy based on the placement of new products in markets and the formation of sales paths.

V CONCLUSION

In conclusion, innovative benchmarking is an activity of an enterprise based on improving production and influencing market conditions. According to research, each stage of the innovation life cycle requires different benchmarking methods and approaches, strategies, and tactics.

The system of innovative benchmarking measures is inextricably linked not only with the modernization of production but also with the dynamics of capital accumulation and flow.

Innovative benchmarking is important for businesses that want to make more money than their competitors and form a superior competitive strategy based on innovation and innovation. Innovative benchmarking also involves not only the sale of a new product or an existing product in the market but also the sale of licenses for inventions and know-how on a new product or technological process and the improvement of equipment for its manufacture.

The effectiveness of reforms related to the radical improvement of the automotive industry in our country requires increasing the work and market activity of the industry. The work and market activity of the industry is directly related to the investment process, its efficiency, and capacity, which is reflected in the mass placement of shares of joint-stock companies in the domestic and international stock markets.

Market activity in the automotive industry requires increasing production efficiency and quality, increasing the export potential of enterprises, and increasing competitiveness in international and national markets through a market-oriented benchmarking strategy.

Since establishing the automotive industry in Uzbekistan, the industry has been provided with significant benefits. Measures have been identified to support the initiative. Over the past years, due to several reforms, the sector's exports have increased. However, due to the failure of benchmarking to assess the effectiveness of benchmarking in the automotive industry, the processes of their formation, the behavior of dominant consumers in the market, the level of profitability, exports of passenger cars in 2017-2018 decreased from 130.2 million USD to 29.3 mln. USD., maintaining a positive growth rate of truck and bus exports with an average relative growth rate of 20 percent.

In the future, measures will be taken to improve the benchmarking of the industry, including the organization of production of new models of cars on a single unified platform, the development of targeted programs to attract investment and drawing concessional credit lines from foreign banks and export credit agencies to finance localization projects. - It is expedient to implement measures systematically.

Based on the above, to improve the benchmarking system of the automotive industry in our country, it is expedient to implement the following:

1. Due to the insufficient use of benchmarking-mix elements in domestic automotive companies' development of benchmarking strategies, it is necessary to ensure the active participation of existing automotive enterprises in the "global value chain (GVCs)" as effective benchmarking strategies.

2. Since the development of benchmarking strategy in the automotive industry reflects the company's capabilities, its current market position, the direction of development, taking into account the factors affecting the internal and external environment in the risk environment, the decision to choose a benchmarking strategy is individual for each enterprise. Therefore, a detailed, clear benchmarking plan should be developed and implemented rather than identifying specific enterprise activities using particular internal parameters.

3. Competitiveness of the automotive industry, first, the superiority of the company's products in many respects over other competitors; secondly, it is necessary to ensure the competitiveness of the enterprise through product competitiveness, as the enterprise is based on the implementation of clear competitive advantages that allow it to sell its products in the market on the most favorable terms for itself.

4. As a result of the development of benchmarking strategies for benchmarking research in the automotive industry and benchmarking strategies to bring new products to market, it is desirable to improve the enterprise benchmarking system and increase the volume of products on the market.

5. It is proposed to diversify regions, products, and their transportation in the automotive industry, implement benchmarking strategies based on the establishment of new initiatives, to increase production and export potential in the regions while providing priority strategies for diversification, focus and cost.

VI References

[1] Decree of the President of the Republic of Uzbekistan dated January 17, 2019 PF-5635 "On the state program for the implementation of the" Year of Active Investment and Social Development ".

[2] Resolution of the President of the Republic of Uzbekistan dated June 1, 2018 PP-3028 "On measures to further develop and improve the management of the automotive industry in 2017-2021."

[3] Bankin A., Content branding for real sales. - SPb: Peter, 2017, 272 p..

[4] G. Bekvit, Four keys to marketing services. - M.: Alpina Pablisher, 2017, 252 p..

[5] S.N. Berdyshev, The secret of effective internet advertising., Practical guide. - M.: Dashkov K., 2018, p. 120.

[6] P. Bojuk, Benchmarking research., Book. - M.: Yurayt, 2017, p. 280.

[7] M. Gorshteyn, Modern benchmarking - M.: Dashkov and Ko, 2017, p. 404.

[8] A.Karasev, Benchmarking research and situational analysis. Textbook and workshop for applied bachelor's degree. - M.: Yurayt, 2017, p.315.

[9] Fatxuddinov R.A., Strategic benchmarking: Textbook for higher education, 5-Edition. - SPb.: Peter, 2008. - p.368.

[10] Harding G., Industrial products benchmarking. / Per. s angl. - M .: Sirin, 2002, p.272.

[11] Shkardun V.D., Benchmarking bases of strategic planning: Theory, methodology, practice: Monograph. - M .: Delo, 2005, p.376.

[12] Ergashkhodjaeva Sh., Sharifxojaev U., Benchmarking management. Textbook. - T .: TSU, "Economy" Publishing House, 2019,– 324 p..

[13] S.A. Salimov, Marketing management. Textbook. - T .: Aloqachi ”2010, p.252.

[14] G. B. Muminova, The use of innovative benchmarking strategies in the development of the market of information and communication services., 08.00.11 - Benchmarking (Economics)., Abstract of the dissertation for the degree of Doctor of Philosophy (PhD) in Economics. - T .: Academy Publishing Center, 2019. p.54.

Acta of Turin Polytechnic University in Tashkent, 2022, 31, 70-73
Published Online March 2022 in Acta TTPU (http://www.acta.polito.uz/)

ANALYSIS OF THE TECHNICAL CONDITION OF THE WEIGHT CHECKING WAGON TYPE 640-VPV-277 OF THE JOINT STOCK COMPANY "UZBEKISTON TEMIR YULLARI"

Adilov N.B.
Tashkent State Transport University
Email: adilovnodir1991@gmail.com

Abstract– In this article, the assessments of the technical condition of the metal structure of the weighing wagon 640-VPV-277 were studied. When wagon carrying out calculations of the metal structure of a weight-checking wagon, the wall thickness will be taken taking into account its decrease by the average wear value to determine whether the strength of the wagon structure complies with the required standards.

Key words– Freight wagon, six-axle wagon, railway pivot beam, end beam, longitudinal beam.

I Introduction

One of the main conditions for the gradual development of the railway transport of the independent Republic of Uzbekistan is the renewal and replenishment of the fleet of freight and passenger wagons with modern domestically produced wagons that meet international standards, as well as extending the service life of existing wagons for their optimal use in operation [1-3].

In order to increase the efficiency and volume of rail freight transportation in the absence of other ways to increase the throughput and wagon carrying capacity of wagon-intensive sections, as well as with limited lengths of receiving and departure tracks at stations, the most promising is the introduction of wagons with heavy axle loads [4]. In this case, to determine the weight of the rolling stock in the railway industry of the republic, weight-checking wagons used for periodic checks should be operated.

Mechanized checking of all types of wagon scales that require periodic checks is provided by weight checking wagons. The weighing wagon performs mechanized verification of various types of wagon scales, thereby ensuring the accuracy and fidelity of the readings of weight measuring instruments.

At the moment, it is required to design and manufacture new and modernized weighing wagons to replace the old ones with an expired service life, but this takes a lot of time. In other words, before the release of new models of weighing wagons, as well as to achieve optimal performance indicators for currently used wagons, it is required to increase their service life. Increasing the service life of these wagons requires an assessment of the current technical condition and residual resources of these wagons [5-6].

At the first stage of the analysis of the technical condition of the metal structures of the 640-VPV-277 weighing wagons, it is necessary to identify faults that affect their service life by visual inspection.

At the second stage of the analysis, it is necessary to determine the wear values for the elements of the metal structure of the 640-VPV-277 weighing wagon for comparison with standard indicators and taking them into account when conducting strength studies.

For this purpose, a survey and analysis of the main load-bearing elements and structural parameters of the bodies of weighing wagons 640-VPV-277 was wagon carried out.

The weighing wagon model 640-VPV-277, located at regional railway junction Karshi, was built in 1966. The date of the last depot repair is 28.10.11. The weight of the wagon is 126 tons.

When checking the bodies from the outside, it was determined that there was corrosion on the side wall skins under a layer of paint. In this case, it is required to clean the bodies of the existing paint and weld the rust spots with new sheets. In the end walls and pillars of the body as a whole, there are no serious defects.

Welds of studs to side wall skins and welds from cross beam to stud welds need to be checked and re-welded.

During the inspection inside the weighing wagons, it was revealed that the wooden floor needs to be completely replaced, the monorail (I-beam) needs to be repaired.

It is necessary to restore the supporting part of the monorail by applying corner No. 50. Due to wear, it is necessary to replace the rollers of the bogie hoist inside the wagon.

The metal plates of the weighing wagon model 640-VPV-277 in the area of the junction of the transverse beams with the center beam are destroyed by corrosion. At the time of inspection, the thickness of the metal lining is thirty percent of the nominal. It is necessary to install wear-resistant pads on the sides of the bogies of weighing wagons.

A survey of the technical condition of the main load-bearing elements and structural parameters of the body of this weighing wagon was wagon carried out. The measurement results are shown in figures (8–12).

II Methods

Prior to determining the wear values of the body elements of the weighing wagon 640-VPV-277, schemes of measurement sites were drawn up, shown in Figures (1-7).

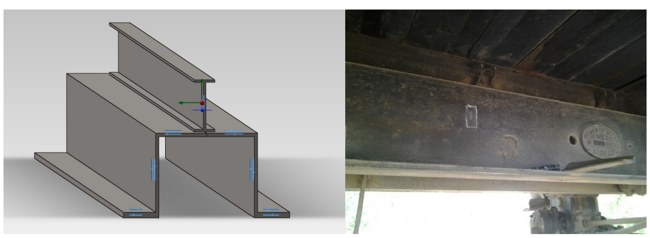

Fig. 1: Measurement of the center beam of the frame of the weighing wagon 640-VPV-277

Beam measurements were performed by the experimental method [7].

Based on the results of measurements of wear thickness h^i, the value of the average thickness h^i_{cp} is calculated taking into account the tolerance "δ=0.2 mm" for cleaning, which is determined by the formula

$$H^i_{mid} = \frac{1}{n} H^i_{mid} - 0,2$$

where n - the number of measurements.

Let us determine the average value of wear of sheets for the elements of metal structures of the weighing wagon according to the formula:

$$H_{mid} = \frac{1}{n} \sum_{i}^{n} H^i_{mid}$$

The results of the average wear values for the beams of the weighing wagon are summarized in figure 12.

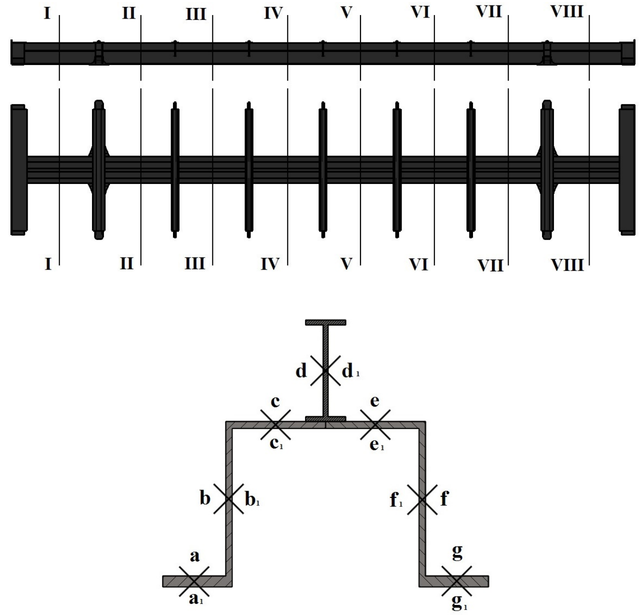

Fig. 2: Scheme of measuring the thickness of wear sheets on the center beam of the frame of the weighing wagon

Fig. 3: Measurement of the pivot beam of the frame of the weighing wagon 640-VPV-277

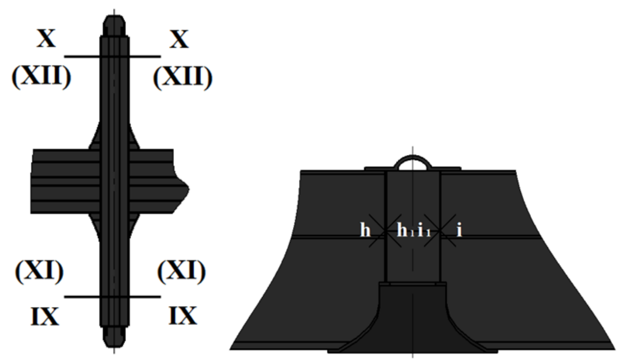

Fig. 4: Scheme of measuring the thickness of wear sheets on the pivot beam of the frame of the weighing wagon

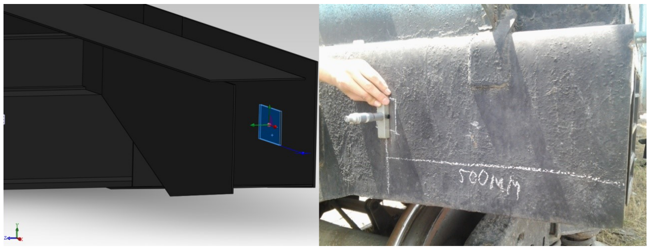

Fig. 5: Measurement of the end beam of the weighing wagon frame

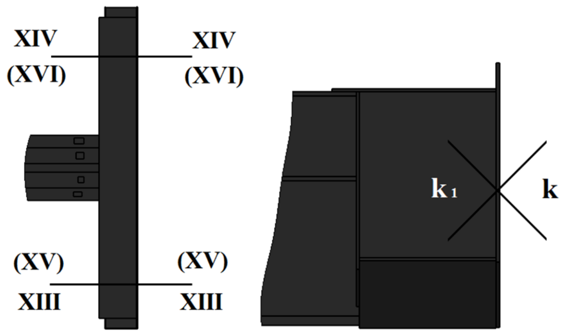

Fig. 6: Scheme of measuring the thickness of wear sheets on the end beam of the frame of the weighing wagon

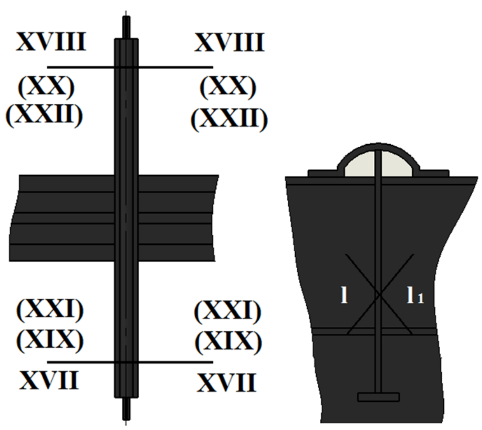

Fig. 7: Scheme of measuring the thickness of wear sheets on the longitudinal beam of the frame of the weighing wagon

III Analysis of the results

At the analysis stage, it is necessary to determine the wear values for the elements of the metal structure of weighing wagons for comparison with standard indicators and taking them into account when conducting strength studies [8-9].

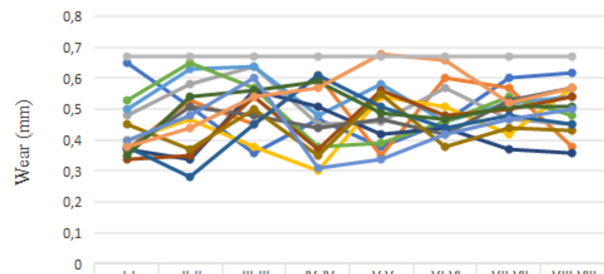

	I-I	II-II	III-III	IV-IV	V-V	VI-VI	VII-VII	VIII-VIII
a	0,65	0,51	0,36	0,47	0,38	0,46	0,6	0,62
a1	0,37	0,53	0,45	0,61	0,35	0,6	0,57	0,38
b	0,48	0,58	0,64	0,45	0,46	0,57	0,47	0,45
b1	0,4	0,47	0,38	0,3	0,54	0,51	0,42	0,57
c	0,5	0,63	0,64	0,48	0,58	0,46	0,52	0,54
c1	0,53	0,65	0,57	0,38	0,39	0,46	0,54	0,48
d	0,37	0,34	0,56	0,51	0,42	0,44	0,37	0,36
d1	0,34	0,35	0,54	0,37	0,56	0,48	0,5	0,54
e	0,37	0,51	0,48	0,44	0,47	0,42	0,53	0,57
e1	0,45	0,37	0,5	0,35	0,55	0,38	0,44	0,43
f	0,38	0,28	0,45	0,61	0,51	0,44	0,48	0,45
f1	0,35	0,54	0,56	0,59	0,49	0,47	0,51	0,51
g	0,4	0,48	0,6	0,31	0,34	0,42	0,47	0,5
g1	0,38	0,44	0,54	0,57	0,68	0,66	0,52	0,57
Hmid	0,67	0,67	0,67	0,67	0,67	0,67	0,67	0,67

Section

Fig. 8: The results of measurements of the wear thickness of sheets on the center beam of the frame of the weighing wagon

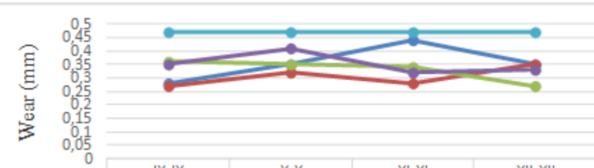

	IX-IX	X-X	XI-XI	XII-XII
h	0,28	0,35	0,44	0,35
h1	0,27	0,32	0,28	0,35
i	0,36	0,35	0,34	0,27
i1	0,35	0,41	0,32	0,33
Hmid	0,47	0,47	0,47	0,47

Section

Fig. 9: The results of measuring the wear thickness of sheets on the pivot beam of the frame of the weighing wagon

IV Conclusions

In the future, when calculating the strength of the mechanical parts of weighing wagons, it is required to take the wall thickness, taking into account its reduction by the value of the average wear indicators [10]. In other words, the value of the average wear must be subtracted from the value of the element sheet thickness. At the same time, it will be possible to find out whether the structural loading strength of the weight-checking wagon 640-VPV-277 is sufficient with the existing load wear required by the standards.

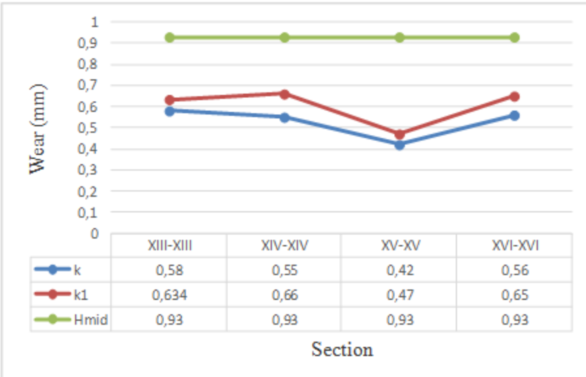

Fig. 10: The results of measuring the wear thickness of sheets on the end beam of the frame of the weighing wagon

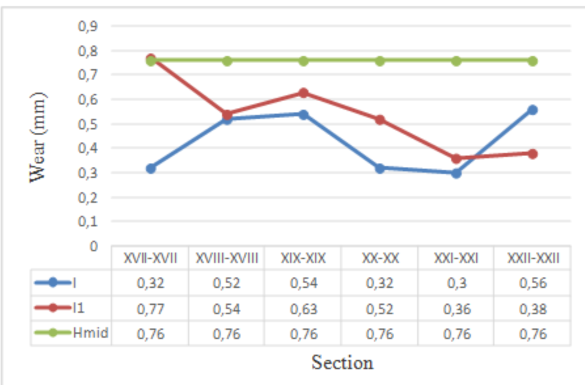

Fig. 11: The results of measurements of the wear thickness of sheets on the longitudinal beam of the frame of the weighing wagon

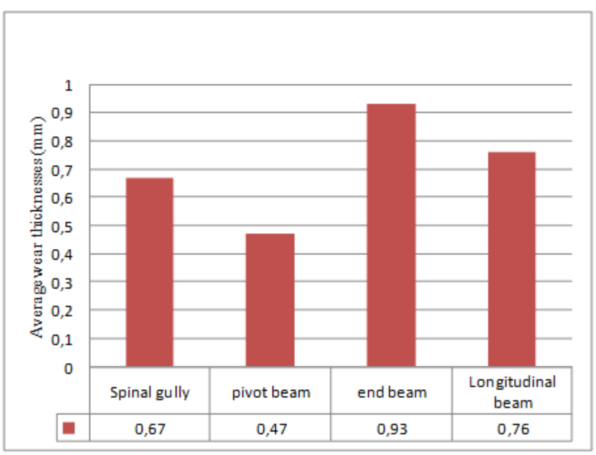

Fig. 12: The results of the average wear thicknesses for the elements of the weighing wagon 640-VPV-277

V References

[1] Decree of the President of the Republic of Uzbekistan dated December 2, 2017 №. PP-3422 "On measures to improve transport infrastructure and diversify foreign trade routes".

[2] Decree of the President of the Republic of Uzbekistan "On the organization of the Ministry of Transport of the Republic of Uzbekistan" February 1, 2019 №. PP-4143.

[3] Decree of the President of the Republic of Uzbekistan dated February 1, 2019 №. PF-5647 "On measures to radically improve the public administration system in the field of transport."

[4] Business plan of the JSC "UZBEKISTON TEMIR YULLARI" for 2021.

[5] Ruzmetov Ya.O., Prospects for the development of wagon building in the Republic of Uzbekistan / Ya.O. Ruzmetov, R.V. Rakhimov // Collection of scientific papers of the VIII All-Russian scientific and practical conference "Problems and prospects for the development of wagon building" (Bryansk, April 18 - 19, 2019). - Bryansk: BSTU, 2019. - P. 147 - 150.

[6] Rakhimov R.V., "Uzbekiston temir yo'llari" AZhning wagon parks: khozirgi holati va rivozhlanish istiqbollari / R.V. Rakhimov, D.N. Zairova // Bulletin of Tashkent State Technical University. - 2018. - No. 2 (103). - S. 136 - 142.

[7] Yadgor Ruzmetov, Nodir Adilov and Shokhruk Sultonov, Strength assessment of the body of a weight checking wagon type 640-VPV. E3S Web of Conferences 264, 05021 (2021) *https://doi.org/10.1051/e3sconf/202126405021*.

[8] GOST 30414-96., Scales for weighing vehicles in motion. General technical requirements. - Minsk.: IPK Standards Publishing House, 1997. - 8 p.

[9] Ikonnikov E.A., Means for measuring mass and weight verification tools used in railway transport. - M.: Route, 2003. - 40 p.

[10] Norms for the calculation and design of new and modernized wagons of railways of the Ministry of Railways of the 1520 mm gauge (non-self-propelled). – M.: GosNIIV-VNIIZhT, 1996. – 317 p.